TEMPERATURE SENSITIVITY OF INTEGRATED OSCILLATORS

by

Richard Adams

Memorandum No. ERL-M247

17 May 1968

ELECTRONICS RESEARCH LABORATORY

College of Engineering
University of California, Berkeley
94720

ACKNOWLEDGEMENT

The author is especially indebted to Professor D. O. Pederson for his guidance in conducting the research and preparing this thesis. The author also wishes to acknowledge the important and fruitful discussions with Professor W. G. Howard, the essential assistance given by W. J. Walsh in the writing of the computer programs, and the considerable help and many technical suggestions of Dorothy McDaniel in the laboratory fabrication of the circuits. The encouragement, artwork, and editorial assistance of my wife Kathryn were invaluable in the preparation of the final report.

The author is also pleased to acknowledge the support received from the Graduate Fellowship and the support furnished the integrated circuits research group of the Electronics Research Laboratory by the Joint Services Electronics Program under Grant AF-AFOSR-139-67 and the U. S. Army Research Office - Durham under Contract DAHC04-67-C-0031.

TABLE OF CONTENTS

I. INTRODUCTION

1.1 Prologue

Near-harmonic monolithic integrated oscillators based on conventional RC oscillator designs have inherently poor frequency constancy[1]. The oscillation frequency in such circuits has a large sensitivity to temperature which typically causes a frequency deviation of greater than 10% over the temperature range $0^{o}C$ to $65^{o}C$. The major contribution to this temperature sensitivity of oscillation frequency is the large temperature coefficient of the diffused resistors used in the frequency determining feedback network.

In a monolithic integrated oscillator, all the circuit components are realized on a single epitaxial chip as either diffused structures or MOS devices. Microcircuit integrated oscillators can also be realized in hybrid form. In this case, the complete oscillator is formed by an overlay of thin film and other components on a single or multiple silicon chips that contain active devices and non-critical resistors. However, the monolithic oscillator is attractive because of size, reliability and cost.

The disadvantage of the monolithic oscillator is its inferior frequency constancy. The subject of this thesis is the analysis of

the monolithic oscillator temperature sensitivity problem and the development of compensation techniques to correct this deficiency.

1.2 History

The specific constraints of monolithic active RC oscillators were first considered by Hachtel[2,3,4,5]. He devised a method for the realization of integrated oscillators from integrable bistable circuits. However, he made no attempt in his designs to control temperature sensitivity. Therefore, all of the oscillators he realized had large frequency variation with temperature. Howard generalized Hachtel's monolithic oscillator synthesis method to include all two device RC imbedded oscillators[6]. Since Howard's oscillators were used as voltage controlled oscillators in a phase-locked loop, there were no requirements on the temperature sensitivity in this application that were violated by the inherent sensitivity of the monolithic realization.

To date, in applications where the sensitivity of oscillators realized in monolithic form is unacceptable, microcircuit oscillators have been realized in hybrid form. One example is the RC twin-T oscillator of Berry, et al, that used low temperature coefficient thin film resistors in the frequency determining network to achieve a .1% frequency duration over a 75 ^{o}C range[7]. An alternative solution is given by the oscillators described here. A fully monolithic temperature compensated integrated oscillator is realized that has a frequency performance comparable to the thin film hybrid version over a temperature range.

1.3 Temperature Sensitivity Considerations

The Wien-type oscillator shown in Fig. 1.1 is typical of the RC oscillators considered. This oscillator will, as will all RC oscillators, produce an output frequency which is temperature sensitive because of (i) changes in the frequency determining feedback elements R_1, R_2, C_1, C_2; (ii) changes in the nature of the amplifier nonlinearity; and (iii) changes in the gain level in the internal amplifier with temperature.

The nonlinear contributions (ii and iii above) are studied by a computer-aided analysis of the generalized form of Lienard's equation[8]:

$$\ddot{x}(f(x)\dot{x} + g(x) = 0 \qquad (1.1)$$

For this equation, a form of $g(x)$ is found for a given $f(x)$ such that the oscillation frequency sensitivity to gain changes can be set equal to zero. In monolithic oscillator realizations, negative feedback is used in the amplifier to make the gain depend to a first order on the ratio of resistors with the same temperature coefficient. In this case, the nonlinear contributions to temperature sensitivity are negligible compared to the sensitivity caused by the frequency determining feedback elements in (i) above.

The temperature coefficient of MOS capacitors in the monolithic realization is very small. Therefore, the major problem is to compensate for the large temperature coefficient of the diffused feedback

resistors R_1 and R_2 of Fig. 1.1. Two basic compensation techniques are possible. In one, the shaping of the root locus of the linearized system can be used. In this method, a controlled gain sensitivity compensates for changes in the open-loop poles and zeros due to temperature changes of resistance values. The disadvantage is the increase in the non-linear contributions to temperature sensitivity.

In the second method, the individual RC products are made invariant using Miller-effect multipliers to provide compensating temperature sensitivity for the diffused resistors. In this case, the gain requirement for the monolithic realizations can be made to be almost independent of temperature. This is the method used to achieve the final compensated design.

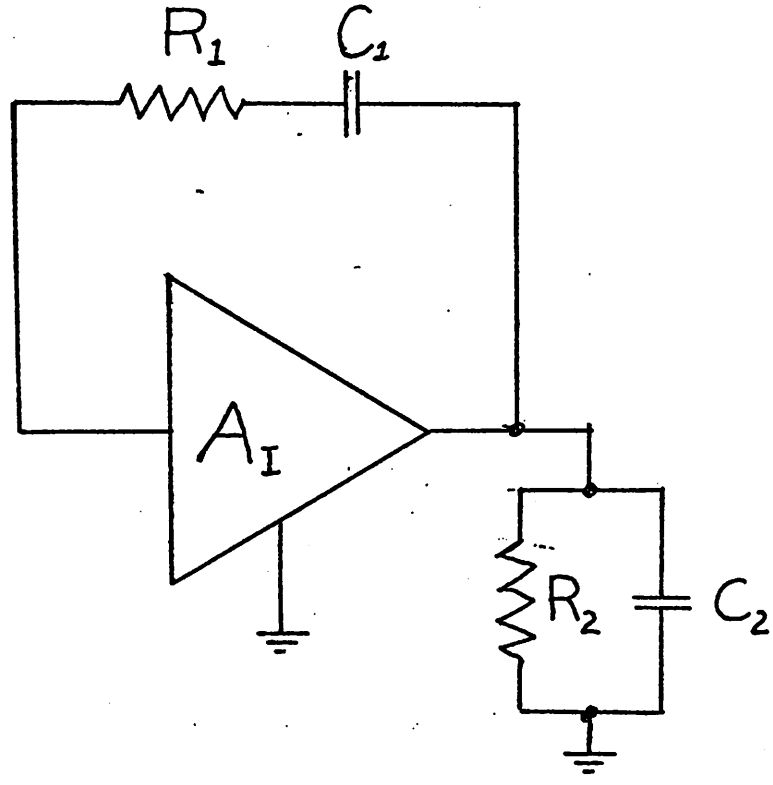

Fig. 1.1 Basic Current Amplifier, Wien-type Oscillator

II. OSCILLATOR CONFIGURATIONS

2.1 Introduction

Near-harmonic oscillators can be realized by using passive RC imbedding of either single or multiport active devices. In the case of the single-port realization, the active device must have an input impedance for small signal excursions about an operating point that is both inductive and has a negative real part at the oscillation frequency. Examples of such single port oscillators are the tunnel diode oscillator of D. K. Lynn, et al, and the unijunction transistor

oscillator of Hachtel[9,10].

Oscillators based on negative immittance inverters (NII) or negative immittance converters (NIC) are not included in the class of single port realizations. An ideal NII is a two port network that has an input impedance that is equal to the negative reciprocal of the terminating load impedance. An ideal NIC has an input impedance that is the negative of the terminating load impedance. A potential oscillator configuration which is based on an NIC realization is shown in Fig. 2.1. Pederson and Pepper have shown that this is totally equivalent to the Wien-type configurations[11], cf. Fig. 1.1.

The oscillators considered here do not depend on the inductive effect of any single port device and therefore are based necessarily on multiport active devices. This is because in the frequency range of interest, there is no direct integrable analog to the inductor. In addition, the active devices considered are three terminal devices which are assumed to have no appreciable charge storage effects. Under these constraints, an RC system which has passive RC imbedding of the idealized active three terminal devices and no closed feedback paths has only negative real natural frequencies. An oscillator is formed by using a closed feedback path. This is the form of the RC feedback oscillators considered in this thesis.

For convenience, the single loop RC feedback oscillators considered are arbitrarily classified as positive or negative feedback oscillators depending on the angle condition used to specify the root locus. Definitions of possible signal paths and feedback loops

are necessary before the class of an oscillator can be determined.

2.2 Signal Path Classification

In an actual oscillator design, there may be several discernable feedback loops and multiple signal paths between two circuit nodes. The classification of the oscillator as a positive or negative feedback type is based on the angle condition that specifies the root locus. For the purpose of discussion and definition of oscillator types, the following definitions of feedback loops and signal paths are given.

> 1. Multiple signal path. A multiple signal path provides several signal transmission routes that are not in the form of closed loops between two points in the circuit. A single branch of a multiple signal path may be broken without opening any closed feedback loop or breaking the continuity of any overall transmission path.

An example of a multiple signal path is the bridged-T network in Fig. 2.2. Forward transmission is not eliminated by opening either path, e.g., R_1.

For the classification of feedback loops, a distinction is made between loops that depend on nonlinear behavior to achieve a circuit function and those that do not. In the latter case, the loop is characterized as linear even though nonlinear effects may occur. As an example of this distinction is the simple Wien-type oscillator of Fig. 1.1 which is based on a feedback loop that is considered linear, even though the amplifier nonlinearity limits oscillation amplitude.

On the other hand, certain compensation techniques require feedback loops that are inherently nonlinear and would be classified as a nonlinear feedback loop. The definition of nonlinear feedback loop is given by:

> 2. Nonlinear feedback loop. A nonlinear feedback loop has a circuit function that cannot be characterized by a linear circuit model.

For the linear feedback loops, another distinction can be made. The oscillator circuit may contain gain blocks that contribute no dominant natural frequencies to the system (i.e., no significant charge storage effects). These gain blocks may contain feedback loops to control gain levels. If they do, it is convenient to classify such feedback loops so as to distinguish them from loops that have dominant open-loop poles. Therefore, one may define:

> 3. Gain control feedback. Gain control feedback is used only to control gain levels and contributes no dominant natural frequencies to the system.

The voltage amplifier of a Wien-type oscillator is typically realized as the two transistor series-shunt feedback pair shown in Fig. 2.3. The overall negative feedback loop in the amplifier is classified as gain control feedback.

Feedback loops that are not stated as being gain control or nonlinear in the subsequent work are assumed to be of the remaining

It may appear that there is an anomoly for certain non-minimum phase oscillators. This problem occurs for configurations that produce an odd number of open-loop zeros on the positive real axis. For this case, the dc feedback polarity is the reverse of a minimum phase configuration. If the minimum phase configuration has a positive dc feedback polarity, the non-minimum phase configuration with one zero on the positive real axis has a negative dc feedback polarity. However, it is natural to expect the class of an oscillator not to be changed by this modification of the positions of open-loop zeros. Indeed, under the definition given, the class of an oscillator does not change by moving an odd number of zeros to the right half plane.

As an example, the root locus for the Wien-type oscillator shown in Fig. 1.1 is shown in Fig. 2.6. For this locus, the complex root positions always move on a circle with a center at the zero. This is expressed by the positive feedback angle relation:

$$2\theta_1 - (180-\theta_2) = 0 \qquad (2.6)$$

where θ_1 and θ_2 are indicated on Fig. 2.6. This is the equation for a circle with center at the zero as shown on the figure. This locus is a circle regardless of the position of the zero.

This example extends to the three $j\omega$ axis phase plots for a left half plane, origin, and right half plane open-loop zero shown in Fig. 2.7 respectively. As is seen, the definition classifies the oscillator as a positive feedback type in each case since the root locus is still determined by the same angle condition.

To avoid possible confusion, it is noted that this classification as positive or negative feedback depends on the absolute value of the return difference phase, not its relative value with respect to its base-band value.

2.4 Minimum or Basic Oscillator Realization

In order to determine some of the characteristic properties of the oscillator classes, it is desirable to consider some fundamental configurations of each class. The configurations considered are fundamental in the sense that they are minimum complexity realizations. The fundamental oscillator configurations are called basic oscillators, the definition of which is given by:

> 1. Basic oscillator. A basic oscillator contains no multiple signal paths, multiple feedback loops, or nonlinear feedback loops. It is realized with the minimum number of dominant open-loop poles.

With this definition, the basic oscillator of each class can be considered. It is impossible to achieve a near-harmonic oscillator with a system that has a single natural frequency. A system with two open-loop poles and an open-loop zero to the right of these poles can be made to oscillate with the application of positive feedback. A typical root locus is shown in Fig. 2.6. An oscillator system represented by this root locus is a positive-feedback oscillator. A possible realization in basic form is the Wien-type oscillator of Fig. 1.1.

It also is possible to construct an oscillator that contains only two open-loop poles and obeys the rules of negative feedback. An example of such a two pole, negative feedback configuration has two finite open-loop transmission zeros and the root locus shown in Fig. 2.8(a). The open-loop poles and zeros of the root locus are determined by the circuit element values of the possible corresponding configuration shown in Fig. 2.8(b) where the block A is a differential amplifier with both an inverting and non-inverting output. The normalized circuit values are only used to indicate the possibility of the example. However, by the Fialkow-Gerst relation, this system cannot be obtained by any unbalanced configuration[12]. This is contrary to the condition of the basic oscillator definition and consequently this root locus does not characterize a basic negative feedback oscillator. To achieve a basic negative feedback oscillator, a minimum of three open-loop poles are required.

The basic oscillator definition implies a ladder form of RC driving point imbedding of the gain blocks, so that all the open-loop poles and zeros lie on the negative real axis. This leads to a restriction on the open-loop transmission zeros. In order to produce an oscillation with the application of negative feedback, either all the open-loop zeros must lie to the left of all the open-loop poles, or they must all lie to the right of the open-loop poles. A typical ladder-type realization of the former case is shown in Fig. 2.9 with its accompanying root locus.

In the more general case where the restriction to a basic oscillator is removed, the condition pointed out Howard exist[13]. The

positive feedback oscillator requires an odd number of poles and zeros to the right of the pair producing harmonic oscillation and the negative feedback oscillator requires an even number of poles and zeros to the right of the pair producing harmonic oscillation. In monolithic realizations where dc blocking capacitors are not permitted, Howard points out that designs should be selected that do not have positive feedback at dc to prevent possible resultant bias instability. This condition implies either negative feedback at dc or an open-loop transmission zero at the origin.

2.5 Basic Positive Feedback Oscillators

In general, a linear, time-invariant model of a feedback oscillator can be represented by the block diagram shown in Fig. 2.10. The blocks are assumed to be unilateral, have no interaction, and have transfer functions which are rational functions in s. If the input variable is x_{in} and the output variable is x_o, the closed-loop transfer function is

$$T(s) = \frac{x_o(s)}{x_{in}(s)} = \frac{H(s)}{1 + H(s)G(s)} \tag{2.7}$$

where $H(s)G(s) = N(s)$ and $N(s)$ is given by Eq. 2.3. If $H(s)$ and $G(s)$ are given by

$$H(s) = \frac{H_N(s)}{H_D(s)}$$
$$G(s) = \frac{G_N(s)}{G_D(s)} \tag{2.8}$$

where the subscripted terms are polynomials in s,

$$N(s) = H_N(s)G_D(s) \tag{2.9a}$$

$$D(s) = H_D(s)G_D(s) + H_N(s)G_N(s) \tag{2.9b}$$

The closed-loop poles are given by the zeros of D(s). The closed-loop root locus for positive feedback is specified by

$$\text{Arg } [H(s)G(s)] = 2n\pi \qquad n = 1,2,... \tag{2.10}$$

The closed-loop pole positions on the root locus are determined by the loop gain and satisfy the relation

$$|H(s)G(s)| = 1 \tag{2.11}$$

For analysis of the basic positive feedback oscillator system, the simple Wien-type configuration is considered. The final form of the transfer function is independent of whether the current amplifier or voltage amplifier configuration of Fig. 2.11 is considered. For the basic system, the open-loop zero occurs at the origin due to the series capacitor in the feedback loop. For both configurations, the idealized linear closed-loop system equation, which is given general form by Eq. 2.7, about the quiescent operating point is

$$T = \frac{A}{1 - \frac{A_s}{R_1 C_2} \Big/ [s^2 + (\frac{1}{R_1 C_1} + \frac{1}{R_2 C_2} + \frac{1}{R_1 C_2})s + \frac{1}{R_1 R_2 C_1 C_2}]} \qquad (2.12)$$

For oscillation, the starting condition requires

$$A \geq 1 + \frac{R_1}{R_2} + \frac{C_2}{C_1} \qquad (2.13)$$

When the equality is satisfied, the oscillation is harmonic and the frequency of oscillation is given by

$$\omega_o^2 = \frac{1}{R_1 R_2 C_1 C_2} \qquad (2.14)$$

Because of the nature of charge-control devices, a positive feedback oscillator without transformers cannot be realized with a single device. Moreover, the configurations discussed here are based on npn bipolar transistors (BJT). Configurations requiring complimentary pnp transistors are not considered because of the difficulty in realizing complimentary structures in monolithic circuits.

Howard obtained all possible two transistor positive feedback oscillators with RC one-port imbedding[14]. He mentions a difference between driving point and transfer function imbedding. This distinction was necessary for his derivation which was based on driving point

realization of the imbedding. The form of the imbedding required depends on the zero location of the transfer function. Driving-point imbedding can be used when the zeros of transmission of the transfer function lie on the negative real axis.

Howard's configurations are based on the controlled resistance model of bistable circuits by Hill, Pederson, and Pepper[15]. Howard's method of obtaining the possible RC oscillator configurations is based on an ac model and does not directly include biasing considerations of monolithic realizations. An alternate approach is used in this thesis to obtain positive feedback oscillator configurations and is based on the basic oscillator. The oscillator is realized as either an interacting pole configuration or a non-interacting pole configuration.

When each of the open-loop poles of a feedback system is produced by an independent RC product, the poles are said to be non-interacting. This must be true irrespective of where the loop is opened. Interacting poles occur when a resistance or capacitance value appears in more than one RC product. As an example, the Wien-type oscillators considered to this point have interacting poles. For the basic positive feedback oscillator, minimum total gain to produce harmonic oscillation is achieved for non-interacting poles. This requires that the RC elements producing each of the poles be separated by unilateral gain blocks. This requirement is the basis for obtaining two transistor, non-interacting pole, basic positive feedback oscillator configurations.

For the basic oscillator, a series capacitor is contained in the positive feedback loop to produce a transmission zero at the origin and prevent positive feedback at dc. If a single resistance and capacitance produce each pole, sixteen configurations are possible. Six examples are shown in Fig. 2.12. Approximate voltage gain, current gain, transimpedance, and transadmittance circuits are shown in Fig. 2.13. The voltage and current gain circuits have a gain that is approximately the ratio of a load resistance and a feedback resistance. The transimpedance and transadmittance circuits have a transfer value that depends approximately on a single feedback resistance value. These circuits are used to complete the realization of the two transistor oscillator configurations.

It is also possible to obtain non-interacting pole oscillator realizations with a resistor and capacitor in the emitter lead of a transistor. These realizations are not considered because the appearance of transistor parameters in the RC product determining the open-loop pole position is deamed undesirable.

In the other case, the system has interacting open-loop poles and isolation of RC pairs producing the poles is not permitted. Thus, the system with inter-acting open-loop poles contains a single gain block. In the single gain block, gain control feedback usually is used to make the gain function independent of transistor parameters. For the two transistor gain blocks considered here, the gain control feedback can be applied individually to each transistor or as an overall feedback loop. For example, in the current amplifier gain

block which is realized as a shunt-series pair, the feedback may be local as shown in Fig. 2.14a or it may be overall as shown in Fig. 2.14b.

The basic oscillator configurations are obtained by placing the single active gain glock with negligible charge storage effects in RC imbedding as shown in Fig. 2.15. With these configurations, the RC transfer function still should have a zero of transmission at the origin to prevent positive DC feedback. Again, the gain block can have one of four forms. If the gain block is a voltage or current amplifier, the RC transfer function for the positive feedback oscillator is of the form

$$T_{V,I} = \frac{\frac{s}{R_1C_1}}{s^2 + \left(\frac{1}{R_1C_1} + \frac{1}{R_2C_2} + \frac{1}{R_1C_2}\right)s + \frac{1}{R_1R_2C_1C_2}} \qquad (2.15)$$

If the gain block is a transconductance or transresistance, the form of the denominator remains the same. The numerator still has a zero at the origin, but is dimensionally modified so the overall open-loop transfer function is dimensionless. For example, if the gain block is transconductance, the proper form of the RC transfer function is a transimpedance.

The topology of the network depends on the type of RC transfer function being realized, and is fixed as either a T, π, or L configuration. In each case, two physical realizations of the transfer function

are possible. If the network is the L configuration used with the voltage or current amplifier, the two physical realizations are identical except for the trivial reversal of the physical locations of resistor and capacitor in the series feedback pair. If a transimpedance is being realized, a π topology is required and the two possible physical realizations are shown in Fig. 2.16.

A typical final circuit based on the current amplifier with overall gain control feedback and the L topology for the RC network is shown in Fig. 2.17. This circuit is realizable in monolithic form and is the basic circuit for two of the oscillators actually realized in Chapter V.

Another positive feedback oscillator design that has interacting poles and has not been mentioned contains one of the dominant poles in the gain block. For the current amplifier, Wien-type oscillator of the above example, the modified oscillator is constructed by removing the shunt feedback capacitance C_2 and placing it in the gain control feedback loop as shown in Fig. 2.4. However, the internal feedback loop can no longer be calssified as a gain control feedback loop. Even though this oscillator is a multiloop configuration and no longer of basic form by the definition, it is a natural extension of this development and is included here as a fundamental form.

That this form is not a fundamental departure from basic forms can be seen from physical reasoning. To a first order, the shunt capacitor in the negative feedback loop can be placed from the base

to the collector of the input transistor without modifying the circuit performance. Since the input stage has voltage gain, this circuit is equivalent to a capacitor shunting the input transistor base to ground with a value multiplied by the voltage gain of the input transistor. In this equivalent form, the oscillator would classify as a basic oscillator.

If a hybrid π model of the intrinsic base region of the transistor is used in the analysis and the admittance in the positive and negative feedback loops of the oscillator are not specified as to configuration, the oscillator circuit model shown in Fig. 2.18 can be considered. The node equations may be used to analyze the circuit of Fig. 2.18. In terms of this equation, the closed-loop transfer function between the input node and the output node is of the form:

$$Z_{21} = \frac{V_o}{I_i} = \frac{\Delta_{12}}{\Delta} \tag{2.16}$$

where Δ is the determinant of the nodal admittance matrix and Δ_{12} is the cofactor of the matrix element in the first row and second column. The natural frequencies of the system are given by the zeros of Δ.

For the circuit of Fig. 2.18, the determinant has been calculated in complete form to avoid possible errors caused by initial cancellation of apparently nondominant terms. The determinant has a dominant term that is at least an order of magnitude larger than

any other term. After appropriate cancellation, the dominant term is

$$\Delta(s) = g_{m1}g_{m2}(Y_RY_E - Y_LY_F) + \ldots \qquad (2.17)$$

where the admittances are those shown in Fig. 2.18. All subsequent terms are of order $1/\beta_o$ or $1/\beta_o^2$ of this term and contribute only a few percent to the dominant term*. Harmonic oscillation is achieved when this term has a pair of pure imaginary zeros. The admittance Y_R is chosen to contain a series capacitor to prevent positive feedback at dc. In order to obtain the imaginary pair of natural frequencies, Y_L or Y_F must contain a parallel RC pair. These two cases are those previously shown in Figs. 2.4 and 2.17. The circuit in Fig. 2.17 has been realized in monolithic form. The experimental description of this realization is contained in Chapter 5.

2.6 Negative Feedback Oscillator

The basic negative feedback oscillator can be represented by the same block diagram and closed-loop transfer function as the positive feedback oscillator. This representation is shown in Fig. 2.10 and expressed by Eq. 2.7 of the previous section. The negative feedback oscillator is different from the positive feedback oscillator in the angle condition that specifies the root locus. For

---

* The result of Eq. 2.17 is confirmed by a first order analysis of the positive feedback loop for this circuit which has an open-loop transfer of Y_RY_E/Y_LY_F. Thus, the denominator of the closed loop transfer function is $Y_LY_F - Y_RY_E$.

the negative feedback oscillator, the root locus is given by equation

$$\text{Arg } [H(s)G(s)] = (2n+1)\pi \qquad n = 1,2,... \tag{2.18}$$

which differs from positive feedback by the angle π. The closed-loop pole position on the root locus still satisfies the magnitude condition

$$|H(s)G(s)| = 1 \tag{2.19}$$

In contrast to the positive feedback oscillator, the basic negative feedback oscillator can be realized with a single transistor. An arbitrary numerical example to show this is the ladder configuration shown in Fig. 2.19. The open-loop transfer function for this configuration is

$$T_r = \frac{V_o}{V_{in}} = \frac{G^2 g_m}{C^3S^3 + 4.2C^2GS^2 + 3.61G^2CS + .21G^3} \tag{2.20}$$

The starting condition is satisfied for $g_m = 14.952$ mhos and the harmonic frequency of oscillation is

$$\omega_o = \frac{3.61G}{C} \tag{2.21}$$

A possible circuit for $G = 10^3$ mhos and $\beta_o = 150$ is shown in Fig. 2.20.

The ladder-type realization with all of the zeros at infinity has a minimum overall starting gain of 8 when the three poles are equal. This can only be accomplished for the case of non-interacting poles which require a realization of the form of Fig. 2.21. The overall gain requirement for equal R's and C's is

$$A_T = A_{v_1} A_{v_2} A_{v_3} = 8 \tag{2.22}$$

With additional gain elements allowed for isolation of poles, the total number of configurations possible is greatly increased. These are not enumerated here but can be developed by the same techniques used for positive feedback oscillators. It is noted that any given root locus may have several realizations.

2.7 Nondominant Effects

In addition to the intended natural frequencies of the system, there are natural frequencies produced by parasitics and active device charge storage. Models of both field effect and bipolar transistors that include charge storage effects of the intrinsic transistor region and extrinsic effects such as junction capacitances are adequately described in the literature[16,17].

Integrated transistors made in our laboratory have another consideration not normally needed in the usual transistor models. Because of the lack of buried layer technology, the transistors realized have considerable collector series resistance[18]. It is

usually on the order of 500 ohms. The integrated transistor also has on the order of 5 pF collector to substrate capacitance at V_{rev} = 5 volts. These effects reduce the current at which saturation occurs and lowers the cutoff frequency respectively. A modified transistor model to include these effects is shown in Fig. 2.22. In this model, y_{π}, y_{μ}, and g_m are the usual hybrid π parameters modeling the intrinsic base region of the transistor. The series base resistance is r_x and the series collector resistance is r'_c. C_o is the collector to subdiode capacitance.

The effects of base-width modulation also can be of significant importance in a circuit design. A large base width modulation causes a small transistor output resistance r_o. If the transistor has a large collector load impedance, base width modulation effects can cause a significant reduction in gain. Experience in our laboratory has shown that shallow transistor structures show a marked decrease in base width modulation over deep structures for equivalent short-circuit current gains and, thus, that this effect can be minimized.

Resistors are typically realized with p-type base diffusions into the n-type epitaxial layer. These resistors are actually RC transmission lines. However, for the dimensions of resistors and frequencies considered here, these distributed effects are not significant and the resistors behave as lumped elements. A further discussion of this point is provided by Hodges[19].

The effects of the nondominant poles depend upon the circuit use and configuration. The problem often encountered is a modifica-

tion of the root locus that produces outband peaking. These nondominant natural frequencies may cause the oscillator to break into parasitic oscillation. A Wien-type oscillator may exhibit parasitic oscillation due to nondominant natural frequencies as shown in Fig. 2.23. This root locus is determined by a computer-aided analysis of the linearized system model that included charge storage effects. If the nondominant natural frequencies are removed by more than an order of magnitude from the dominant natural frequencies, their effect on the dominant portion of the root locus is proportionally small. Therefore, an analysis based on the dominant portion of the root locus alone may be completely adequate. The experimental results of Chapter 5 indicate that this is the case for the oscillators considered here. However, if a higher frequency of oscillation is considered, these nondominant effects may not remain insignificant. In this case, their effect must be included in the design.

2.8 Allowable Elements and Tolerances

Because of the physical limitations of a monolithic realization, there are definite restrictions on allowable elements. These restrictions are of two types. First, the various devices in a monolithic realization must be compatible. There must be no conflicting processing requirements for the circuit elements to be realized. For example, at the present time in our laboratory, it is difficult to obtain good bipolar transistors and junction field effect transistors

in the same circuit[20].

The other restriction has to do with the total available area for the circuit realization. The total circuit resistance, capacitance, and circuit complexity are limited by the area required per unit resistance and capacitance as well as the total number of active devices required. The circuit area required for a given design depends on the amount of resistance and capacitance that can be obtained per unit area and the area required to realize an active device. These limitations usually are imposed by the facilities available.

The effective usage of circuit area on the monolithic chip depends to some degree on the initial ruby-lith mask accuracy, the resolution maintained to the final mask and the final mask alingment accuracy. The Motorola text contains a discussion of the fabrication requirements[21]. This laboratory can yield satisfactory results with 1/2 mil (10^{-3} in) line widths and 1 mil spacing. MOS capacitance per unit area depends on oxide thickness, as does the yield. Good results have not been obtained for thicknesses less than 1500 $\mathring{A}$.

An approximate empirical formula for the total area required by a realization in this laboratory is given by

$$A_{total} = 5C_T + 4R_T + 100N_{BJT} + A_I$$

where A_I is the area used by isolation in square mils and is dependent on circuit design and layout. C_T is given as total capacitance

in picofarads, R_T is total resistance in kilohms, and N_{BJT} is the number of bipolar transistors required. For example, if a circuit for a Wien oscillator requires 2 bipolar transistors, 400 pF of capacitance, 15kΩ of resistance, and 100 square mils of isolation, at least 2360 square mils of area are required.

A point of interest is the minimum frequency of oscillation that can be obtained for the realization of a given configuration with a specific circuit area*. For example, the minimum frequency of oscillation for a Wien-type basic oscillator occurs for equal R's and equal C's for fixed total resistance and capacitance[23]. In this case the frequency is given by

$$f_o = \frac{1}{2\pi RC}$$

The use of chip area for realizing resistance and capacitance to give the minimum frequency of oscillation under this constraint is obtained by setting the total differential of frequency equal to zero:

$$df = \frac{\partial f}{\partial R} d + \frac{\partial f}{\partial C} dc$$

This gives the ratio of capacitance to resistance to achieve minimum oscillation frequency. For a typical 70 by 70 mil circuit area, A_{total} equals 4900 square mils. If the realization requires 10 kΩ

---

* Pinch-effect resistors are not considered[22].

bias circuit resistance and two bipolar transistor, the minimum frequency by the above derivation is approximately 2.4 kHz. In actual circuit designs,where there may be additional complexity and additional oxide thickness is used to raise capacitor yields, a reasonable design frequency is of the order of 100 kHz. This frequency is low enough to avoid the effects of parasitic natural frequencies which occur at a few megahertz for circuits realized in this laboratory.

2.9 Operating Point Considerations

It is often desirable to design circuits that do not depend critically on operating point. This is usually accomplished by designing transfer functions that depend on the values of ratios of resistors. However, circuits can be successfully designed that depend on the operating point. One such circuit is the compensated selective amplifier by Gaash that depends on a transistor transconductance g_m[24].

One circuit of potential interest in subsequent chapters requires accurate bias control. It provides a voltage transfer function with a controlled nonlinearity. For the example cited below, the operating point must be controlled so that the collector voltage of the transistor is exactly 1/2 the supply voltage and is temperature insensitive. The biasing circuit to accomplish this is a direct adaptation of Widlar's scheme[25]. Wildar's circuit to control the operating point accurately is shown in Fig. 2.24a with values

chosen so that V_{CE} is one half of V_{CC}. This produces an approximately symmetric nonlinearity in the transfer function as also shown in Fig. 2.24(b). This nonlinearity can be modified by the inclusion of the diode network shown in Fig. 2.25 to achieve the symmetrically shaped nonlinear gain characteristic shown in Fig. 2.26. The application of this circuit to the nonlinear compensation of transfer oscillators is discussed in Chapter 3.

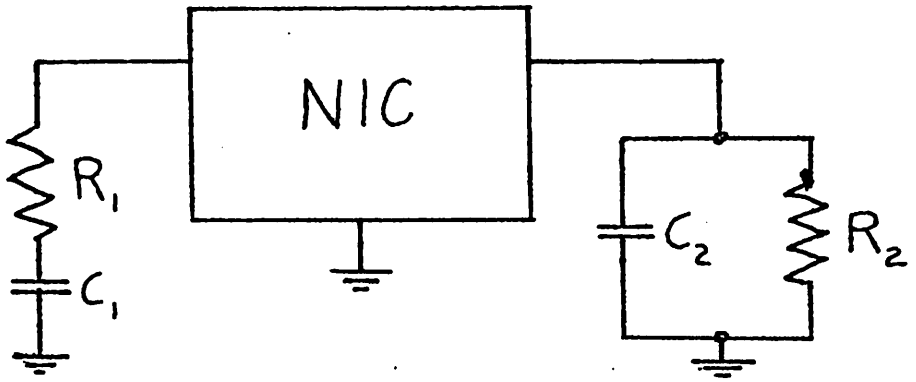

Fig. 2.1 Negative Impedance Converter Oscillator

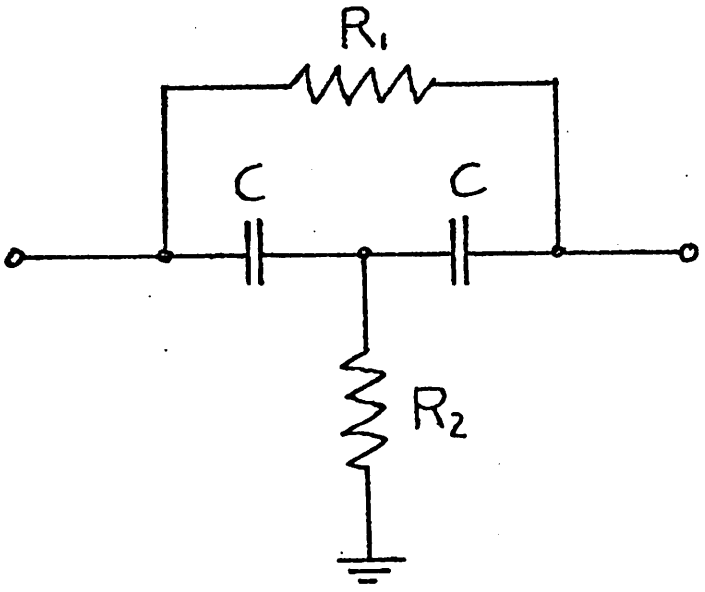

Fig. 2.2 Bridged-T Network

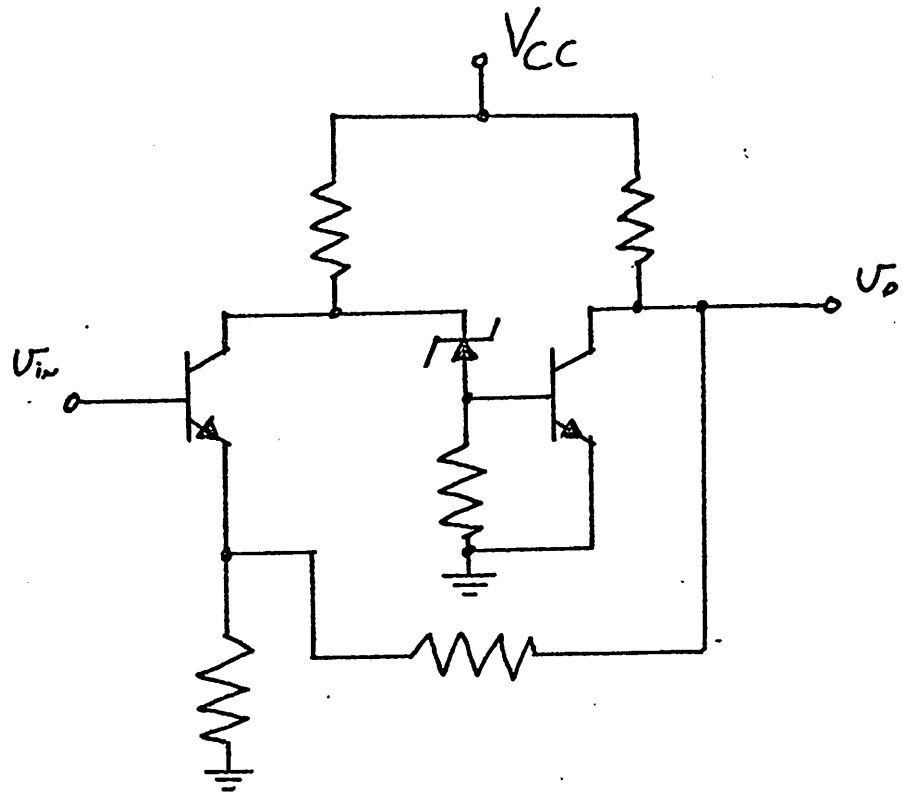

Fig. 2.3 Voltage Amplifier for Wien-type Oscillator

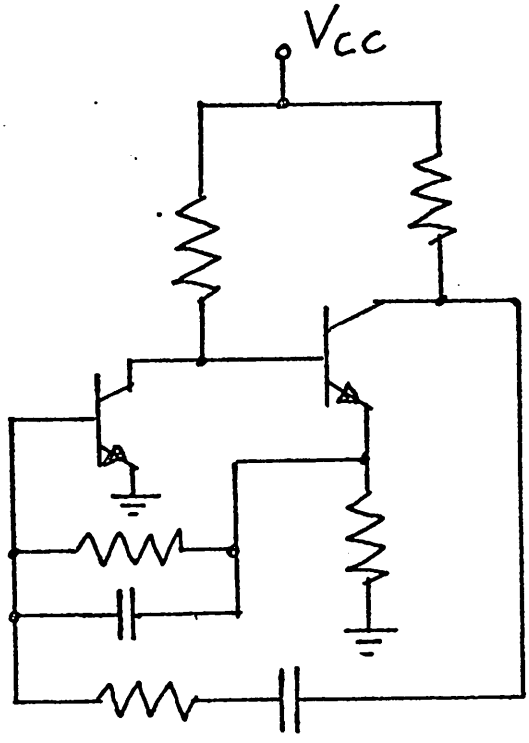

Fig. 2.4 Modifier Wien-type Oscillator

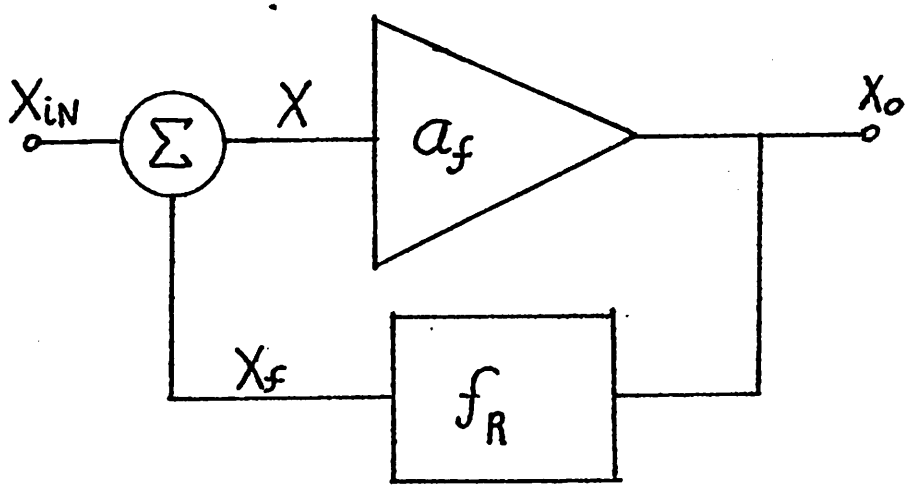

Fig. 2.5 Oscillator Classification Test

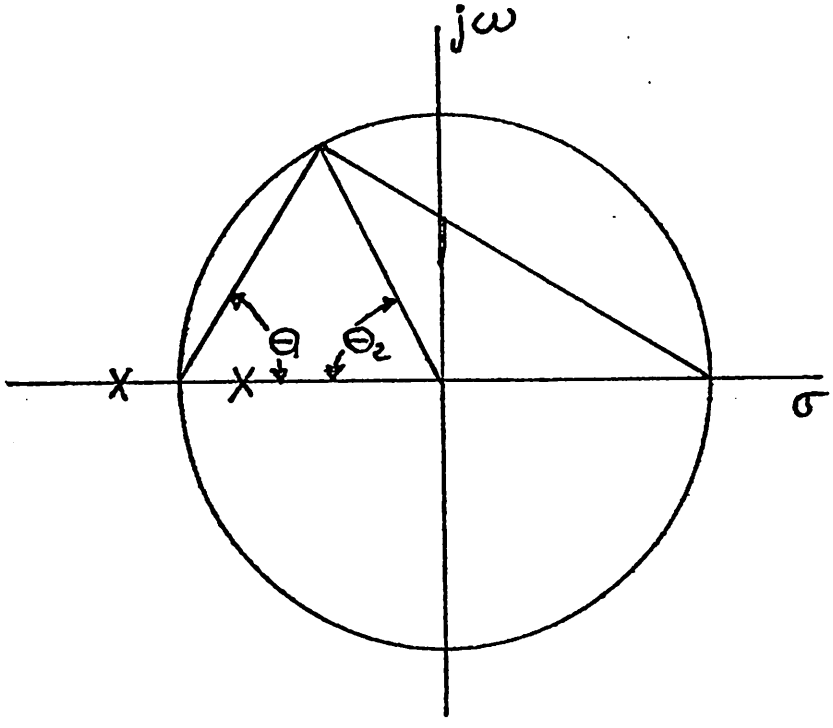

Fig. 2.6 Current Amplifier, Wien-type Oscillator Root Locus

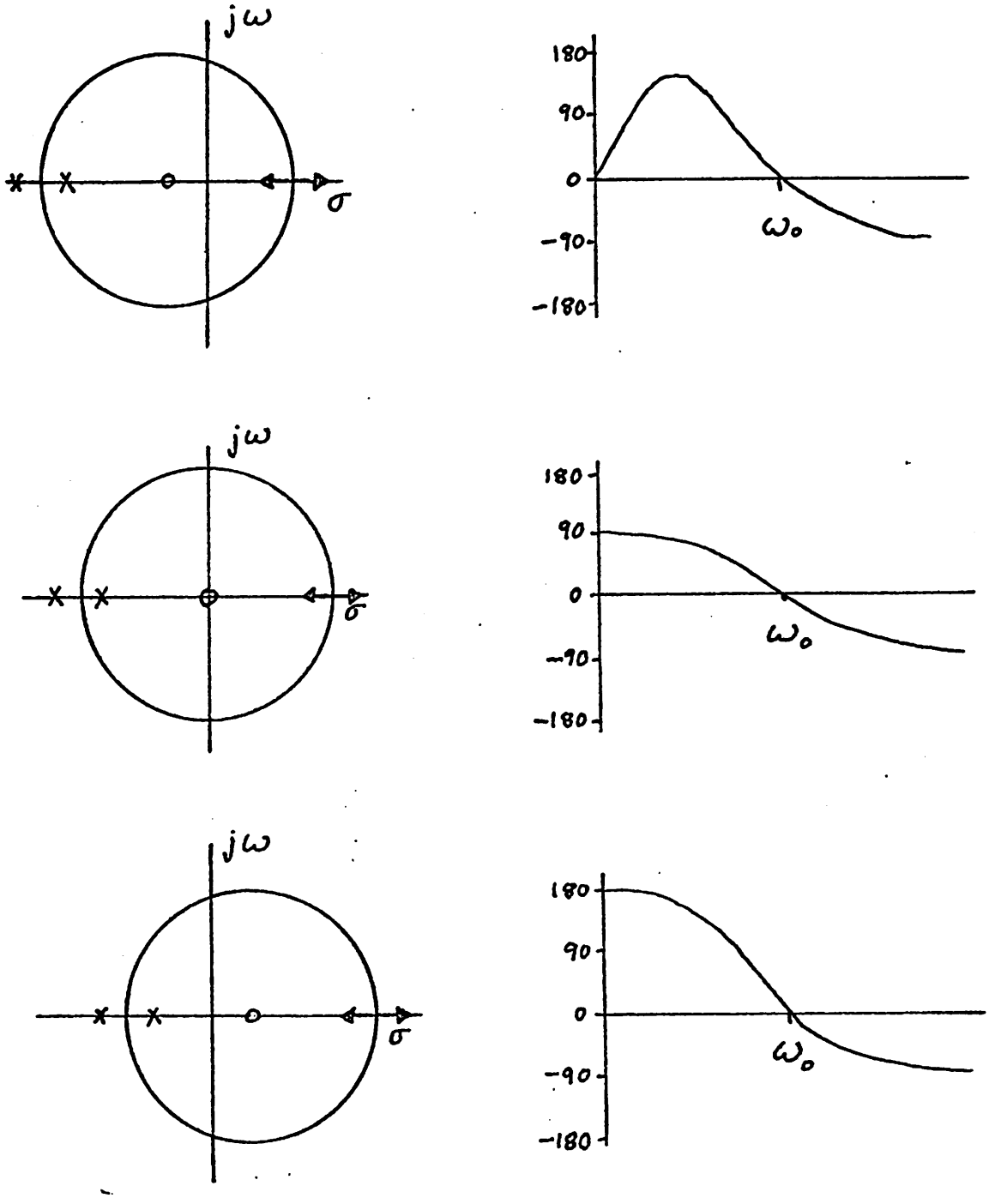

(a) Root Locus

(b) Return Difference Phase

Fig. 2.7 Wien-type Oscillators for Different Open-loop Transmission Zeros

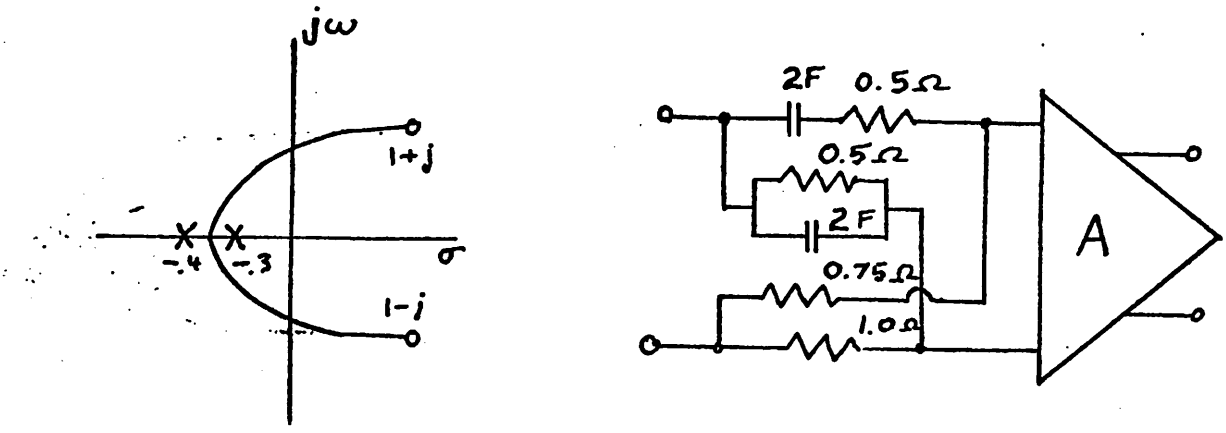

(a) Root Locus (b) Circuit Configuration

Fig. 2.8 Two Pole, Negative Feedback Oscillator

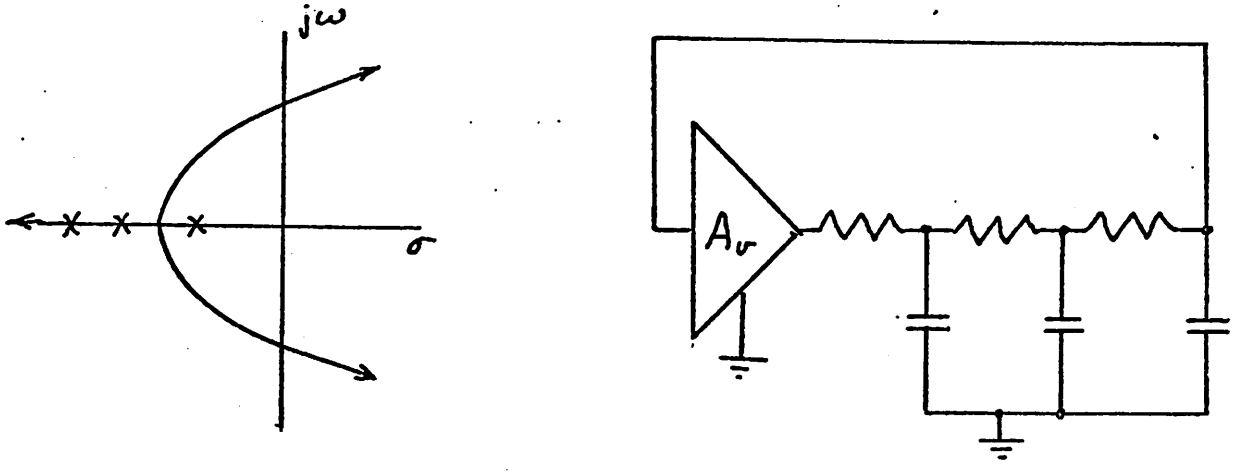

(a) Root Locus (b) Circuit Configuration

Fig. 2.9 Basic Negative Feedback Oscillator

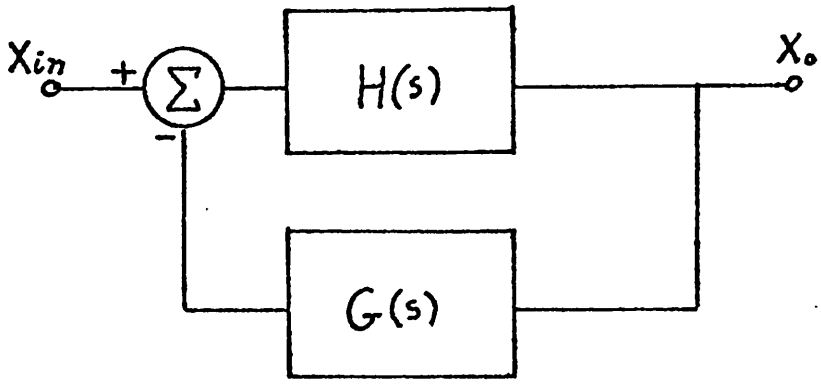

Fig. 2.10 General Feedback System

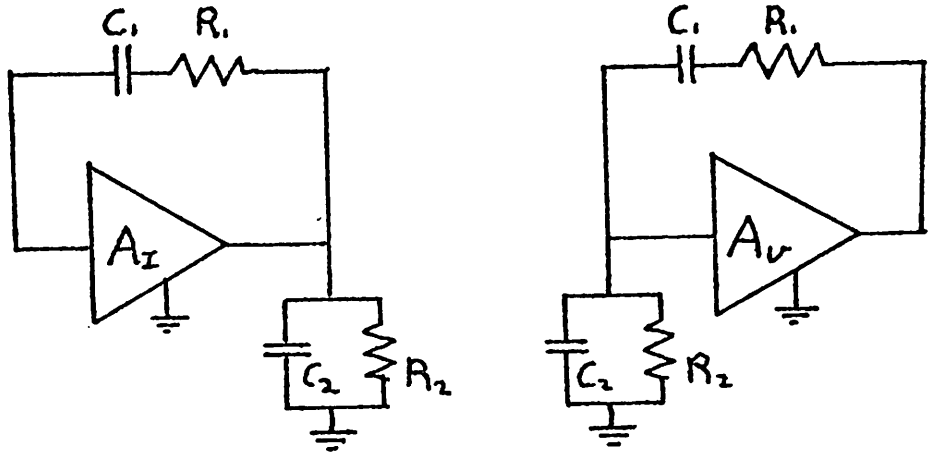

(a) Current Type (b) Voltage Type

Fig. 2.11 Current Amplifier and Voltage Amplifier Wien-type Oscillators

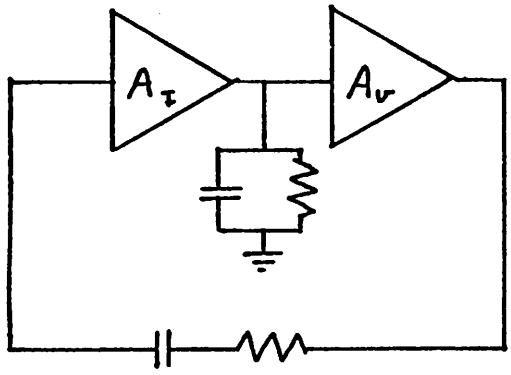

(a)

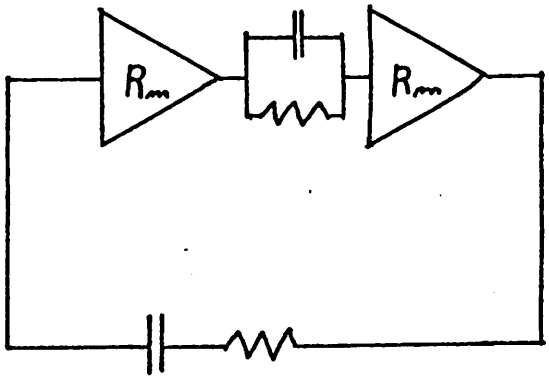

(d)

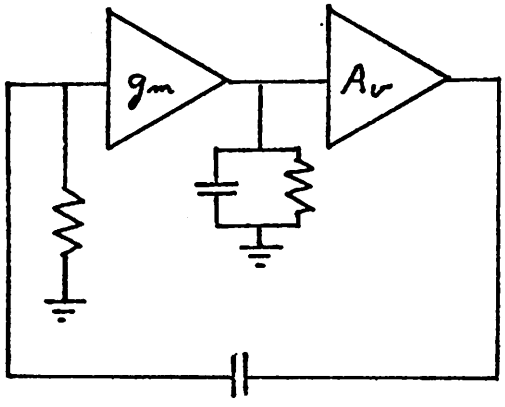

(b)

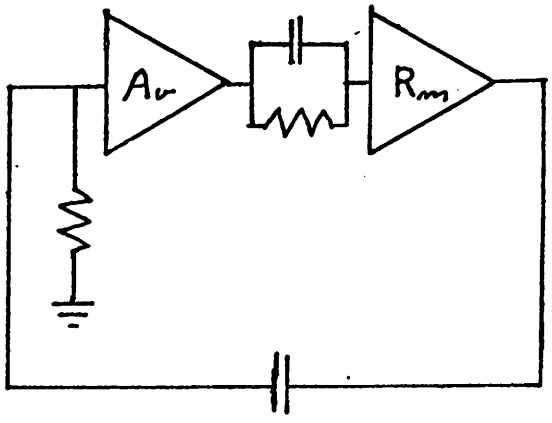

(e)

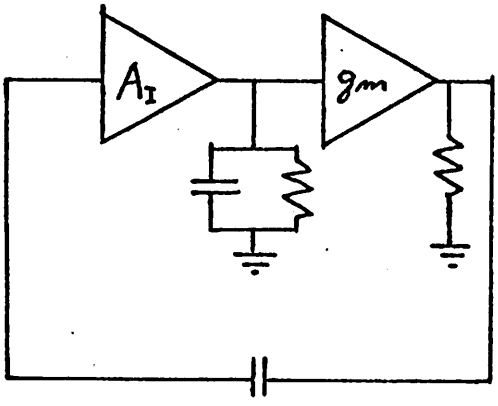

(c)

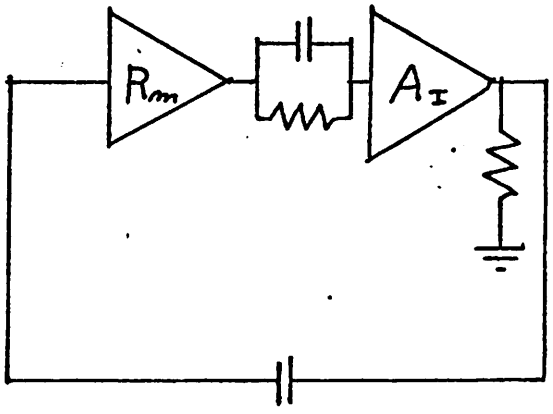

(f)

Fig. 2.12 Basic Positive Feedback Oscillators, Non-interacting Poles, 6 Examples

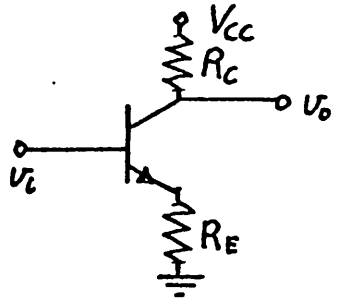

(a) $V_o \approx \frac{R_C}{R_E} V_i$

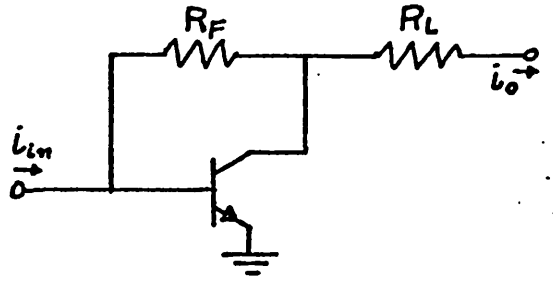

(b) $I_o \approx \frac{R_F}{R_L} I_i$

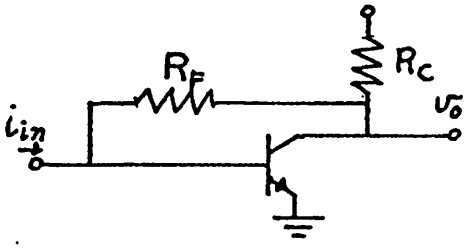

(c) $V_o \approx R_f I_{in}$

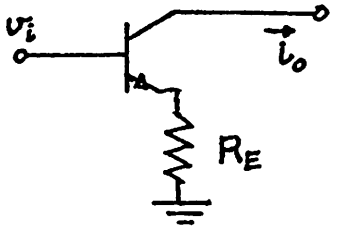

(d) $I_o \approx \frac{1}{R_E} V_i$

Fig. 2.13 Transfer Function Approximate Realization

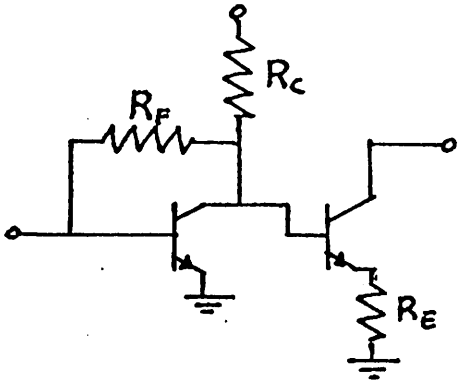

(a) Local Feedback

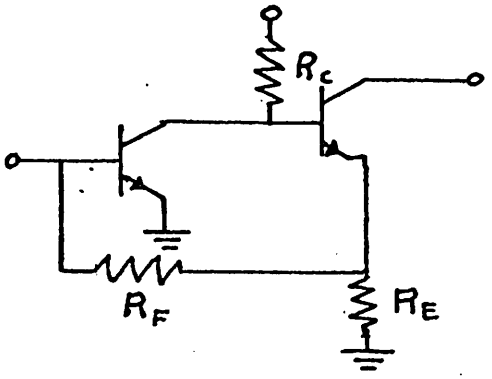

(b) Overall Feedback

Fig. 2.14 Current Amplifiers, Shunt-Series Pair

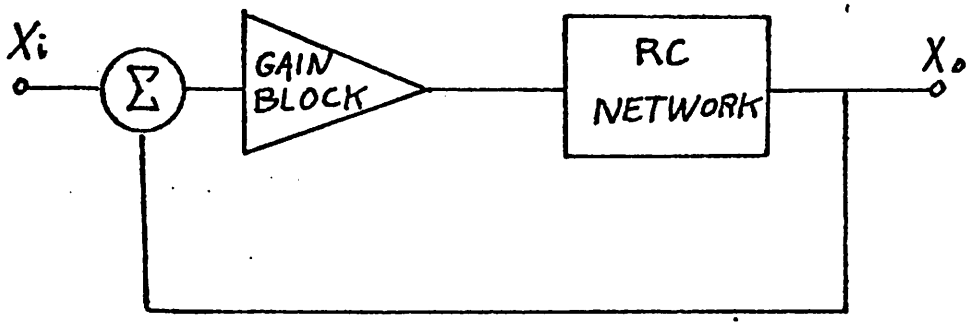

Fig. 2.15 Basic Positive Feedback Oscillator, General Model for Interaction, Poles

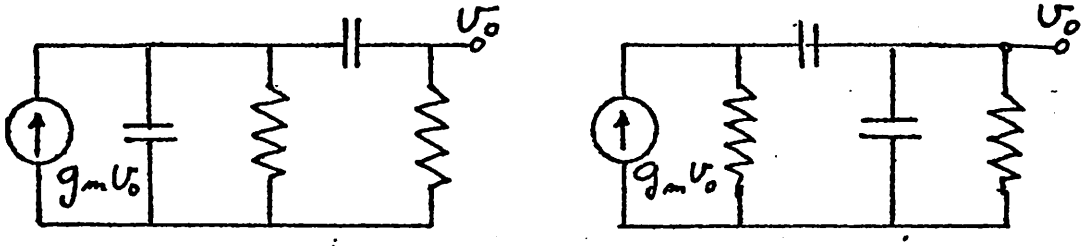

(a) Circuit #1

(b) Circuit #2

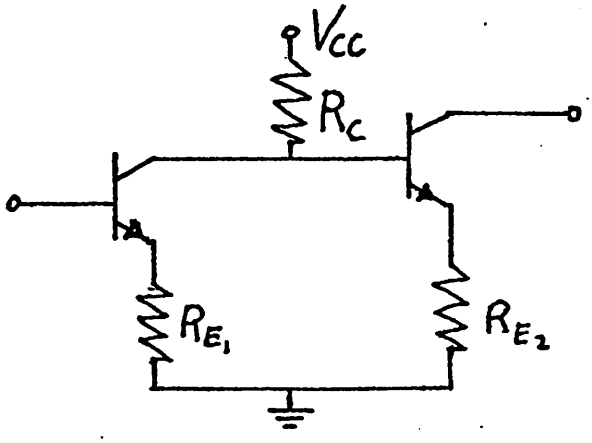

(c) Approximate g_m Realization

Fig. 2.16 Transconductance Positive Feedback Oscillators

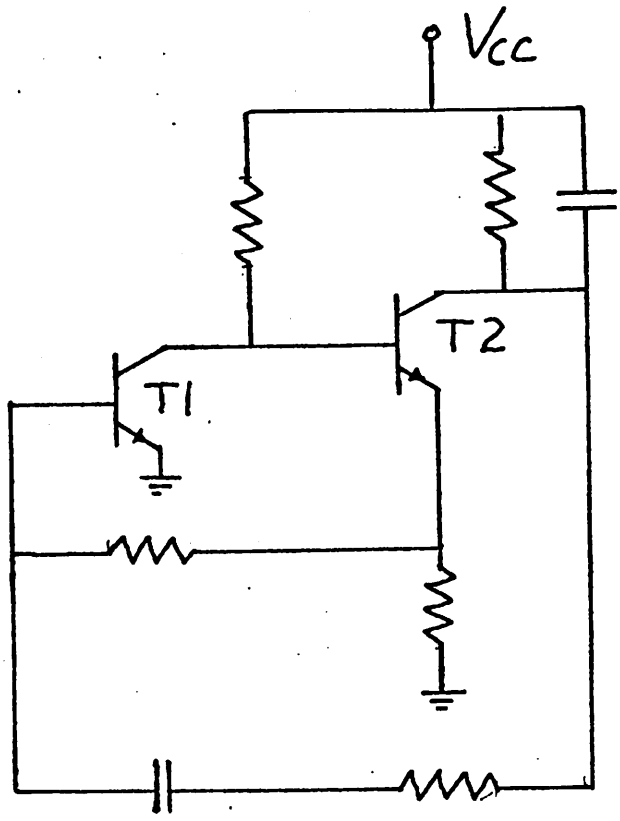

Fig. 2.17 Current Amplifier Wien-type Oscillator

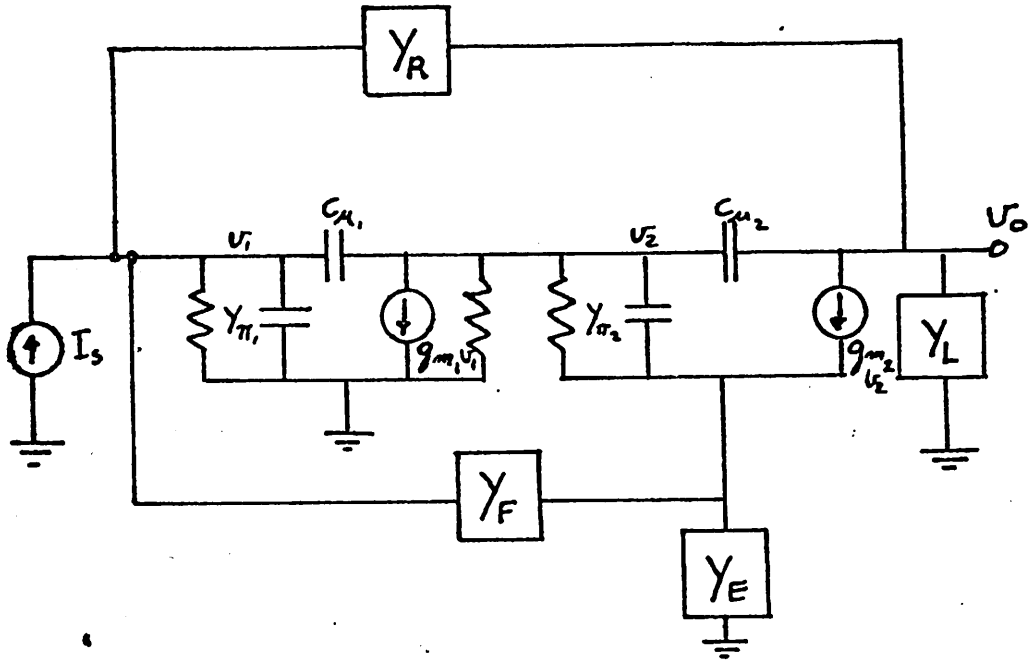

Fig. 2.18 Circuit Model of Oscillator

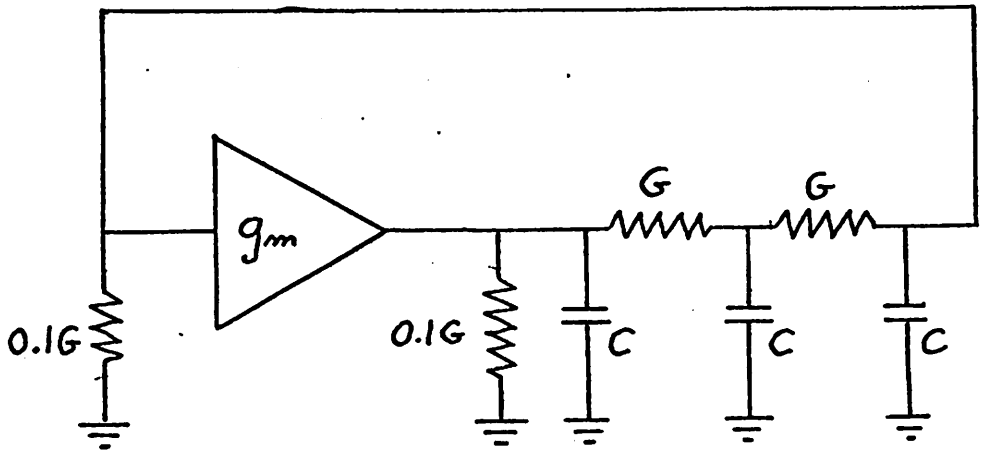

Fig. 2.19 Negative Feedback Oscillator

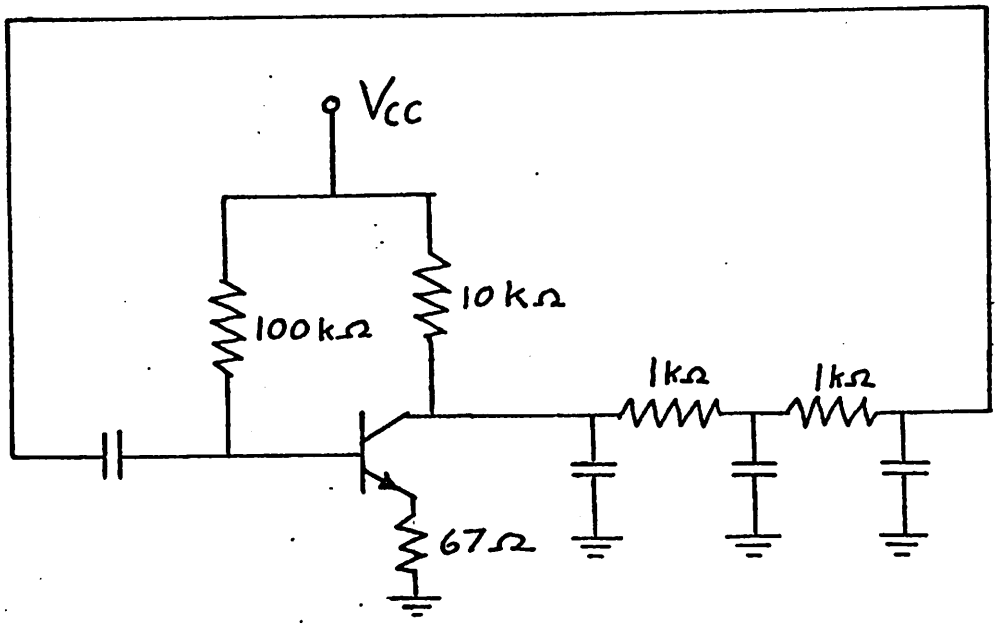

Fig. 2.20 Circuit Diagram of Negative Feedback Oscillator

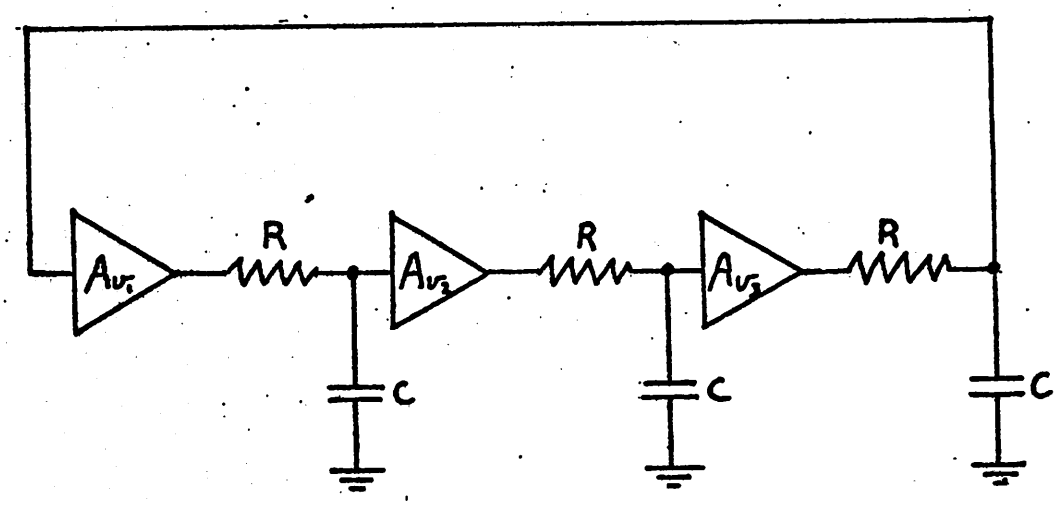

Fig. 2.21 Minimum Gain Ladder-type Negative Feedback Oscillator

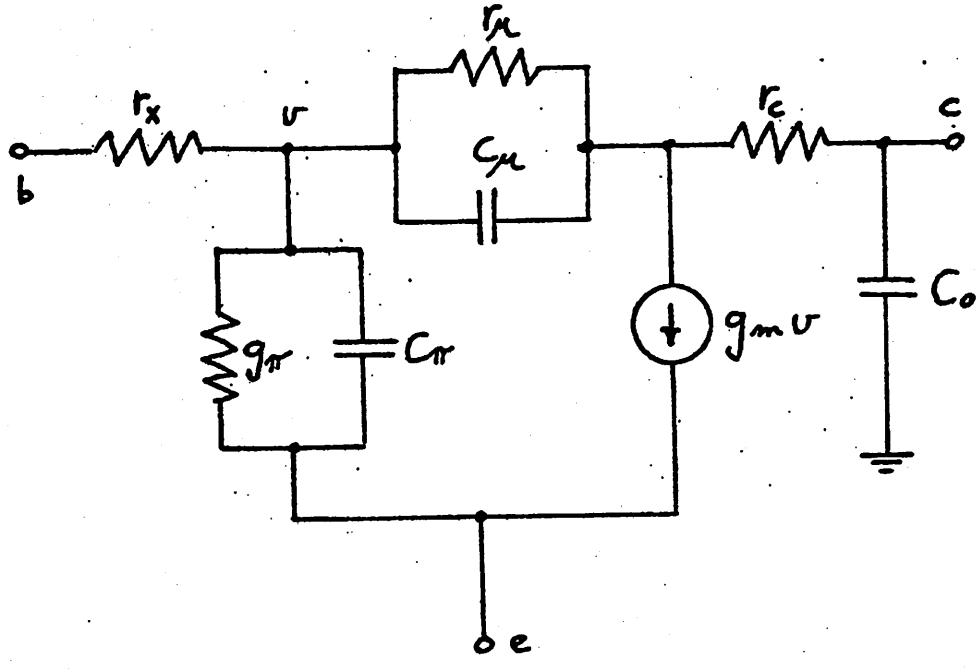

Fig. 2.22 Integrated Circuit Transistor Model

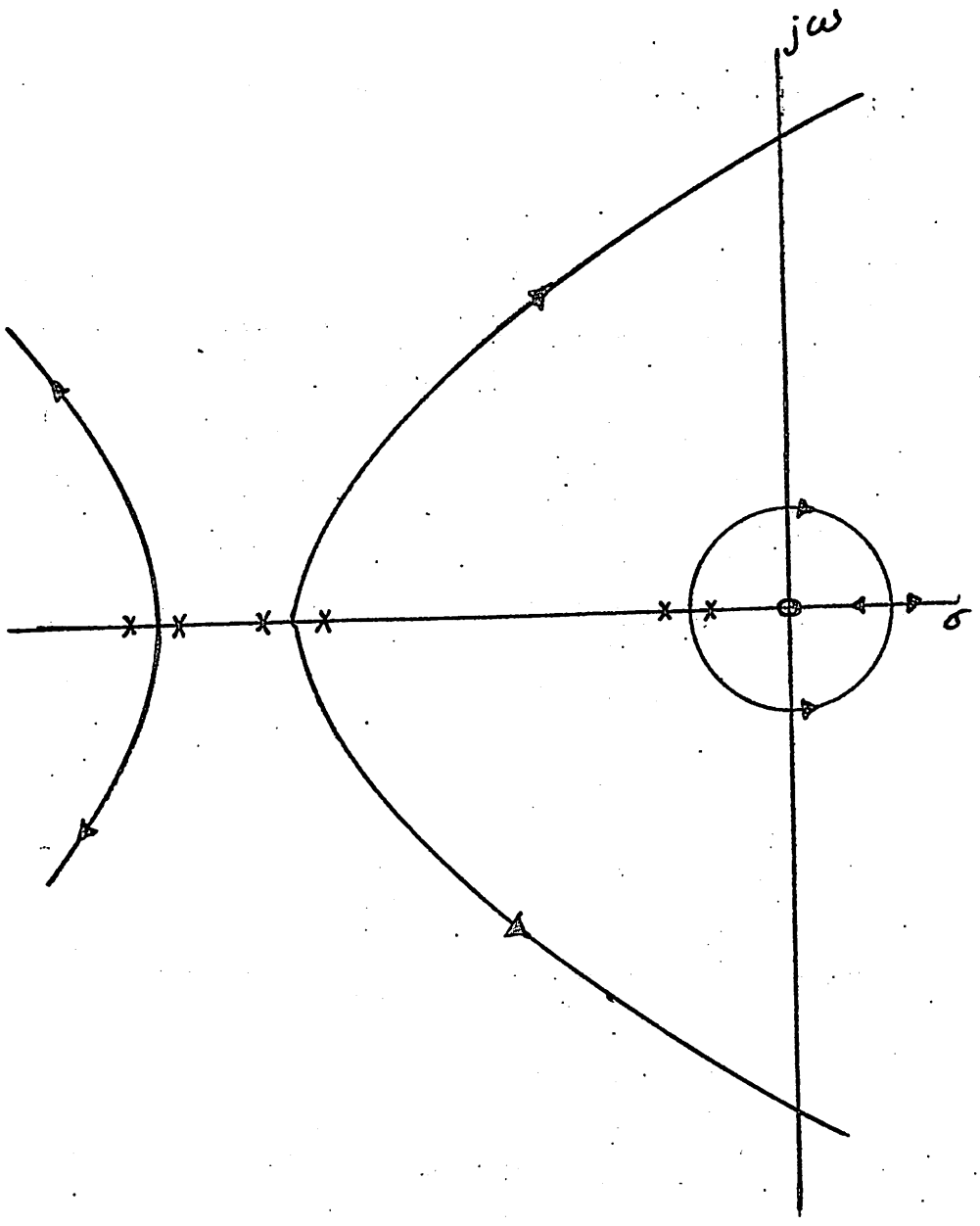

Fig. 2.23 Outbound Peaking due to Parasitics, Overall Root Locus

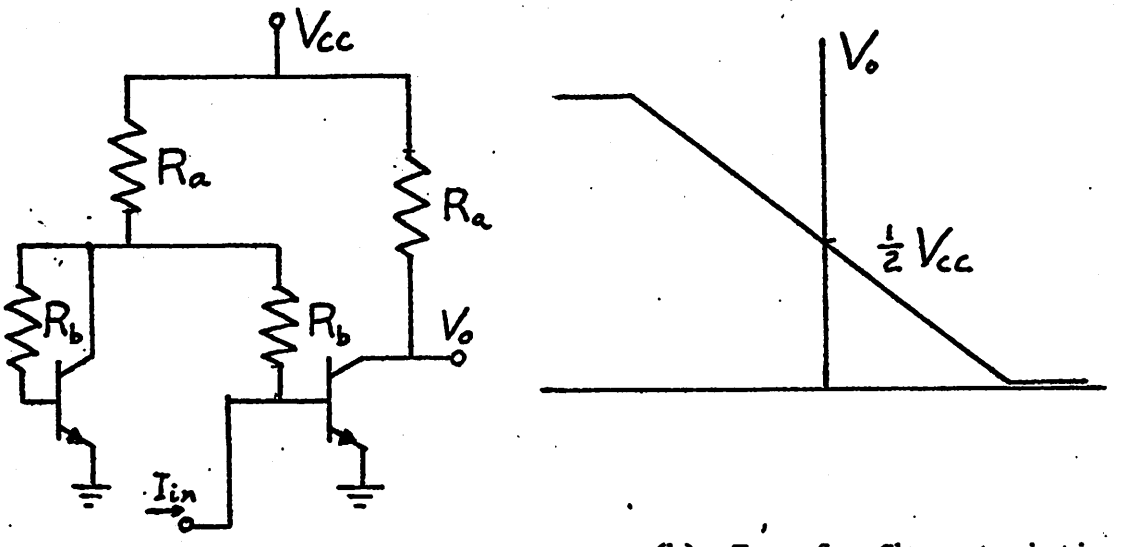

(a) Amplifier

(b) Transfer Characteristic

Fig. 2.24 Amplifier and Approximate Transfer Characteristic

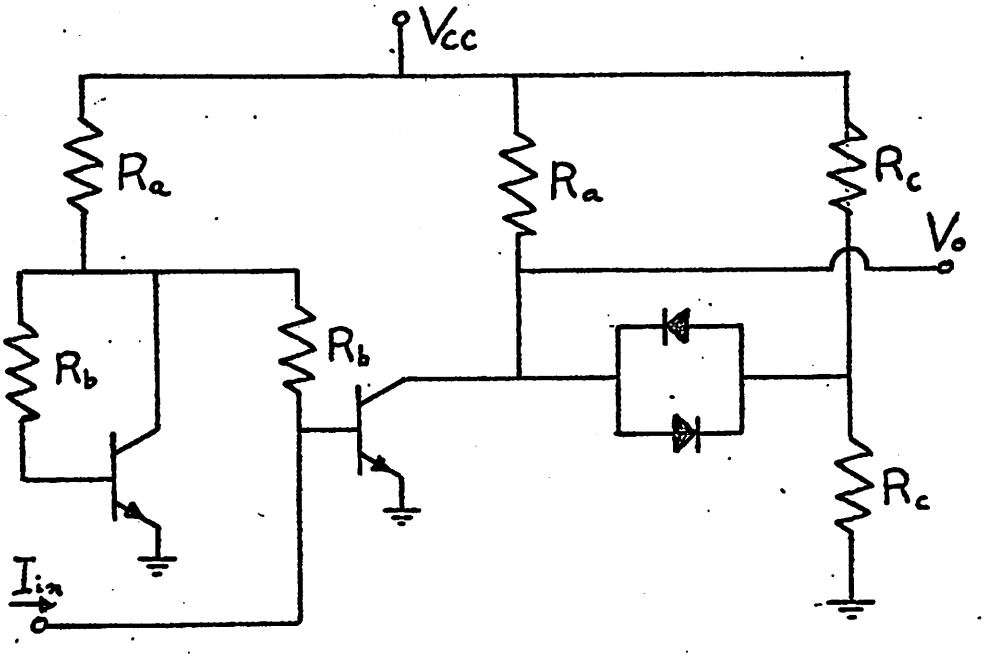

Fig. 2.25 Amplifier for Modified Transfer Characteristic

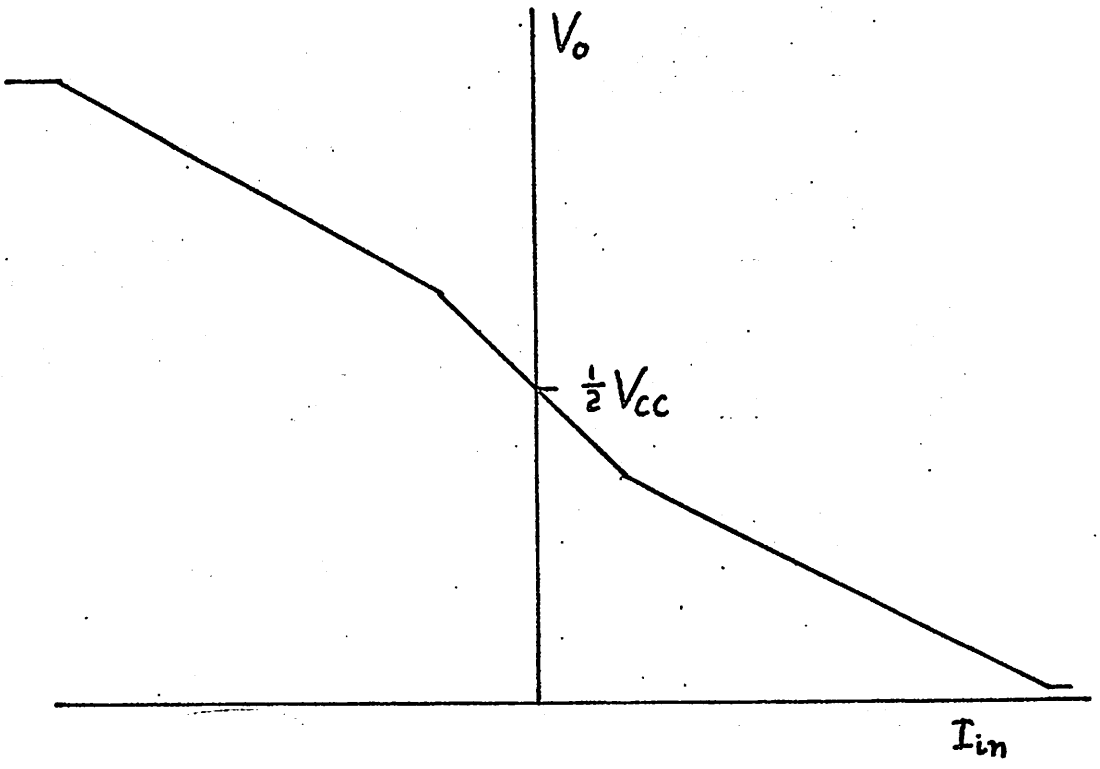

Fig. 2.26 Modified Transfer Characteristic

III. OSCILLATOR SENSITIVITY

3.1 Introduction

Chapter 2 defines two types of basic oscillators and the feedback loops that they may contain. Some of the design constraints imposed by a totally integrated monolithic oscillator are considered and the resultant possible configurations for positive and negative feedback oscillators are developed.

In this present chapter, the sensitivity problem is considered specifically. First, the temperature sensitivity of circuit elements comprising an oscillator realization are studied. Then a temperature sensitivity formulation is derived for a linear model of the oscillator system. Finally, consideration is turned to the nonlinear effects and their contribution to the temperature sensitivity of the oscillator.

A generalized form of the Groszkowski-Shohat result is derived, indicating possible frequency variations due to distortion of a harmonic output. Since explicit forms are required for sensitivity due to nonlinear effects, both digital and analog computer results of nonlinear second and third order oscillators are presented. These results combined with the results of the linear analysis lead to a complete formulation of the sensitivity problem.

3.2 Sensitivity Coefficient

Several sensitivity coefficients may be defined. In this study, two particular sensitivity coefficients are used. The first is the classical sensitivity coefficient which is given by Bode[26]. The classical sensitivity coefficient for a variable x that depends on a parameter G is defined by

$$S_G^x = \frac{G}{x}\frac{dx}{dG} = \frac{d(\ln x)}{d(\ln G)} \tag{3.1}$$

This is the sensitivity definition used when the parameter G is not temperature. When the parameter of interest is temperature, it is convenient to define another sensitivity coefficient to indicate the fractional change of the dependent variable on temperature. This sensitivity coefficient is defined by

$$\gamma_T^x = \frac{1}{x}\frac{dx}{dT} = \frac{d(\ln x)}{d(T)} \tag{3.2}$$

It is to be noted that if x is the product of several sensitive components x_i, the total classical or temperature sensitivity of x is the sum of the sensitivities of each of the components. For example, the total temperature sensitivity of x is given by:

$$\gamma_T^x = \frac{d \ln x}{dT} = \frac{d \ln(x_1 x_2 \ldots x_N)}{dT} = \frac{d \ln x_1}{dT} + \frac{d \ln x_2}{dT} + \ldots \qquad (3.3)$$

The temperature sensitivity is expressed in parts per million per ^{o}C (ppm/^{o}C).

3.3 Element Sensitivity

The temperature sensitivity values of the different circuit elements used in the final design are based on experimental results. Previous theoretical results used a temperature sensitivity expression for the common emitter current gain (β_o) of a bipolar transistor of the form

$$\gamma_T^{\beta} = \frac{2}{T} \qquad (3.4)$$

where T is the temperature in degrees Kelvin[27]. Experimental results in this laboratory have shown this expression to be accurate for deep structure transistors with nondegenerately doped emitters. However, additional experimental investigation has shown that there is some dependence on processing. For the case of the shallow transistor with a degenerately doped emitter, an approximate empirical

expression based on experimental results obtained in this laboratory is given by

$$\gamma_T^{\beta} = \frac{430}{T^2} \tag{3.5}$$

This expression gives both a smaller sensitivity at room temperature and a smaller derivative of sensitivity. The experimental sensitivities obtained for both types of bipolar transistors are shown in Fig. 3.1. Included in the figure is a graph of Eq. 3.4.

Resistance sensitivities often are assumed to be constant with temperature. In the case of higher resistivities, the is not too bad an approximation. However, as with transistor current gain β_o, the resistance sensitivities are processing dependent. The lower resistivity realizations show a larger sensitivity dependence on temperature. Experimental results obtained in this laboratory for two resistivities are shown in Fig. 3.2. Resistor sensitivities are also somewhat dependent on geometry. Experiments show variations of 5 to 10% for different geometries. Hess, et al, have done a more extensive experimental investigation of diffused resistor temperature coefficient[28]. Their work includes the temperature coefficient dependence on surface impurity concentration, background concentration, and junction depth.

MOS capacitors are usually assumed to have zero temperature sensitivity. To a first order, the assumption is well satisfied for the MOS capacitors realized over an n^+ region. A typical

experimental MOS capacitor sensitivity is shown in Fig. 3.3

3.4 Total Oscillator Sensitivity

The oscillators considered in this thesis are all of such a nature that they can be represented by a single nonlinear differential equation and have a single unstable singularity. All the nonlinearities of the nonlinear equation are assumed to depend on the same single variable. A linearized model for the oscillator system can then be obtained by Taylor series expansion about the singularity[29], as discussed below.

For an initial example, the current amplifier Wien-type oscillator which has been discussed in Chapter 2 and experimentally realized as described in Chapter 5 is considered. The circuit for this particular oscillator is repeated in Fig. 3.4. For clarity in the discussion, the following definitions are made. A_I indicates a circuit block that performs as an ideal current amplifier, F(i) is the input-output relation of the gain block:

$$i_o = F(i)$$

where i is the input current, and A is the linearized gain given by:

$$A = \frac{d}{di} F(i) \Big|_{i=0}$$

The open-loop transfer function for the first-order model is given by

$$T_I = \frac{\left(\frac{1}{R_1C_2}p\right) F(i)}{p^2 + \left[\frac{1}{R_1C_1} + \frac{1}{R_2C_2} + \frac{1}{R_1C_2}\right]p + \frac{1}{R_1R_2C_1C_2}} \tag{3.6}$$

where p is the differential operator, p = d/dt, and F(i) is the idealized current transfer function of the transistor amplifier which is assumed to contain the system nonlinearity. For proper choice of biasing elements, the transistors are biased to a single, stable, operating point with both transistors in the active mode and the open-loop transfer function can be linearized about the operating point to give:

$$T(p) = \frac{A\frac{1}{R_1C_1}p}{p^2 + \left(\frac{1}{R_1C_1} + \frac{1}{R_2C_2} + \frac{1}{R_1C_2}\right)p + \frac{1}{R_1R_2C_1C_2}} \tag{3.7}$$

The gain A of the closed-loop system can be adjusted so the single singularity becomes unstable and periodic oscillations result.

For this oscillator the closed-loop system equation is

$$p^2 + \left[\left(\frac{1}{R_1C_1} + \frac{1}{R_2C_2} + \frac{1}{R_1C_2}\right)p + \frac{1}{R_1R_2C_1C_2}\right]i - \frac{1}{R_1C_2}p\,F(i) = 0 \tag{3.8}$$

where it is noted that the quiescent input current is zero due to the series capacitor. For $R_1 = R_2 = R$, $C_1 = C_2 = C$, and f(i) = d/di (i-F(i)), this can be normalized with respect to time to give

$$\ddot{x} + f(x)\dot{x} + x = 0 \tag{3.9}$$

where $\dot{x} = 1/RC\ di/dt$. Eq. 3.9 is recognized as Lienard's equation.

For this system, the linear contributions to sensitivity are caused by temperature changes in R and C which track closely with temperature variations. This represents changing the time normalization of Eq. 3.9 and therefore adds directly to period changes caused by the modification of f(x) with changing temperature. The temperature sensitivity of the generalized form of Lienard's equation is considered in detail in a later section.

In the general case, there may be resistive and capacitive values that do not track closely in temperature and contribute non-negligible terms to the system equation. The elements of the hybrid π model of the bipolar transistor might be significant and yet not track the passive elements closely with temperature change. However, if all the nonlinearities appear as single valued coefficients of a single variable in the differential equation, the total temperature sensitivity can still be written as the sum of a linear contribution and a nonlinear contribution.

For example, consider a general third order nonlinear equation of the form

$$a_3(x)\frac{d^3x}{dt^3} + a_2(x)\frac{d^2x}{dt^2} + a_1(x)\frac{dx}{dt} + a_o(x)x = 0 \qquad (3.10)$$

If the coefficients are suitably well behaved, each may be expressed as a Taylor series expansion*:

$$\begin{aligned} a_o(x) &= a_{o1} + a_{o2}x + a_{o3}x^3 + \cdots \\ a_1(x) &= a_{11} + a_{12}x + a_{13}x^3 + \cdots \\ a_2(x) &= a_{21} + a_{22}x + \cdots \\ a_3(x) &= a_{31} + a_{32}x + \cdots \end{aligned} \qquad (3.11)$$

If a time scaling is performed so that $\tau = t/K$, Eq. 3.10 becomes:

$$\frac{a_3(x)}{K^3}\frac{d^3x}{d\tau^3} + \frac{a_2(x)}{K^2}\frac{d^2x}{d\tau^2} + \frac{a_1(x)}{K}\frac{dx}{d\tau} + a_o(x)x = 0 \qquad (3.12)$$

However, if the coefficient a_{ij} of Eq. 3.11 are scaled simultaneously with the time scale so that

$$\tilde{a}_{ij} = K^i a_{ij} \qquad (3.13)$$

---

* This Taylor series expansion is not necessary for this discussion but is convenient for clarity.

Eq. 3.10 becomes

$$a_3(x)\frac{d^3x}{d\tau^3} + a_2(x)\frac{d^2x}{d\tau^2} + a_1(x)\frac{dx}{d\tau} + a_o(x)x = 0 \qquad (3.14)$$

If Eq. 3.10 has a periodic solution $x(t)$, Eq. 3.14 has a periodic solution $x(\tau)$ and $x(t) = x(\tau)$. Therefore the scaling of the coefficients of Eq. 3.10 according to Eq. 3.13 is equivalent to time scaling.

Any variation of the coefficients caused by a temperature change may cause the period of $x(t)$ to change. That portion of the coefficient variation that satisfies the scaling relation of Eq. 3.13 is considered to be the linear contribution to temperature sensitivity of oscillation frequency. It is expressed by $\gamma_{TL}^{f_o}$ in the relation

$$\Delta f_{o\,(\text{linear contribution})} = f_o\,\gamma_{TL}^{f_o}\,\Delta T \qquad (3.15)$$

From Eq. 3.13, it can be seen that the scaling K is related to $\gamma_{TL}^{f_o}\,\Delta T$ by

$$K = \frac{1}{1 + \gamma_{TL}^{f_o}\,\Delta T} \qquad (3.16)$$

Any coefficient variation with temperature that violates Eq. 3.13 is considered a nonlinear contribution to sensitivity. For

example, if a particular coefficient a_{ij} has a temperature induced variation

$$\tilde{a}_{ij} = (K)^{i} a_{ij} + \delta \tag{3.17}$$

the term δ causes the nonlinear contribution. The nonlinear contribution is expressed by $\gamma^{f_o}_{TNL}$ in the relation

$$\Delta f_{o(\text{nonlinear})} = f_o \gamma^{f_o}_{TNL} \Delta T \tag{3.18}$$

Since the linear contribution effects only the time normalized system, it can be seen that the two sensitivities add directly to give the total temperature sensitivity of oscillation frequency as

$$\gamma^{f_o}_{T} = \gamma^{f_o}_{TL} + \gamma^{f_o}_{TNL} \tag{3.19}$$

A subclass of oscillators that is of particular interest is one that has the following properties:

a) All the coefficients a_{ij} of Eq. 3.11 have a temperature dependence as expressed by Eq. 3.16.

b) K depends to a first order only on passive elements temperature sensitivities.

c) All the elements of a given type (eg., resistance, capacitance) track closely with temperature (i.e., the temperature coefficient of all resistors is the same).

The temperature sensitivity of oscillation frequency for oscillators in this subclass is primarily due to the linear contribution of the passive elements. The Wien-type oscillators discussed above is in this subclass and exhibits this property.

3.5 Linear Contribution to Basic Oscillator Sensitivity

For a basic positive or negative feedback oscillator which produces a harmonic output, the frequency of oscillation is inversely proportional to an RC product. For a typical Wien-type configuration such as shown in Fig. 3.4, this product contains, to a first-order, only terms involving the passive elements in the frequency selective feedback network. For this case and for many harmonic positive feedback oscillators, the frequency of oscillation is given by

$$f_o = \frac{1}{2\pi \sqrt{R_1 R_2 C_1 C_2}} \tag{3.20}$$

If this expression is accurate for the particular positive feedback oscillator under consideration, its temperature sensitivity is given by

$$\gamma_{TL}^{f_o} = \frac{1}{f_o}\frac{df_o}{dT} = -\frac{1}{2}\frac{1}{R_1}\frac{\partial R_1}{\partial T} - \frac{1}{2}\frac{1}{R_2}\frac{\partial R_2}{\partial T} - \frac{1}{2}\frac{1}{C_1}\frac{\partial C_1}{\partial T} - \frac{1}{2}\frac{1}{C_2}\frac{\partial C_2}{\partial T} \qquad (3.21)$$

If the oscillator operates in a near-harmonic mode over the temperature range considered, this expression can give a fairly accurate prediction of temperature sensitivity for a positive feedback monolithic oscillator as is shown in Fig. 3.5. This figure is obtained from the actual experimental realization of the basic Wien-type positive feedback oscillator of Fig. 3.4. In Fig. 3.5, the temperature sensitivity predicted by Eq. 3.21 using measured values of resistor and capacitor sensitivities is compared with the experimental measured sensitivity. It is seen the difference is less than 5% in the temperature range considered. The details of this realization and these results are described in Chapter 5.

In spite of the good match mentioned above, this linear description is not complete. If the approximation that the oscillator operates in a harmonic mode is poor, or if the resistors and capacitors have a very low temperature sensitivity, this first-order approximation may be completely inadequate.

A more accurate but equally straightforward expression for the linear sensitivity can be obtained based on the particular properties of monolithic integrated circuits. The capacitors realized as MOS devices have a very small temperature sensitivity. Because of the fact that the diffused resistors are realized in the same fabrication processing step and the very close temperature coupling within the

actual circuit chip, there is a close tracking of resistor values with temperature variations. This is to say that the MOS capacitors have essentially a zero temperature coefficient and the resistors have almost exactly equal temperature sensitivities over the temperature range. This can be expressed by

$$\gamma_T^C = \frac{1}{C_i} \frac{\partial C_i}{\partial T} \simeq 0 \qquad i = 1,2,... \tag{3.22}$$

$$\gamma_T^R = \frac{1}{R} \frac{\partial R}{\partial T} = \frac{1}{R_j} \frac{\partial R_j}{\partial T} \qquad j = 1,2,... \tag{3.23}$$

To determine the effect a temperature change has on the system root locus under the conditions of Eqs. 3.22 and 3.23, a brief digression is needed to discuss the concept of root locus and the nature of impedance and frequency scaling.

The concept of root locus is based on a linearized system model. The root locus of an oscillator, which is inherently nonlinear, is obtained from the linearized model of the oscillator about the quiescent operating point.

Impedance scaling is done by multiplying every impedance in the circuit by a common factor K_I. For the elements liable to be encountered in a monolithic circuit, the normalized values of the elements are

$$\begin{aligned} R_{jI} &= K_I R_j & j &= 1,2,... \\ C_{iI} &= C_i/K_I & i &= 1,2,... \\ gm_I &= gm/K_I \end{aligned} \tag{3.24}$$

where the subscript I indicates the impedance scaled value. Since this scaling does not modify open-loop pole position, the root locus is unchanged. If this scaling does not change the open-loop gain level, the closed-loop poles are not modified either. However, if the gain level is changed, the magnitude condition must be used to determine the new closed-loop pole positions on the root locus.

Time scaling corresponds to modifying real time by some factor K_f. The scaled system operates on a time base $\tau = K_f t$. The scaling of the actual system is obtained by modifying the component values by K_f for those elements that contain a time derivative in their model. In the usual monolithic circuit, this means changing capacitor values by K_f

$$C_{if} = K_f C_i \qquad i = 1,2,3,... \tag{3.25}$$

Time scaling is equivalent to frequency scaling of the linearized model which produces a radial shift in the root locus of the system but does not change its form. Thus, the closed-loop poles are only modified in their radial distance from the origin. Their angular position does not change under frequency scaling.

Attention is now returned to the effect of temperature change on open-loop and closed-loop root locus pole positions of the monolithic circuit under the constraint of Eqs. 3.22 and 3.23. For a given temperature change $\Delta T = T_2 - T_1$, the value of MOS capacitors is unchanged and the diffused resistors all undergo an equal percentage change. If γ_T^R is independent of temperature, this is

expressed by

$$\Delta C_i \simeq 0 \tag{3.26a}$$

$$\Delta R_j = R_{jT_2} - R_{jT_1} = R_{jT_1} \gamma_T^R \Delta T \tag{3.26b}$$

In other words, none of the capacitors change in value and the ith resistor has a value at the new temperature T_2 of

$$R_{iT_2} = R_{iT_1} (1 + \gamma_T^R \Delta T) \tag{3.27}$$

This is equivalent to an impedance scaling

$$K_I = (1 + \gamma_T^R \Delta T) \tag{3.28}$$

However, if the whole system is impedance scaled, frequency scaling must be used also since the capacitors do not change with temperature. For zero change in capacitor value, the appropriate frequency scale is equal to the impedance scale.

$$K_f = K_I \tag{3.29}$$

Therefore, the temperature change is equivalent to a simultaneous frequency and impedance scaling of the passive elements. It is noted that this is true even if γ_T^R is not independent of temperature

so long as Eqs. 3.22 and 3.23 are satisfied over the temperature range.

If in an actual monolithic realization the open-loop pole positions are determined by RC products involving only passive resistors and capacitor elements, the above conditions are met and the temperature change can be represented as a simultaneous frequency and impedance scale. This scaling results in a radial shift of the root locus.

The assumption that the RC products contain only passive element values is usually valid for the dominant open-loop poles of typical oscillator realizations. The nondominant poles from active device charge storage effects are typically far enough removed so they do not invalidate the radial movement of the dominant portion of the root locus. This is pointed out in the example discussed in Section 2.7 of Chapter 2. If the open-loop gain level is independent of temperature, the closed-loop poles are also shifted radially with respect to the origin with temperature changes. When the closed-loop poles can be written as a product $(s-s_o)(s-s_1)(s-s_2)\ldots$ and s_o is the natural frequency of interest, its sensitivity to temperature is then expressed by

$$\gamma_T^{s_o} = \frac{1}{|s_o|} \frac{\partial s_o}{\partial T} = - \frac{s_o}{|s_o|} \gamma_T^R \qquad (3.30)$$

This is shown in Appendix A. Of course, if s_o is complex, $\gamma_T^{s_o}$ will be complex.

The example of the Wien-type oscillator in Fig. 3.4 is continued to demonstrate this more detailed formulation. The small-signal, closed-loop, linear system behavior is analyzed on the basis of the equation obtained from the open-loop transfer function given by Eq. 3.6. The second-order, linear differential equation of the system is

$$p^2 i + \left(\frac{1}{R_1 C_1} + \frac{1}{R_2 C_2} + \frac{1-A}{R_1 C_2} \right) pi + \frac{1}{R_1 R_2 C_1 C_2} = 0 \qquad (3.31)$$

where A is the linearized gain of the amplifier given by $A = d/di\ F(i)\Big|_{i=0}$ and $p = d/dt$. The natural frequencies of the system are given in terms of the complex variable s by the roots of

$$s^2 + \frac{1}{RC}(3-A)\, s + \frac{1}{R^2 C^2} = 0 \qquad (3.32)$$

if $R_1 = R_2 = R$ and $C_1 = C_2 = C$. These roots are

$$s_{1,2} = \left(\frac{1}{2RC} \right) \left[-(3-A) \pm \sqrt{5-6A_o+A_o^2} \right] \qquad (3.33)$$

The roots are complex for $1 \leq A \leq 5$ where harmonic oscillation occurs for $A = 3$. For the case where $A = 3.1$,

$$s_1 = \frac{1}{2RC} (0.1 + j\sqrt{3.99}) \qquad (3.34)$$

If the gain A_o is independent of temperature, the root sensitivity to temperature is given by

$$\gamma_T^{s_1} = \frac{1}{|s_1|} \frac{\partial s_1}{\partial T} = \frac{1}{|s_1|} \frac{\partial s_1}{\partial R} \frac{\partial R}{\partial T} = \frac{R}{|s_1|} \frac{\partial s_1}{\partial R} \gamma_T^R \tag{3.35}$$

In terms of Eq. 3.5, this becomes

$$\gamma_T^{s_1} = \frac{-0.1 - j\sqrt{3.79}}{4.0} \gamma_T^R \tag{3.36}$$

This result and Eq. 3.35 are exactly those predicted by the general form of Eq. 3.30. The graphic representation of this solution is shown in Fig. 3.6.

The sensitivity parameter of Eq. 3.30 depends upon an open-loop gain level that is temperature invariant and open-loop pole positions that are determined primarily by RC products of passive elements that satisfy Eqs. 3.22 and 3.23. If the gain level is not invariant, the assumption of radial displacement of the root locus with temperature still holds. Therefore, the new closed-loop pole positions can be determined by first considering the root locus displacement with temperature by application of Eq. 3.30 and then by solving the new gain condition

$$|H(s)G(s)| = 1 \tag{3.37}$$

where H(s) and G(s) are defined by Eq. 2.2. If, on the other hand,

the passive resistors have widely varying geometries or are realized in separate fabrication diffusion processes so that Eq. 3.23 does not hold, or if active element parameters of significant magnitude appear in the open-loop pole products, there is no simple way to determine closed-loop pole sensitivity to temperature. In this case, a more general sensitivity function is needed. An example of such a function for a single feedback loop system with a linear dependence in gain is one that is provided by Gaash[30]. The closed-loop pole position is given in terms of the gain level and the open-loop poles and zeros by

$$ds_o = \left(\frac{[H(s)G(s)]}{s} \right)^{-1}_{s=s_o} \left[\frac{dx}{x} - \sum \frac{p_e}{(s_o+p_e)} \frac{dp_e}{p_e} + \sum_k \frac{z_k}{(s_o+z_k)} \frac{dz_n}{z_k} \right] \tag{3.38}$$

x is the dimensionless open-loop linear gain level, p_e is the eth open-loop pole, and z_k is the kth open-loop zero. If the temperature sensitivity of the gain and each of the open-loop poles and zeros can be determined, the temperature sensitivity of s_o is given by Eq. 3.38. However, this situation does not arise for the oscillator configurations considered.

3.6 Nonlinear Contributions to Basic Oscillator Sensitivity

The linear contribution to oscillator temperature sensitivity

is a complete description of oscillator performance only if the gain condition is satisfied such that all natural frequencies move radially with respect to the origin with temperature changes. Even in circuits designed to satisfy this assumption, second order effects may cause it not to be true. In the remainder of this chapter, the sensitivity of oscillation frequency caused by gain variations with temperature changes is considered. This is basically a nonlinear problem, and for this reason both analytical and computational techniques are used to obtain the results.

Nonlinear analysis of the transistor oscillator has been studied by several people[31,32,33]. In particular, Wilson derived an analytical technique to determine the amplitude and frequency of oscillation for a second-order near-harmonic oscillator having a single nonlinearity[34]. His results are based on an analysis of Lienard's equation for a single analytic nonlinearity. In his analysis, he made the assumption of near-harmonic oscillation. This work on the second-order nonlinear system is extended to cover the generalized form of Lienard's equation. In addition, conditions where the nonlinearity is piecewise linear or where oscillation is not near-harmoinc are studied. Computer-aided analysis is used to obtain the necessary values for the nonlinear sensitivity analysis of typical oscillator.

In contrast to the positive feedback oscillator, the basic negative feedback oscillator is at least a third-order system. Federicks has studied a third-order vacuum tube RLC oscillator and obtained the conditions for the existence of a periodic

solution[35]. D. K. Lynn considered particular forms of specific third-order oscillators and used a perturbation analysis technique to obtain the period of oscillation of the system[36]. Diliberto has provided a perturbation analysis to determine the changes in the period of oscillation due to perturbations of the parameters of an n'th order system[37]. In this thesis, computer-aided analysis is used to obtain specific results for third-order nonlinear models of negative feedback RC oscillators. If excess phase is included in the basic second-order system as another natural frequency, the second-order system becomes a third-order system. Thus, the third-order formulation is used to analyze the effect of excess phase on the nonlinear results obtained for the second-order oscillator.

3.7 Nonlinear Analysis of the Basic Positive Feedback Oscillator

The basic positive feedback oscillator can be adequately represented by a second-order differential equation. The form of the equation is derived for the basic positive feedback oscillator in Section 3.4 and is Lienard's equation

$$\ddot{x} + f(x)\dot{x} + x = 0 \tag{3.39}$$

where $\dot{x} = dx/dt$ and a zero average value for x has been assumed. For studies here, this is generalized to

$$\ddot{x} + f(x)\dot{x} + g(x) = 0 \tag{3.40}$$

Second-order nonlinear systems have received extensive consideration by many authors and are covered well in standard texts[38-40]. In particular, the van der Pol case where $g(x) = x$ and $f(x) = \varepsilon(x^2-1)$ has been studied for all values of ε[41]. However, for situations of interest in this study, $f(x)$ is typically not of the van der Pol form. Moreover, interesting cases occur for nonsymmetric $f(x)$ and $f(x)$ piecewise linear. Therefore, these results are expanded by computer-aided analysis.

The major interest here is the sensitivity of the period of oscillation to changes in the parameters of the normalized nonlinear equation representing the oscillators considered. Intuitive insight to the period of oscillation as related to harmonic content or distortion of the variable x is given by Groszkowski and Shohat[42,43]. Their results are implicit expressions that do not explicitly give the period for given nonlinearities. Moreover, their results do not include the possibility of an example provided by Stoker[44]. He considered a conservative system ($f(x) = 0$ for all x) with a hard restoring force for which the frequency increased as amplitude and distortion increased. A generalized result is derived here that includes the Stoker example and points to possible nonlinear compensation techniques.

3.8 Generalized Relation of Period to Harmonic Content

Groszkowski and Shohat considered systems restricted to the form of Lienard's equation (Eq. 3.39). The theorem stated here

is not restricted to this equation and is stated for the generalized Lienard's equation.

Theorem 1. If $g(x)$ and $f(x)$ of the generalized form of Lienard's equation

$$\ddot{x} + f(x)\dot{x} + g(x) = 0 \tag{3.41}$$

satisfy the conditions:

i. $f(x)$ and $g(x)$ continuous over the range of x
$f(x), g(x) \in C(-\infty,\infty))$

ii. $df(x)/dx$ exists

iii. $f(x)$ and $df(x)/dx$ are bounded

iv. $f(o) < 0$ and a periodic solution $x(t)$ of period T exists

where $x(t)$ can be represented by

$$x(t) = \frac{A_o}{2} + \sum_{n=1}^{\infty} A_n \cos (n\omega t + \psi_n) \tag{3.42}$$

where A_n is the amplitude of the n'th harmonic term and

ψ_n is the phase of the n'th harmonic term;

then a),

$$\int_0^T g(x)dt = 0 \tag{3.43}$$

and b),

$$\int_0^T xg(x)dt = \int_0^T \dot{x}^2 dt \tag{3.44}$$

This theorem is proved in Appendix B. It is noted that for the case where g(x) is odd, the average value A_o of x(t) is zero by Eq. 3.43 of the theorem. Eq. 3.44 of the theorem is the general result relating period of oscillation to harmonic content. It is difficult to obtain a result that more explicitly indicates the relation of harmonic content to period than this expression without first making some assumptions on the nature of g(x). In the case that g(x) is an odd polynomial, g(x) can be expressed

$$g(x) = \sum_m^M a_m x^{2m-1} \tag{3.45}$$

Eq. 3.44 becomes

$$\int_0^T \sum_m a_m x^{2m}\, dt = \int_0^T \dot{x}^2\, dt \tag{3.46}$$

From Parsevals equation[45] this gives

$$\sum_m \sum_n a_m A_n^{2m} = \sum_n n^2 \omega^2 A_n^2 \tag{3.47}$$

where a_m is the mth coefficient of the polynomial and A_n is the amplitude of the nth harmonic. If the sums have finite number of terms, this can be rewritten

$$\sum_n^N \left[\sum_m^M a_m A_n^{2m} - A_n^2 n^2 \omega^2 \right] = 0 \tag{3.48}$$

If $g(x) = x$, Eq. 3.48 becomes

$$\sum_n A_n^2 (1-n^2 \omega^2) = 0 \tag{3.49}$$

which is the result obtained by Shohat. Eq. 3.49 cannot be satisfied unless $\omega \leq 1$. The equal sign only occurs if $A_n = 0$ for $n > 1$, which is the case of harmonic oscillation. Thus, if a temperature increase causes the harmonic oscillation to develop distortion due to increasing gain, the fundamental frequency is sure to decrease. This result is also implied by the calculations of Groszkowski who never directly proves the theorem.

In contrast to this result, the general result of Eq. 3.48 allows for an increase in frequency for increasing distortion. To show this, consider a particular case where the coefficients in $g(x)$ are given by $a_1 = 1$, $a_2 \neq 0$, and $a_n = 0$ for $n \geq 2$. Then Eq.

3.48 becomes

$$\sum_{n} A_m^2 \, (1-n^2 \, \omega^2 + A_2 \, A_n^2) = 0 \qquad (3.50)$$

The a_2 term makes a frequency increase with increasing distortion possible. This result, although not based directly on a physical system, suggests that it may be possible to obtain a physically realizable g(x) that will compensate the system. These details are discussed in the next sections.

3.9 Computer Analysis of the Basic Positive Feedback Oscillator

The second-order nonlinear oscillator equation for the basic positive feedback oscillator is presented in Eq. 3.29 where it is assumed that the active transfer function nonlinearity appears in the first-order differential term of the equation as f(x). For the current amplifier, Wien-type oscillator of Fig. 3.4, this nonlinear term f(x) is obtained in reference to Eq. 3.8 from the current transfer function of the amplifier $i_o = F(i)$ by

$$f(i) = 3 - \frac{d}{di} F(i) \qquad (3.51)$$

The output current i_o, and the input current i are incremental values around the dc quiescent values. If, for example, F(i) = 3.3i-i3 as suggested by Fig. 3.7, then $f(x) = -0.3+2x^2$. The gain

A is defined as the value of the transfer function derivative at the quiescent operating point which for this case is dF(i)/di at i = 0 or 3.3.

There are two steps involved in determining the nonlinear contribution to temperature sensitivity for a given oscillator. The first step involves determining the nonlinearity f(x) as a function of temperature for the particular oscillator being considered. The second step involves finding the relation between the period of oscillation and the nonlinearity f(x). This is accomplished by using the results of the computer study discussed below.

The computer study of the periodic solutions of the second-order nonlinear differential equation is done for forms of f(x) that are representative of typical physically realized gain functions. At the end of this section, after these computer results are determined, an example is given showing the application of these results to a Wien-type oscillator to find the nonlinear contribution to temperature sensitivity.

Computer results for the relation of period to gain are obtained for several different gain curves. The variations in gain curves considered involve both symmetry and the overall shape. These results enable both the sensitivity to be calculated for a given gain curve and the importance of the shape of the gain curve to be considered.

The symmetric gain curves considered are shown in Fig. 3.8. The dependence of period on gain for each of the curves is obtained.

The curves considered vary from piecewise linear to a van der Pol approximation for the active region. The computer results for the van der Pol approximation are compared to a perturbation analysis based on the Krylov-Bogoliobov method at the end of the section[46]. On the basis of the results obtained for the symmetric gain curves, the decision is made to study symmetry variations for piecewise linear curves.

For analysis of the effect of sharpness of cutoff of the gain curve on period of oscillation, four symmetric amplifier curves are studied. These are shown in Fig. 3.7. For each curve, the same relative maximum amplifier output current is assumed and each is symmetric with respect to the bias point. The gain for each is defined as the slope at $x = 0$. Curve one is the van der Pol form up to the amplifier inactive region. The inactive region is represented by a linear segment. Curves two and three consist of linear segments connected by fillets that are circular arcs. Curve two assumes the derivative is zero for x greater than one irrespective of the gain. Curve three assumes a constant radius fillet. Curve four is piecewise linear. The computer program and a description are contained in Appendix C.

The computer results for the last three gain curves are shown in Fig. 3.8. The difference in period between the three solutions occured in the fifth place. This leads to the conclusion that the sharpness of cutoff is not critical when the amplifier gain curve contains a large linear region.

A more noticeable relation between amplitude and frequency sensitivity to gain changes occurs between the piecewise linear and the van der Pol approximation. To supplement the computer study, a perturbation analysis is made for the van der Pol approximation,

$$f(x) = \varepsilon(\mu x^2 - 1) \tag{3.52}$$

and for the case

$$f(x) = \varepsilon(\mu x^4 - 1) \tag{3.53}$$

The details of the perturbation analysis are presented in Appendix F. The dependence of amplitude and fundamental frequency on ε and μ are given in Table 3.1 along with an empirical form for the frequency dependence of the symmetric piecewise linear form of $f(x)$ on ε. In this latter case, ε is defined $\varepsilon = f(o)$. This ε corresponds to the other ε's. It is also interesting to compare the computer result for the van der Pol approximation to the perturbation analysis. This comparison is provided by Fig. 3.9.

An example of the application of these results is the determination of the nonlinear contribution to temperature sensitivity of the current-amplifier, Wien-type oscillator of Fig. 3.4. If the amplifier of this circuit can be modeled as shown in Fig. 3.10, the small-signal current gain is given by

$$A = \frac{g_{m1}g_{m2}(G_E+G_f) + g_{m2}\,G_f\,g_C + \cdots}{g_{m1}g_{m2}\,G_f + g_{m2}\,(Y_1 g_C + G_f g_C) + g_{m1}\,Y_2\,G_f + \cdots} \tag{3.54}$$

where only the terms that contribute more than one percent to the dominant terms $g_{m1}\,g_{m2}\,(G_E+g_C)$ and $g_{m1}\,g_{m2}\,G_f$ for typical circuit values are expressed. The amplifier is also assumed to have a low input impedance Z_{in} and a high output impedance Z_o. Z_o is usually on the order of the output transistor output resistance r_o which is typically greater than 50K. Z_{in} is of the order of 50Ω at base band frequencies for actual circuit values. To a first-order, the current gain is the ratio of resistors given by the dominant term of Eq. 3.42

$$A = \frac{G_E + G_f}{G_f} \tag{3.55}$$

f(x)	Amplitude a	Frequency ω
$\varepsilon(\mu x^2-1)$	$2/\sqrt{\mu}$	$\omega = \omega_o(1 - .0625\ \varepsilon^2)$
$\varepsilon(\mu x^4-1)$	$(\frac{8}{\mu})^{1/4}$	$\omega = \omega_o(1 - .145\ \varepsilon^2)$
Piecewise Linear		$\omega \approx \omega_o(1 - 1.25\ \varepsilon^2)$

Table 3.1 Frequency Sensitivity to Gain

If G_E and G_F track closely with temperature change, it is the second-order terms that cause the gain to be temperature sensitive. If only terms making a significant contribution to the gain sensitivity are included, the gain sensitivity is

$$\gamma_T^{\text{Gain}} \cong -\frac{1}{\beta_o}\left(1 + \frac{g_C}{G_f}\right)\gamma_T^{\beta} \tag{3.56}$$

where it is assumed that the β_o of the two transistors are the same and the gain condition for oscillation is satisfied for A = 3.

For the values of the actual realization considered in Chapter 5, the gain sensitivity has a value of approximately 200 ppm/^{o}K at 300 ^{o}K. If it is assumed that the amplifier can be reasonably represented by a symmetric, piecewise linear gain curve, the computer results show the nonlinear contribution to temperature sensitivity as

$$\gamma_{TNL}^{f_o} \approx 50 \text{ ppm}/^{o}\text{C} \tag{3.57}$$

or less than a 0.5% variation in period over 75^{o}K of temperature change. In comparison to the linear contribution to temperature sensitivity,

$$\gamma_{TL}^{f_o} \cong 2000 \text{ ppm}/^{o}\text{C} \quad , \tag{3.58}$$

the nonlinear contribution is negligible. This is born out by the results obtained in Chapter 5.

3.10 Symmetry Variation

Because of the limited control of element values in the actual realization of an integrated oscillator, a symmetric gain curve would be difficult to obtain. Therefore, the effects of symmetry on sensitivity are of interest. Two results are presented. Firstly, the change in period for changes in symmetry for constant gain is found. Secondly, the change in period for variations in gain at constant offset is found and compared with the symmetrical case. The computer program for these cases was written in modified Fortran II for the IBM 1800 computer as is contained in Appendix D.

In Fig. 3.11 the change in period with change in offset is shown. It is seen that for gain levels that produce almost harmonic oscillation, changes in symmetry have a marked effect on period. Fig. 3.12 shows changes in period for changes in gain for a given nonsymmetric gain curve. These results lead to the conclusion that the period of oscillation is increasingly sensitive to gain variations at low gain levels as the dissymmetry in the gain curve is increased. However, as the gain level increases, the excursions into the cutoff regions increases and the dissymmetry has less effect. With sufficient excess gain, the gain sensitivity for the symmetric and nonsymmetric curves is about the same.

3.11 Additional Computer Results

Three additional computer results for the positive feedback oscillator are obtained. First, the effect of having only partial

cutoff for a piecewise linear gain curve on period sensitivity to gain is studied. Second, the effect of excess phase in the gain function on the sensitivity is considered. Finally, the possibility of compensation as suggested by the frequency relation of Section 3.8 for the generalized Lienard's equation is investigated.

As determined in this section, the period sensitivity to gain is a minimum for the van der Pol approximation to the gain curve, with the piecewise linear gain curve producing the maximum sensitivity. This suggests that the piecewise linear curve, which would be closely realized in an amplifier with a large amount of feedback, such as the Wien-type discussed in Chapter 2, may not be the optimum design. However, accurate gain control is usually obtained by the use of large amounts of feedback. The dilemma can be solved by using a piecewise linear curve that has reduced gain or only partial cutoff in the sections such as on of those shown in Fig. 3.13. The realization of such a modified gain curve is discussed in Section 2.8 of Chapter 2.

Computer results were obtained for two degrees of partial cutoff as shown in Fig. 3.13. These computer results are given in Fig. 3.14 along with full cutoff piecewise linear results. As can be seen in Fig. 3.14, the modified nonlinearity does reduce the gain sensitivity which would in turn reduce the nonlinear contribution to temperature sensitivity of the overall oscillator.

The analysis up to this point of the positive feedback oscillator has been based on a second-order model of the system.

Attention is turned now to a third-order system that is capable of modeling the positive feedback oscillator which has a single non-dominant pole in its amplifier to model excess phase effects. If the positive feedback oscillator is of the Wien-type, the amplifier might contain a nondominant pole of the form $(\alpha p + 1)$ where $\alpha > 0$ as shown in Fig. 3.15. The original second-order system would become

$$\alpha p^3 i + (1 + 3\alpha)p^2 i + (3 + \alpha)pi - p F(i) + i = 0 \qquad (3.59)$$

Computer analysis of period sensitivity to gain was made on this system for a piecewise linear curve. The program is contained in Appendix E. Results were obtained for several values of α. The result for $\alpha = .02$, which corresponds to about 1.2^{o} excess phase in the low frequency slope, shows a slightly greater sensitivity to gain than the model without excess phase. For a 0.3% change in gain, the former shows a .83% change in period and the latter shows a .73% change in period.

The possibility of nonlinear compensation is indicated by the result of Section 3.8. This requires the system to be of the form

$$\ddot{x} + f(x)\dot{x} + g(x) = 0 \qquad (3.60)$$

The computer study again in this case is made for piecewise linear curves. The curves used for f(x) and g(x) are shown in Fig. 3.16.

It is noted that the discontinuity occurs for the same value of x in both curves. A possible realization for these curves is discussed in Chapter 4. The computer results are shown in Fig. 3.17. The particular point of interest is the fact that the period sensitivity to gain has the opposite sign for the g(x) chosen than all the previous cases studied. This is the possibility that is predicted by Eq. 3.44 and Eq. 3.50. From this result it is seen that nonlinear compensation is possible.

3.12 Nonlinear Analysis of Basic Negative Feedback Oscillator

Two systems are studied as representative of the nonlinear considerations in the negative oscillator. The first is the case of a system with non-interacting poles where the third-order equation of the closed-loop system for equal open-loop poles at $s = -\alpha$ is

$$\dddot{x} + 3\alpha\ddot{x} + 3\alpha^2\dot{x} + (1-A\alpha^3)x = 0 \tag{3.61}$$

For the computer study, α is set equal to 1 and the amplifier gain curve is assumed piecewise linear.

Because of programming considerations, only a piecewise linear system is considered. If the piecewise linear system is modeled to represent total amplifier cutoff, the computer results indicate nonsymmetric output waveforms are obtained for a symmetric amplifier characteristic. These results are not considered representative of

an actual physical system. The digital computer results for such a negative feedback oscillator with a third-order model occur because of the nature of the computer model of the mathematical system. This is not necessarily an erroneous result[47]. It can be attributed to the fact that the computer program appears as a delay differential operator rather than a continuous nonlinear operator[48]. Therefore, digital computer results are only obtained for partial cutoff. These results are shown in Fig. 3.18. As with the second order system with a single nonlinearity, the third order system with a single nonlinearity shows decreasing frequency with increasing gain.

For an amplifier that exhibited complete cutoff, a system continuing interacting poles is considered. The system in this case is described by

$$\dddot{x} + 6\ddot{x} + 10\dot{x} + (3+A)x = 0 \qquad (3.62)$$

An analog computer setup that is used to obtain the results is shown in Fig. 3.19. The nonlinearity realization is based on a model provided by Johnson[49]. The results, for which the period is measured to three places, indicate a constant period of 2.22 seconds for gains from 60 to 85. In fact, modifying the coefficient to either $\ddot{x}$ or x does not change the period as long as the starting condition is satisfied. These results suggest that further analysis of the third-order system is in order.

The realizations in this thesis are based on second-order systems.

It has been shown in previous sections that a realization of such a system is possible where the nonlinear contribution to sensitivity is negligible. Therefore, there would be no advantage to a third-order realization and the questions posed by the above results need not be purused further for the purpose of this thesis.

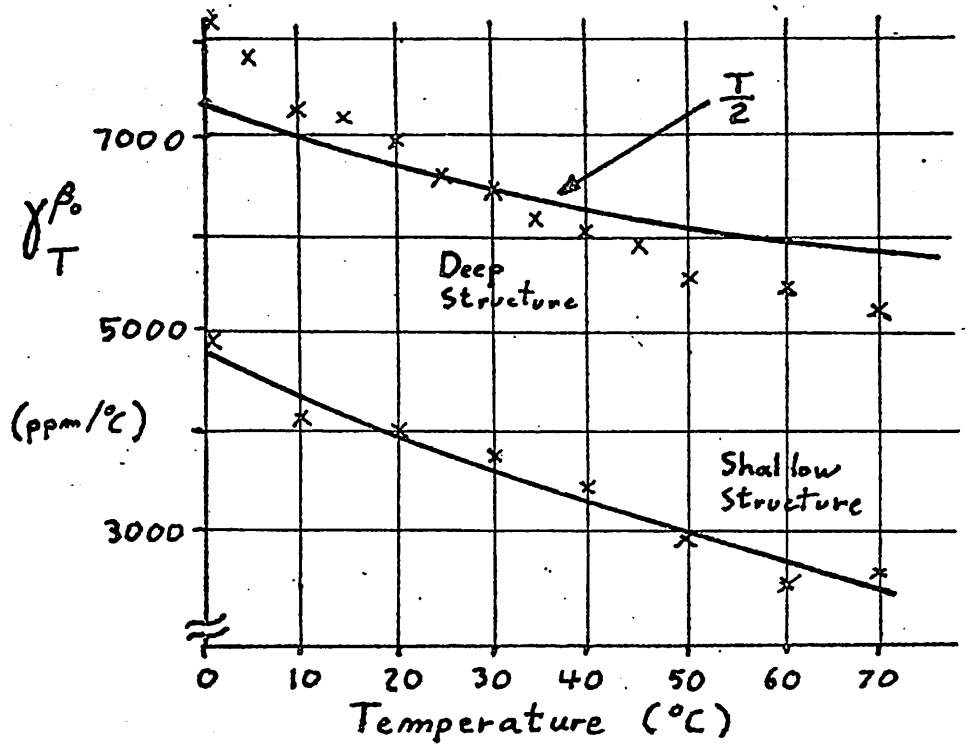

Fig. 3.1 Transistor β_o Temperature Sensitivity

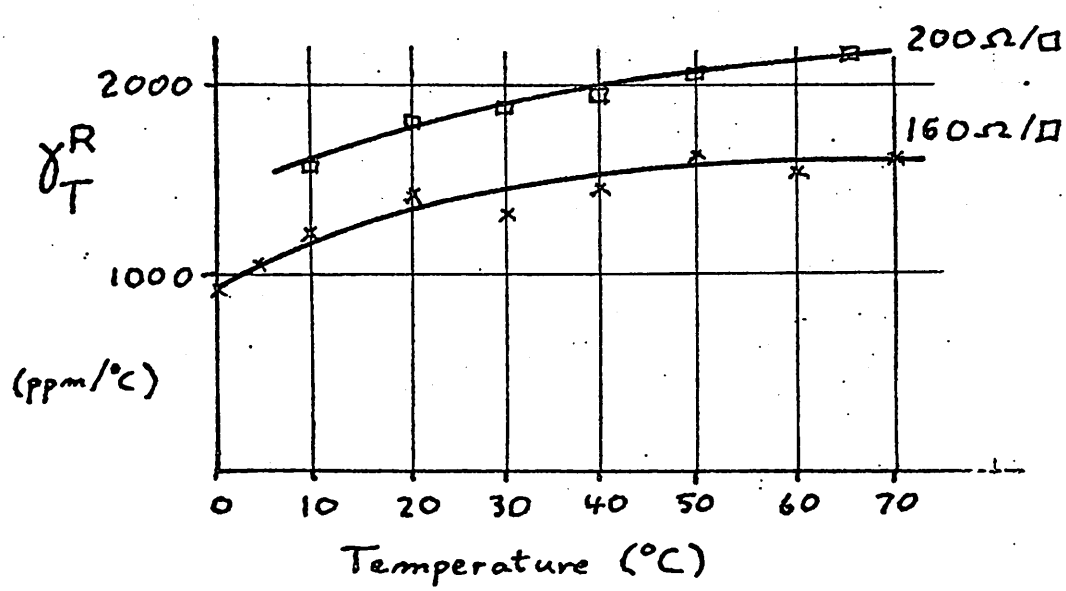

Fig. 3.2 Resistor Temperature Sensitivity

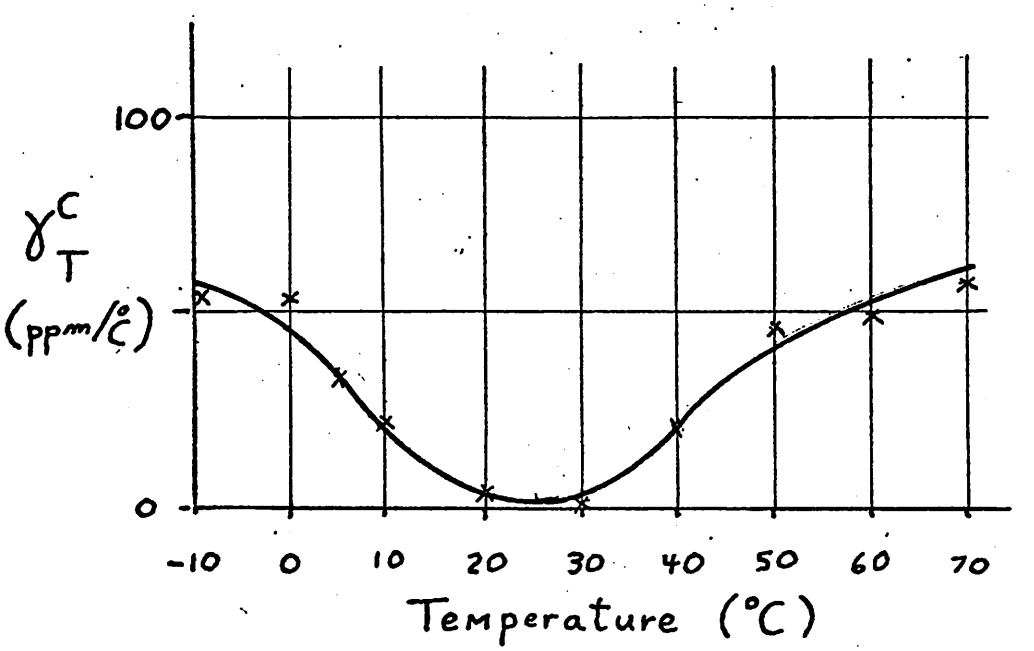

Fig. 3.3 Capacitor Temperature Sensitivity

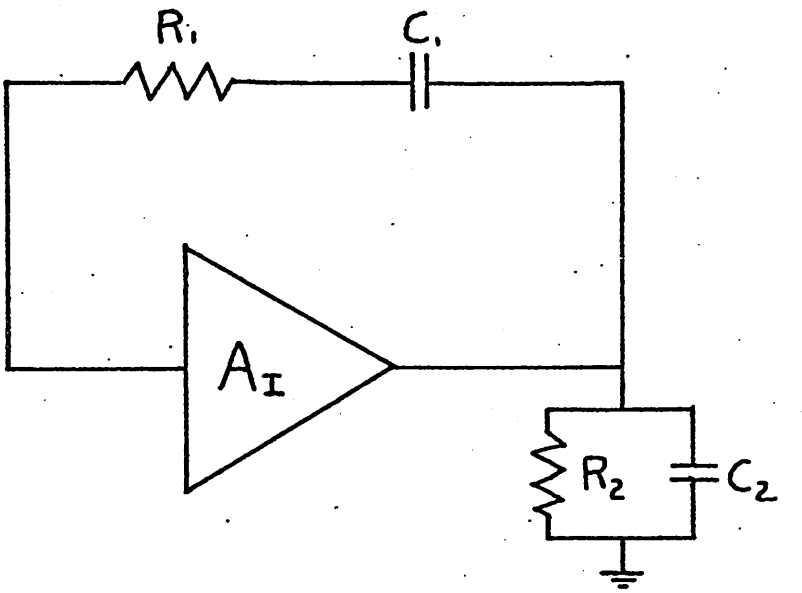

Fig. 3.4 Current Amplifier, Wien-type Oscillator

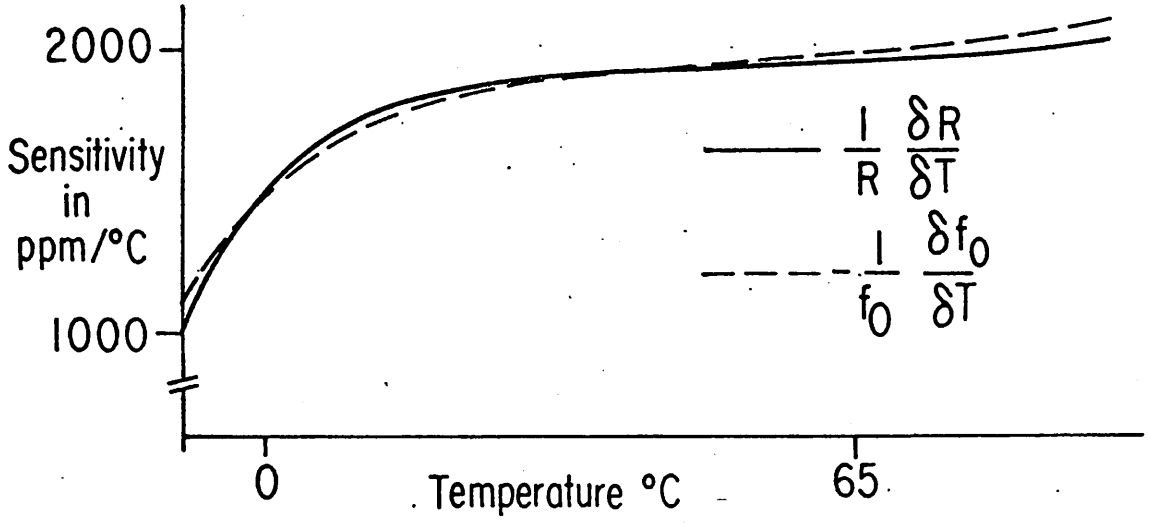

Fig. 3.5 Temperature Sensitivity of Positive Feedback Oscillator due to Linear Term

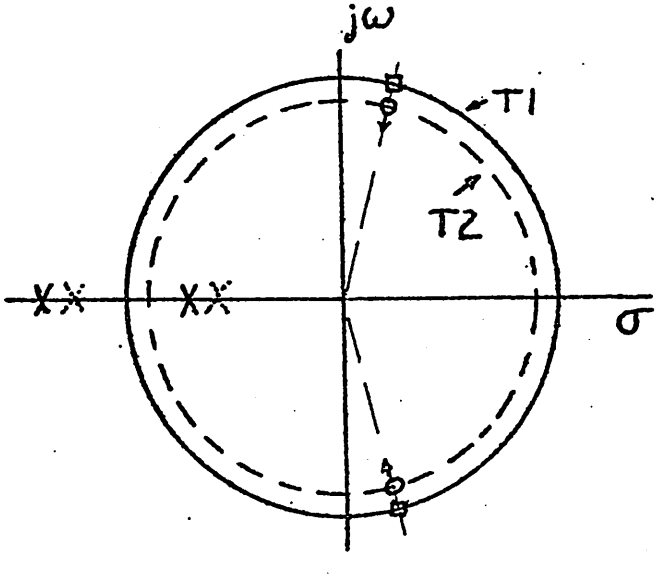

Fig. 3.6 Positive Feedback Oscillator Temperature Sensitivity

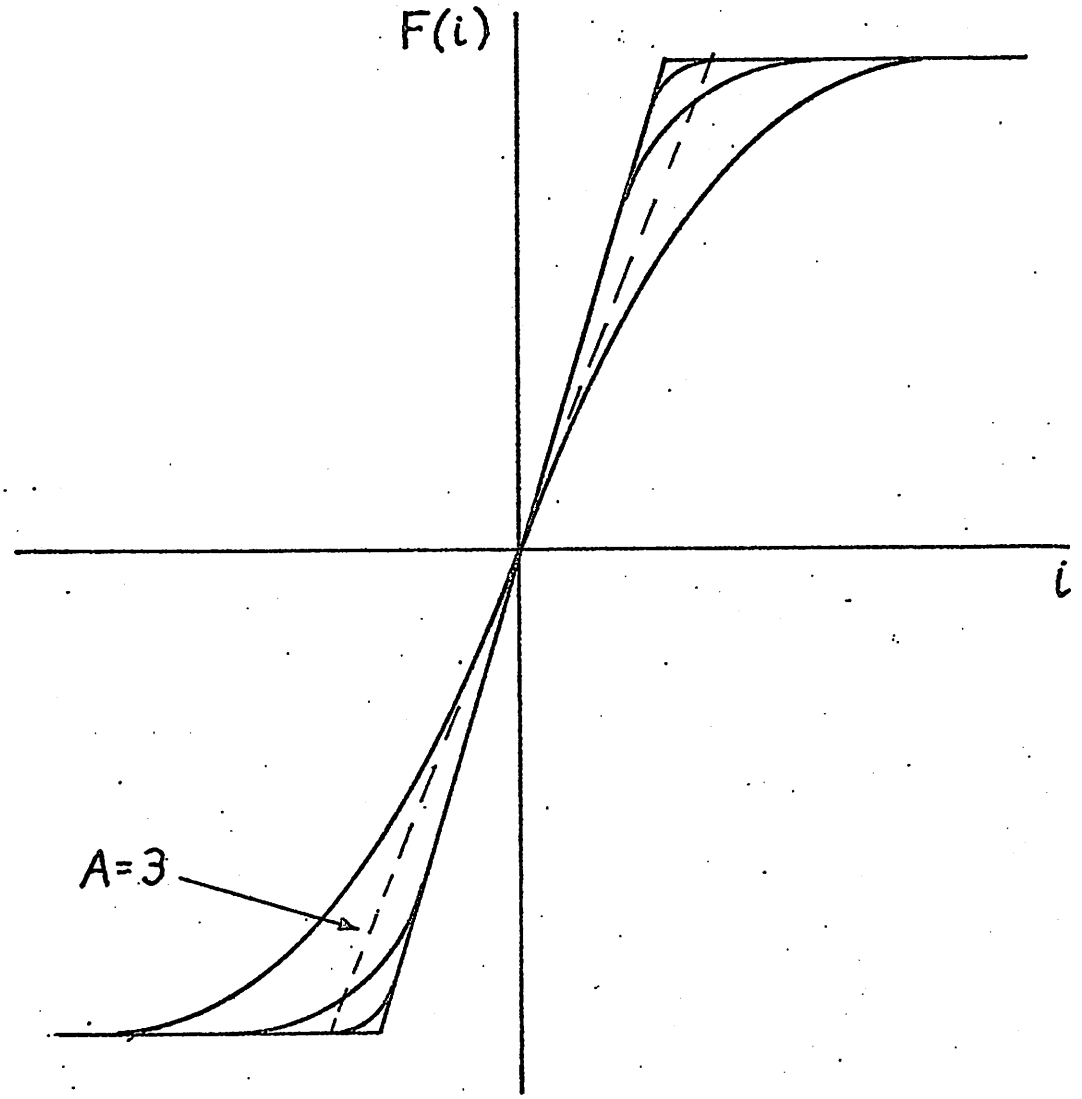

Fig. 3.7 Amplifier Gain Curves for Computer Study

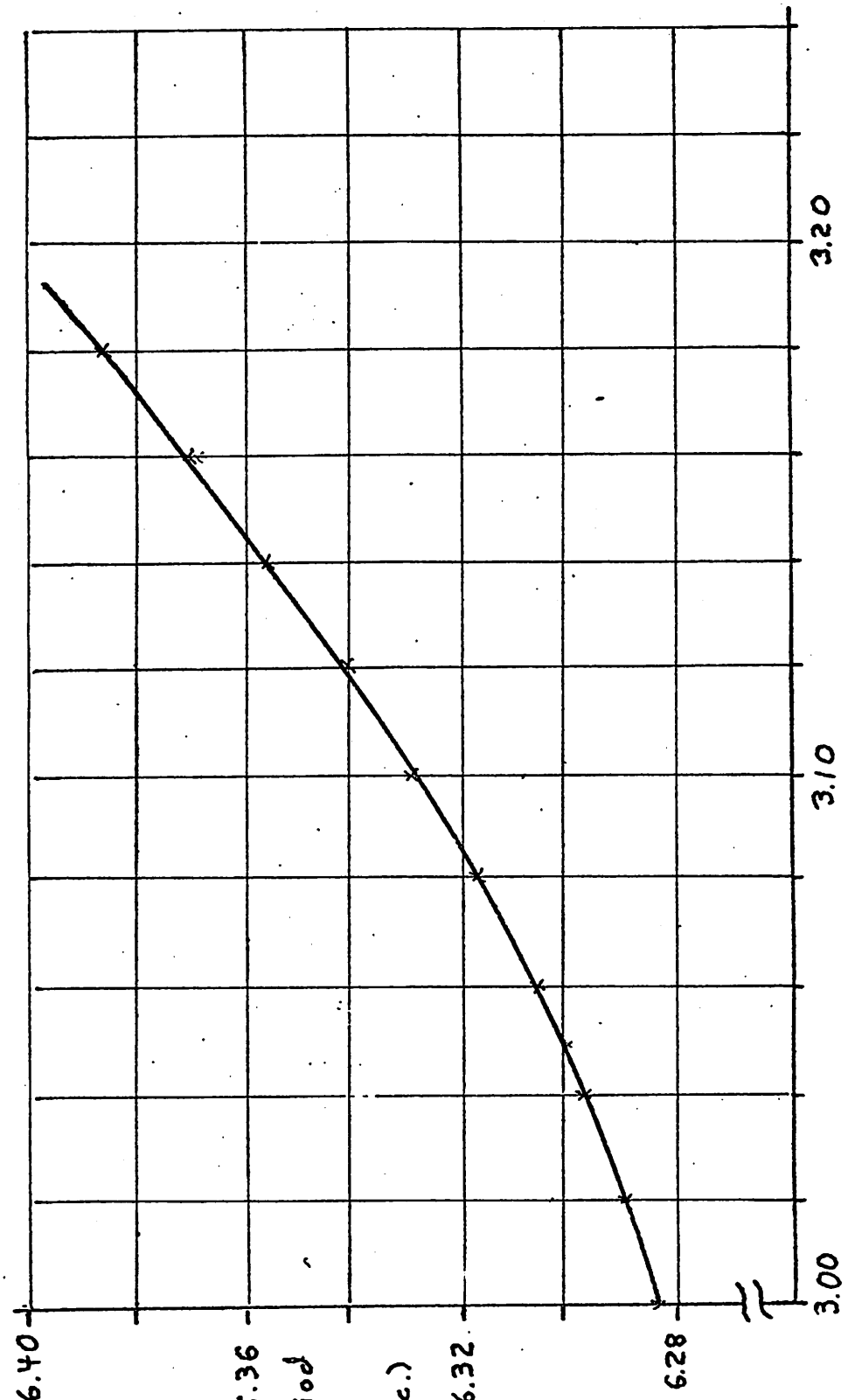

Fig. 3.8 Period Variation with Gain Change

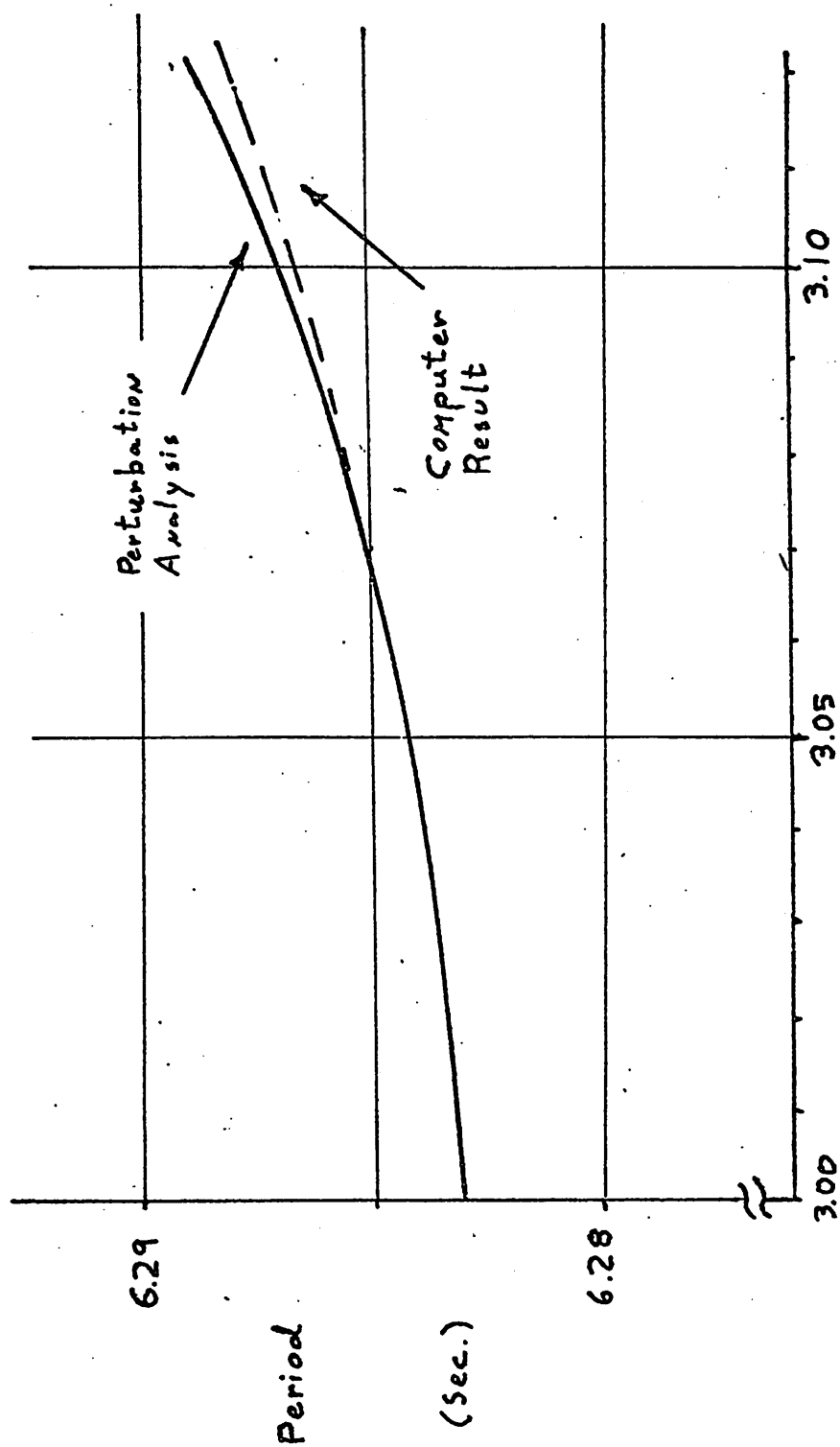

Fig. 3.9 Perturbation and Computer Analysis of the van der Pol Approximation

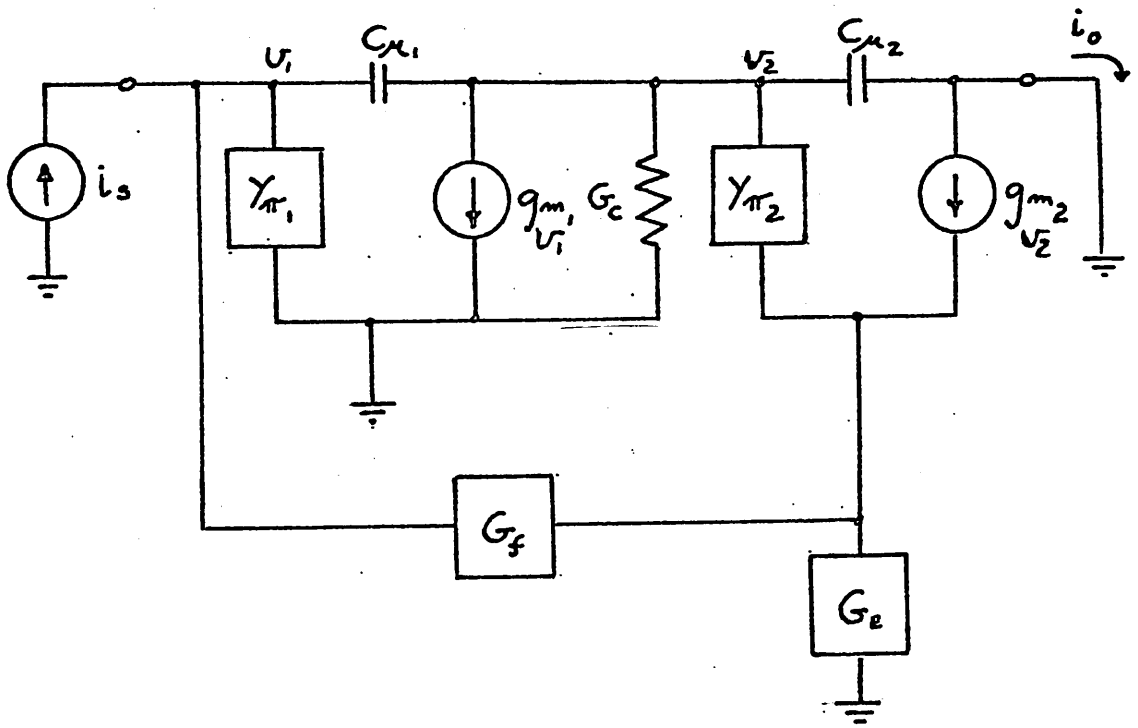

Fig. 3.10 Current Amplifier Circuit Model

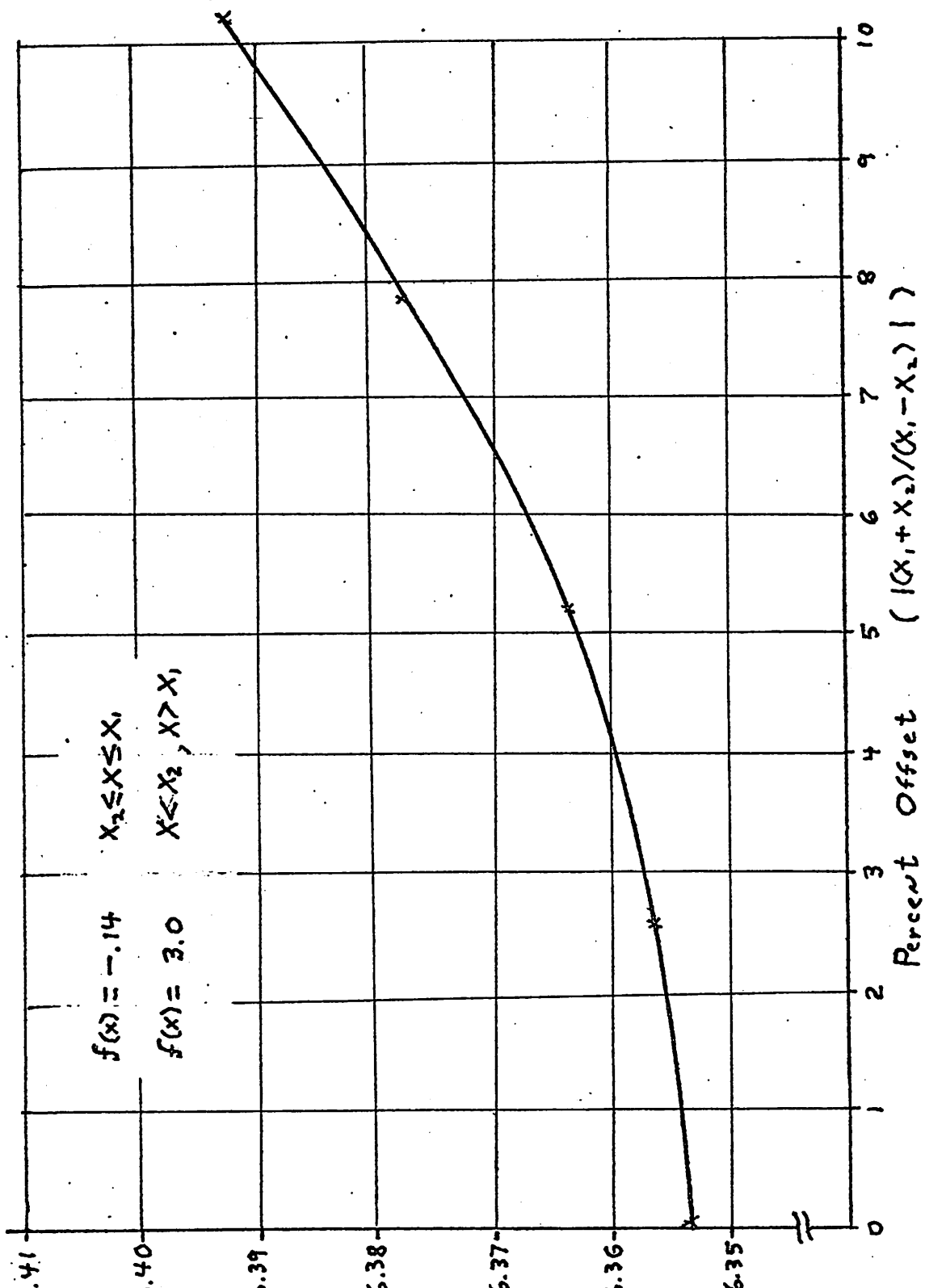

Fig. 3.11 Period Variation with Offset

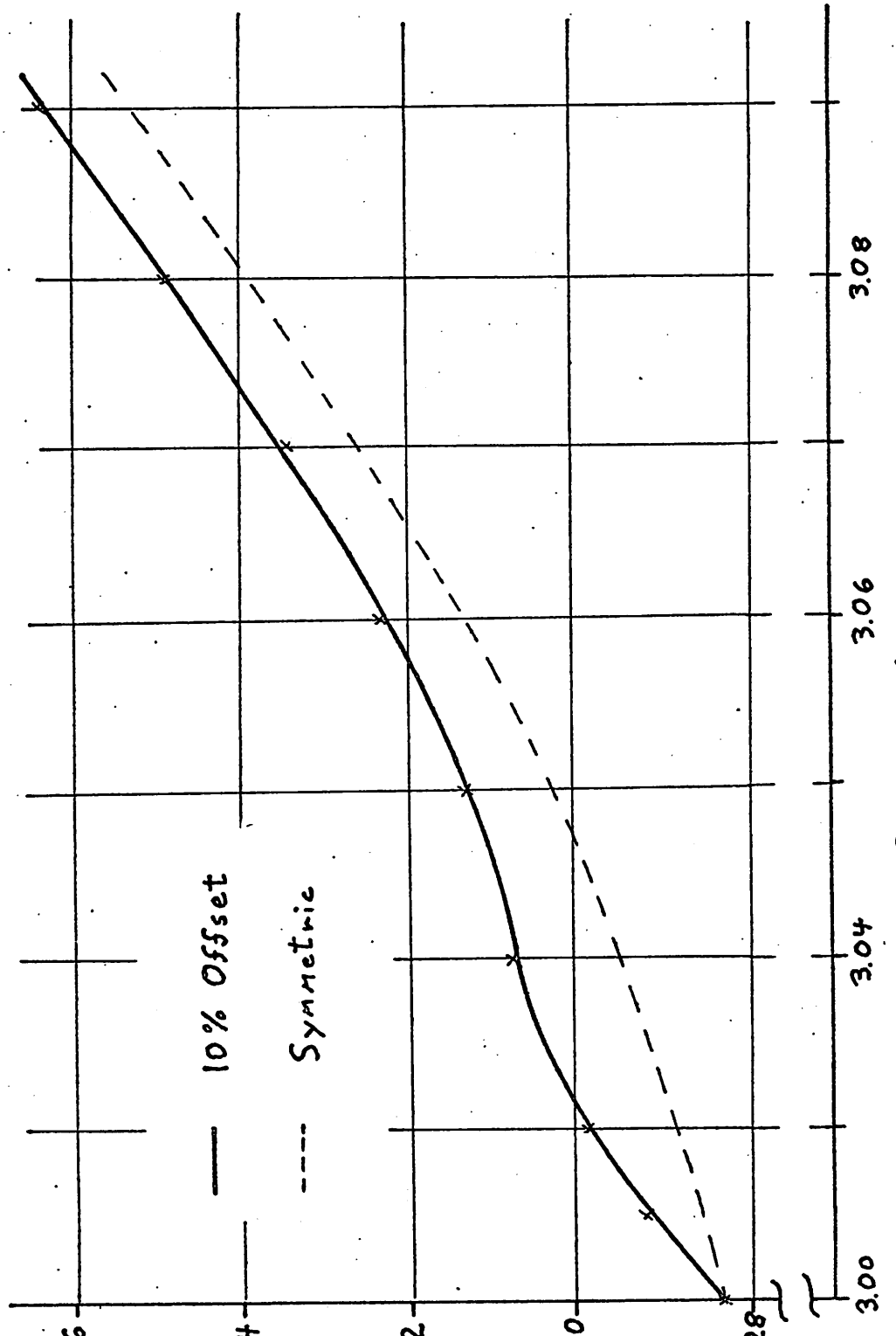

Fig. 3.12 Period Variation with Gain, Nonsymmetric Nonlinearity

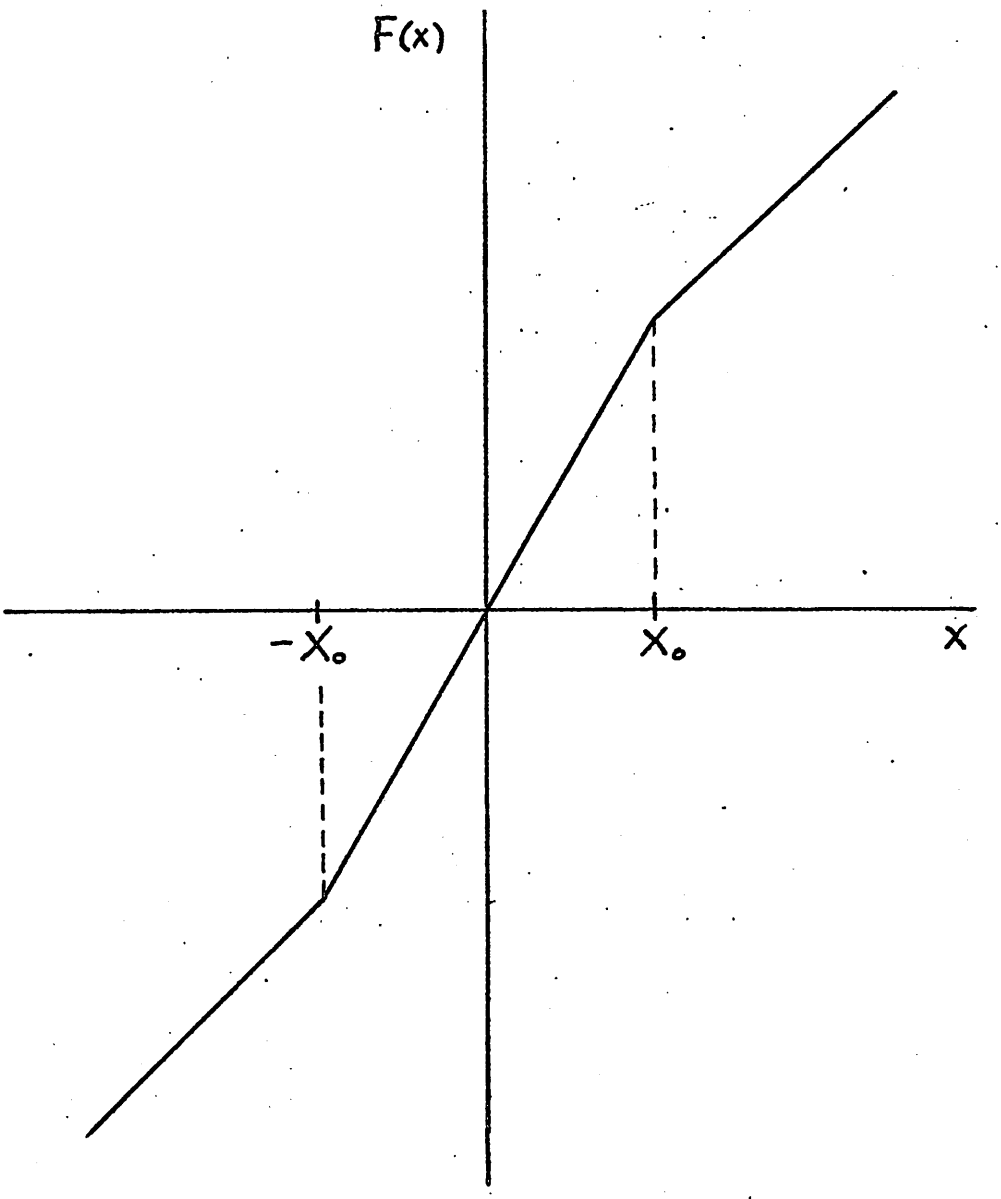

Fig. 3.13 Gain Curves of Computer Analysis

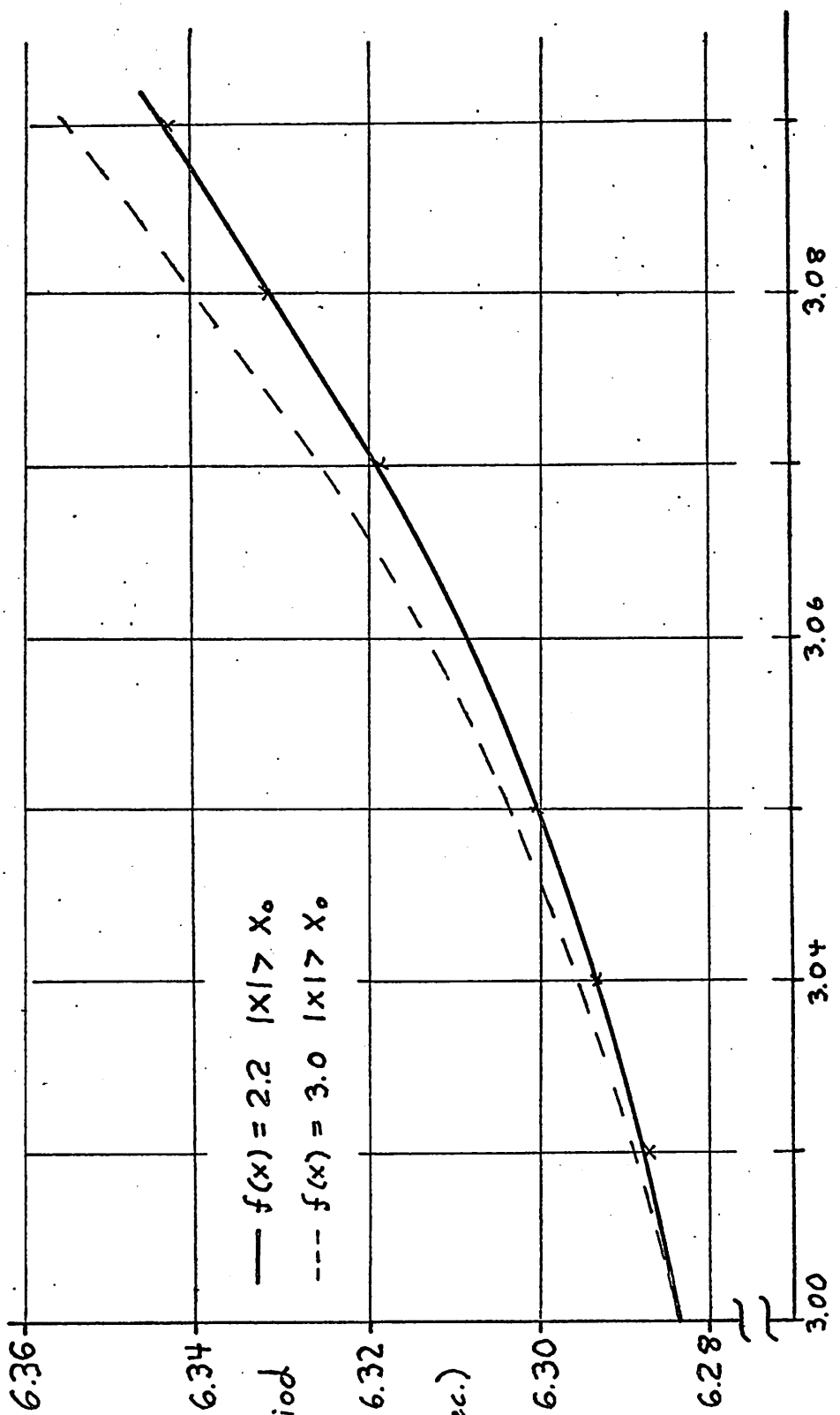

Fig. 3.14 Computer Analysis of Partial Cutoff Gain Curves

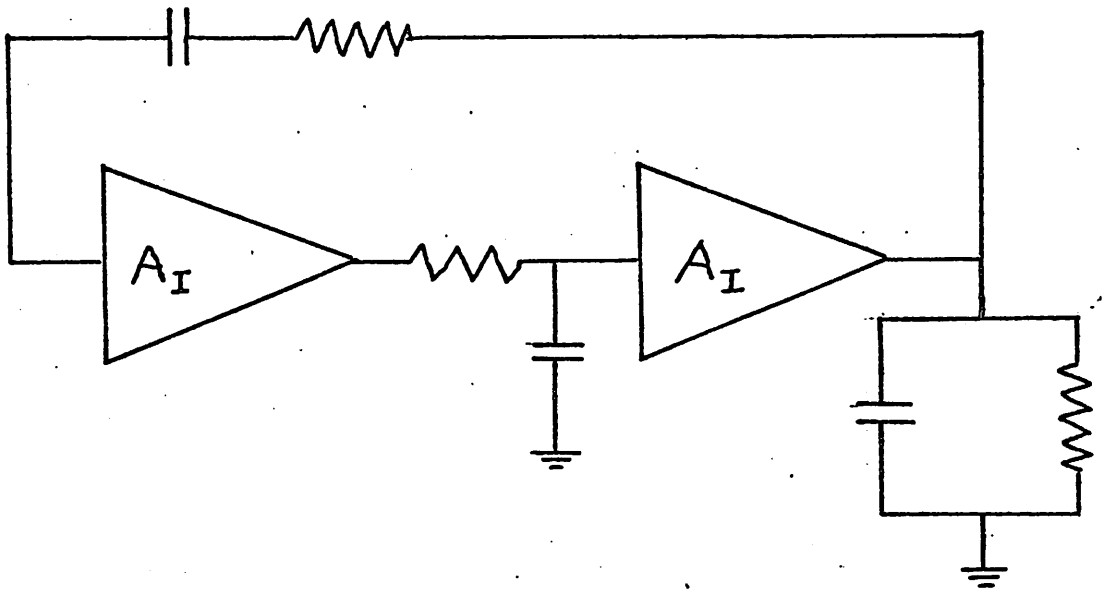

Fig. 3.15 Non-dominant Pole Model for Wien-type Oscillator

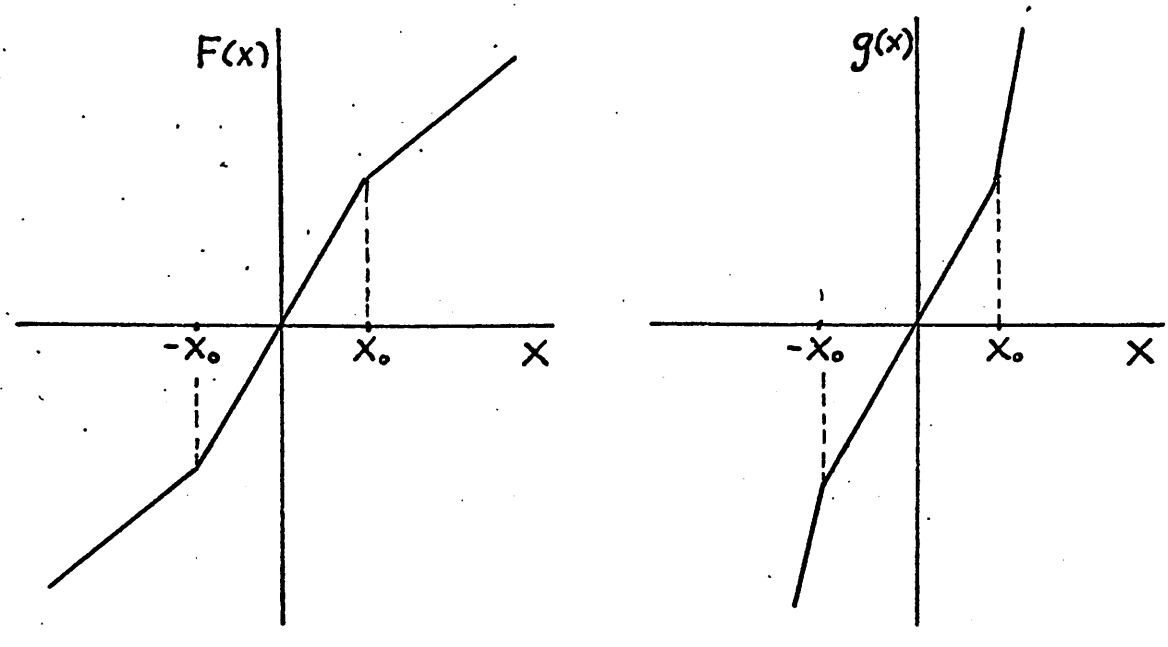

Fig. 3.16 Compensating g(x) for $\ddot{x}+f(x)\dot{x}+g(x)$

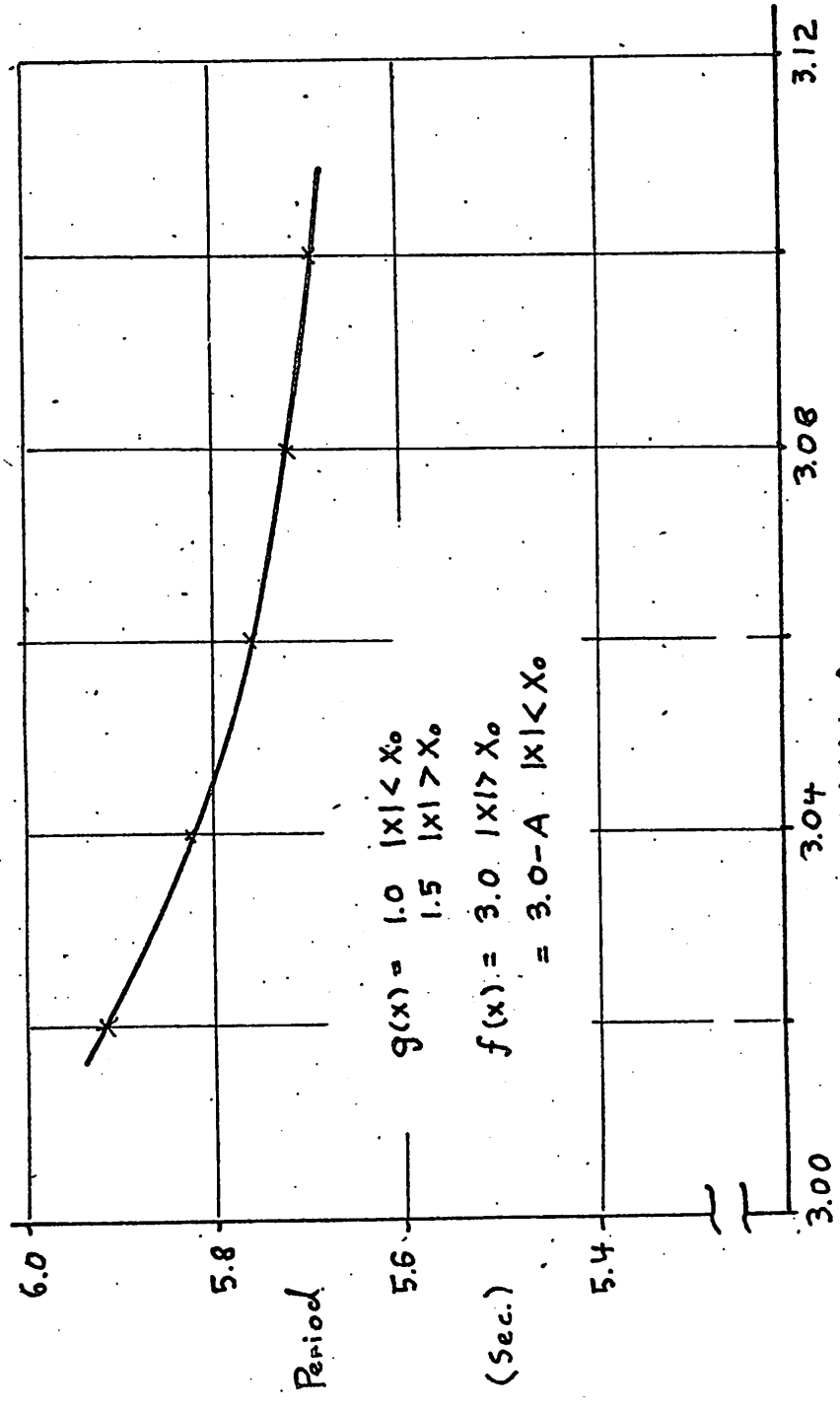

Fig. 3.17 Period Variation with Gain, Compensated Oscillator

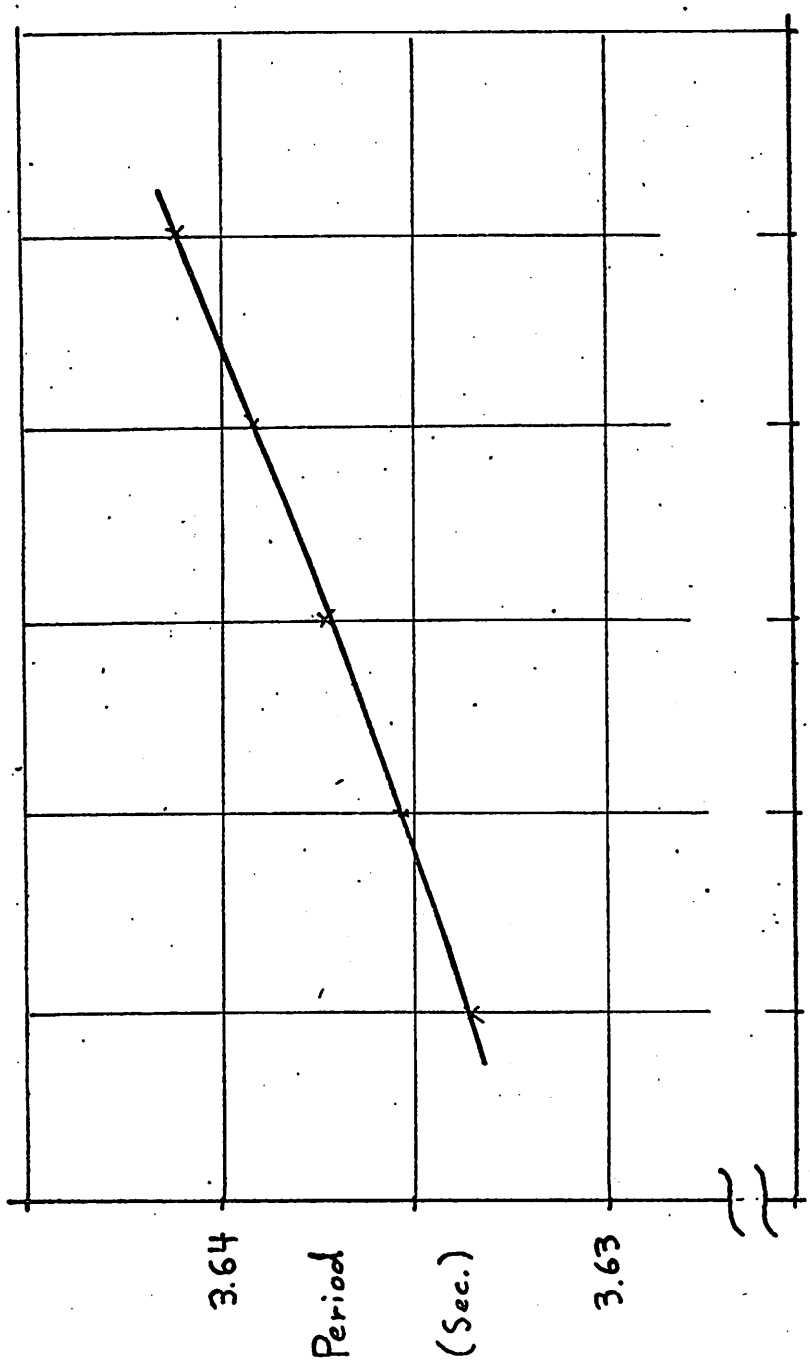

Fig. 3.18 Digital Computer Results, 3rd Order System

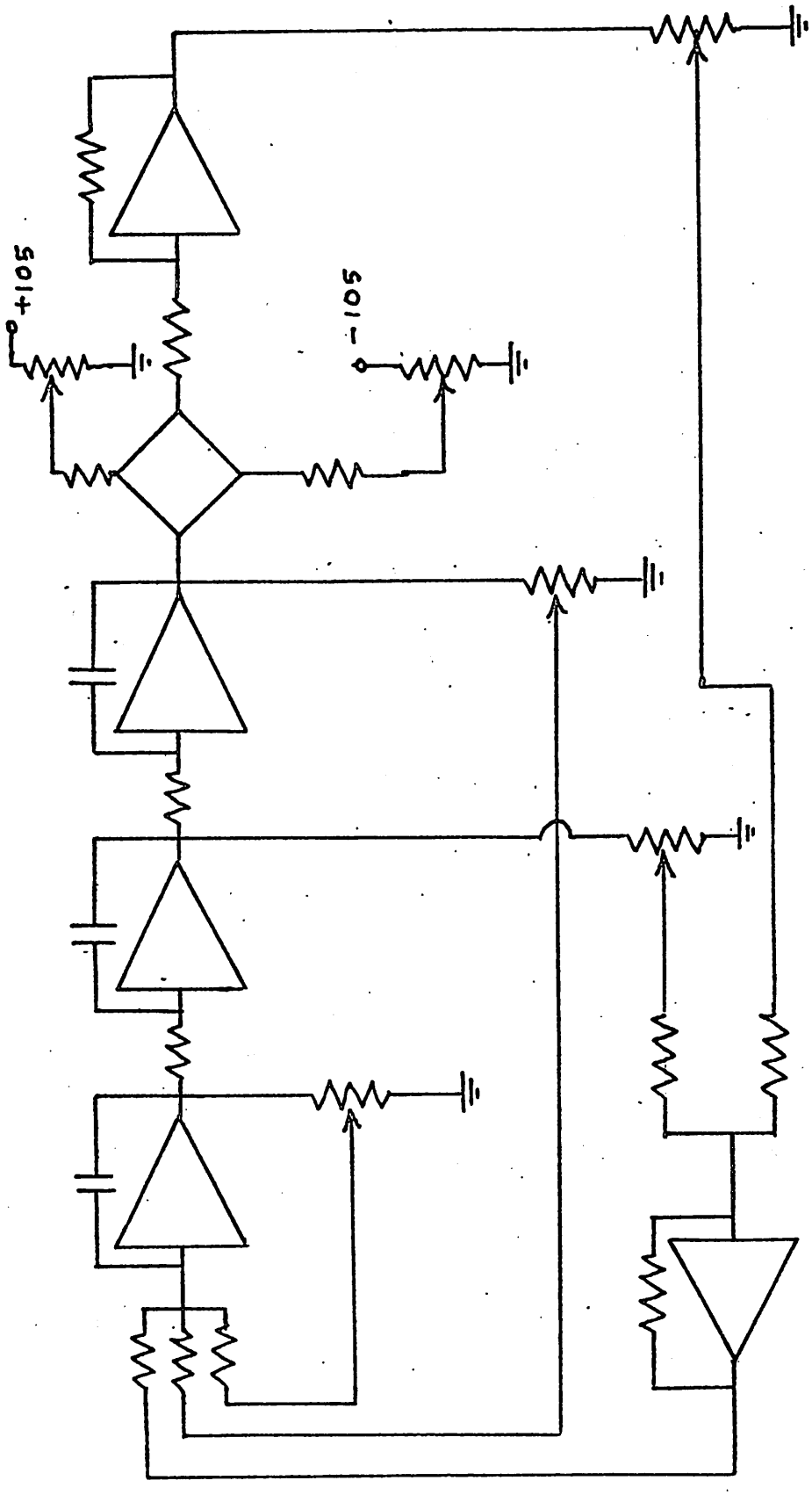

Fig. 3.19 3rd Order Analysis, Analog Computer Setup

IV. TEMPERATURE COMPENSATION OF INTEGRATED OSCILLATORS

4.1 Introduction

The total sensitivity of the basic oscillator is the sum of the linear and nonlinear contributions to the sensitivity as expressed by

$$\gamma_T^{f_o} = \gamma_{TL}^{f_o} + \gamma_{TNL}^{f_o} \tag{4.1}$$

Temperature compensation involves reducing the magnitude of the total oscillator sensitivity $\gamma_T^{f_o}$ that is inherent in the basic oscillator over a specified temperature range. Compensation techniques that modify the linear term $\gamma_{TL}^{f_o}$ of the basic oscillator are called linear compensation techniques and those that modify the nonlinear term $\gamma_{TNL}^{f_o}$ are called nonlinear compensation techniques. The

final compensated oscillator may employ both techniques.

For the oscillators considered in this study, designs are possible that cause the nonlinear contribution $\gamma_{TNL}^{f_o}$ to be negligible compared to the linear contribution $\gamma_{TL}^{f_o}$ in the monolithic realization of the basic oscillator. Therefore, the compensation techniques that are of major interest for these realizations are the linear techniques that minimize the magnitude of $\gamma_{TL}^{f_o}$. It is true that $\gamma_{TNL}^{f_o}$ could be used to compensate the oscillator by offsetting $\gamma_{TL}^{f_o}$, but for the magnitude of $\gamma_{TL}^{f_o}$ encountered in monolithic realizations, this would cause considerable output waveform distortion for oscillators designed to operate over any sizable temperature range. However, situations occur, such as with thin film circuits, where the linear and nonlinear contributions to temperature sensitivity may be of comparable magnitude. In this situation, nonlinear compensation techniques are of interest and so are described briefly in the following section. In the remainder of the chapter, detailed attention is given to linear compensation.

4.2 Nonlinear Compensation

The basic positive feedback oscillators can be modeled adequately by the second-order nonlinear equation

$$\ddot{x} + f(x)\dot{x} + x = 0 \tag{4.2}$$

As is shown in Chapter 3, the sensitivity of the oscillation period

to temperature caused changes in f(o) depends on the form of f(x). For near-harmonic oscillators, the period of oscillation is less sensitive for a van der Pol approximation for the amplifier gain F(x) that determines f(x) than a piecewise linear form of F(x). However, a large amount of negative feedback is usually employed in typical designs to minimize the sensitivity of f(o) to temperature as discussed in Chapter 2. This feedback causes f(x) to have an approximate piecewise linear form in the basic oscillator as shown in Fig. 4.1(a).

The advantages of gain control by negative feedback can be combined with the lower gain sensitivity of the van der Pol approximation by including a diode-resistor network in the amplifier to produce the modified f(x) as shown in Fig. 4.1(b). This modified nonlinearity is shown to have a reduced gain sensitivity in Chapter 3. The required gain curve might be obtained by the use of a circuit such as shown in Fig. 2.23 of Chapter 2.

As is proved in Chapter 3, a zero nonlinear contribution to sensitivity due to temperature caused gain changes cannot be obtained for Lienard's equation as given by Eq. 4.2. In order to achieve a zero of the nonlinear contribution, the second-order nonlinear equation must be of the form

$$\ddot{x} + f(x)\dot{x} + g(x) = 0 \tag{4.3}$$

The computer results of Chapter 3 show that it is possible to select a g(x) such that $\gamma_{TNL}^{f_o}$ is zero. A possible circuit that

would include the reduced gain sensitivity for partial cutoff in f(x) and a compensating g(x) is shown in Fig. 4.2. This circuit depends on the offset voltage of the diode as shown in Fig. 4.3. The approximate forms of f(x) and g(x) for this circuit are shown in Fig. 4.4. From Chapter 3, it is seen that this form of g(x) can offset the gain sensitivity that would be due to f(x) alone. The numerical details of such a realization would depend on the actual circuit. However, this does demonstrate that in principle it is possible to compensate the nonlinear contribution to temperature sensitivity.

4.3 Linear Compensation

Linear compensation reduces the total temperature sensitivity of the oscillator by altering the linear contribution $\gamma_{TL}^{f_o}$. Since it is possible to design a monolithic circuit so that the nonlinear contribution to temperature sensitivity is negligible compared to the inherent linear contribution, the linear compensation techniques of interest reduce the magnitude of $\gamma_{TL}^{f_o}$ of the basic oscillator. Of course, this compensation should be accomplished so that it does not increase the magnitude of $\gamma_{TNL}^{f_o}$.

The basis of linear compensation is to modify the small-signal model of the system to reduce the temperature sensitivity of the dominant natural frequencies of this model. In this respect, linear compensation techniques are applicable to both oscillators and band-pass amplifiers. However, the final formulation may be quite

different for the two since the oscillator inherently contains nonlinear considerations. A temperature sensitive Q in the bandpass amplifier usually is undesirable. However, the same is not true of the oscillator*. The negative Q of the oscillator is the ratio of the negative real part to the imaginary part of the linearized model natural frequency and represents the degree by which the starting condition has been satisfied. The temperature sensitivity of the negative Q for the oscillator then appears in the nonlinear term, $\gamma_{TNL}^{f_o}$, of the temperature sensitivity. This contribution is then in the nonlinear considerations of the design rather than the linear considerations. Therefore, the optimum circuit in the two cases for any given criterion may be quite different.

Linear compensation techniques for the oscillator are divided into two categories. The first of these is based upon a root locus that is shaped so that temperature-controlled gain variations can be used to offset the closed-loop pole temperature sensitivity. This method is based on the work of Gaash[50].

The other method is based on making each of the open-loop poles individually insensitive and then combining the net result in an overall feedback loop that has a desensitized loop gain. The closed-loop system forms the desensitized oscillator. This scheme is called Miller-type compensation because the individual desensitized poles which may appear in minor feedback loops always can be considered as Miller-effect circuits.

---

* Q has the dimensions of energy stored over energy dissapated per cycle and is used as a measure of selectivity in bandpass networks.

4.4 Root Locus Shaping Compensation

The definition of the basic oscillator assures that all the open-loop poles and zeros lie on the negative real axis. With such open-loop pole and zero locations, it is impossible to produce a root locus that has a portion near the imaginary axis in the right-half-plane that lies on a radial from the origin. However, this condition is exactly that required to achieve linear compensation.

A possible design is to provide additional signal paths to remove the above restriction on open-loop pole and zero position. With such a design it may be possible to obtain the required shaping of the root locus. In particular, redundant signal flow paths permit the realization of complex open-loop transmission zeros. As is shown in the example below, these zeros can be used to obtain the desired root locus. For this root locus, temperature-controlled gain can be used to achieve insensitivity.

A single-loop ladder realization of the basic negative feedback oscillator is shown in Fig. 4.5. This circuit has the root locus shown by the solid line in Fig. 4.6. The open-loop gain has been adjusted to give the closed-loop pole position shown. From the results for the linear model in Chapter 3, a temperature increase would cause the root locus and closed-loop poles to shift to the dotted line shown in Fig. 4.6. It can be seen that the open-loop gain, which now controls the position of closed-loop poles on the dotted root locus, cannot be adjusted to return the closed-loop poles to their original position. To make it possible

to return the closed-loop poles to their original position by gain adjustment, the root locus at the higher temperature must still go through the original closed-loop pole positions. Such a root locus is one that has a portion in right-half-plane that lies on a radial from the origin since temperature changes cause the root locus to shift radially.

A possible realization that has the required root locus is the modified negative feedback oscillator shown in Fig. 4.7. In this circuit, the multiple signal path of the bridged-T network permits the realization of complex transmission zeros. This circuit can be adjusted to obtain the root locus and closed-loop poles shown in Fig. 4.8. An increase in temperature shifts the root locus radially inward as shown by the dotted line. If the gain were temperature invariant, the new closed-loop pole position would be

$$s_{oT2} = s_{o_{T1}} + \gamma_T^{s_o} \Delta T \tag{4.4}$$

where ΔT is the temperature increase, $s_{o_{T1}}$ is the original closed-loop pole, and $\gamma_T^{s_o}$ is the temperature sensitivity of s_o due to passive resistor temperature sensitivity, as is discussed in Chapter 3. By Eq. 3.30 of Chapter 3, this becomes

$$s_{o_{T2}} = s_{o_{T1}} - \frac{s_{o_{T1}}}{|s_{o_{T1}}|} \Delta T \tag{4.5}$$

Since the shifted root locus still goes through $s_{o_{T1}}$, it is possible

to add a temperature controlled gain shift to make $s_{o_{T2}} = s_{o_{T1}}$. With the required temperature controlled gain term included, Eq. 4.5 becomes

$$s_{o_{T2}} = s_{o_{T1}} - \left[\frac{s_{o_{T1}}}{|s_{o_{T1}}|} + \gamma_G^{s_o} \frac{\partial G}{\partial T} \right] \Delta T \qquad (4.6)$$

where G is the open-loop gain level. The required gain sensitivity is obtained by setting the bracketted term in Eq. 4.6 equal to zero.

The requirement of root locus shaping is made clear in the example by Eq. 4.6. $\gamma_T^{s_o}$ of Eq. 4.4 is a complex number for the system natural frequencies that produce oscillation. The only parameter in the gain term of Eq. 4.6 that can be complex is $\gamma_G^{s_o}$. Therefore, in order to set the coefficients of ΔT equal to zero, the argument of $\gamma_G^{s_o}$ is a function of both the gain level G which determines the closed-loop pole s_o and the shape of the root locus. The root locus of a basic oscillator cannot satisfy this argument equality condition and thus root locus shaping by the use of a non-basic configuration such as demonstrated in the above example is required.

This form of compensation could also be achieved by the use of a twin-T network. However, a more complicated form than the simple 3-pole twin-T would have to be used.

4.5 Miller Effect Compensation

In the previous section, the closed-loop poles are made temperature insensitive by shaping the root locus and utilizing temperature-

controlled gain variations. No attempt was made to desensitize the open-loop poles. Controlling the open-loop pole sensitivities, however, does represent another alternative to achieve temperature compensation. It is this alternative that is discussed in this section.

If it is possible to make the open-loop poles and the open-loop gain level temperature insensitive, the closed-loop system has temperature-insensitive natural frequencies. It is possible to make each of the open-loop poles temperature insensitive by the temperature compensation method applied in the last section. Each pole is realized individually in a minor feedback loop that has a temperature controlled gain to make the insensitive. The insensitive natural frequency of the closed minor loop then becomes an open-loop pole of the major loop of the overall system. In a single-pole feedback loop, no root locus shaping is necessary over the basic root locus to achieve gain control compensation since both the temperature-induced resistance changes and the controlled gain changes move the pole along the real axis.

The design requirement for temperature compensation of the minor-loop, closed-loop pole is to control the magnitude and sign of the gain temperature sensitivity to offset the inherent pole sensitivity. For the particular overall open-loop pole in question, say p_e, the minor loop requirement for insensitivity of p_e is

$$\gamma_T^{p_e} = \gamma_{G_m}^{p_e} \frac{\partial G_m}{\partial T} \tag{4.7}$$

where p_e is the open-loop pole of the major loop, $\gamma_T^{p_e}$ is the temperature sensitivity of p_e due to the temperature sensitivity of the passive resistor, and G_m is the minor-loop, open-loop gain. This is the zero sensitivity requirement of Eq. 4.6. Now, however, $\gamma_T^{p_e}$ and $\gamma_G^{p_e}$ are both real rather than complex since both can be represented as shifts in position on the real axis for a temperature increment. Therefore, no special root locus shaping is required.

The reason that this form of temperature compensation is called Miller-effect compensation is that all the typical minor loop realizations for a single pole can be considered as Miller-effect circuits. In fact, it is convenient to base the design on Miller-effect circuits. An example in point is the circuit of Fig. 4.9a which might be used to achieve a single, negative-real, temperature insensitive pole. This circuit can be redrawn as shown in Fig. 4.9b where it is recognized as a Miller multiplier of the conductance G_2.

If the circuit of Fig. 4.9 is idealized as shown in Fig. 4.10, the input resistance is of the form

$$R_{in} = R(1+A_v) \tag{4.8}$$

where A_v is the gain of an ideal unilateral voltage amplifier and is assumed real. Further, it is assumed that $R_{in} = \infty$, and $R_o = 0$. The temperature sensitivity of R_{in} is:

$$\gamma_T^{R_{in}} = \frac{1}{R_{in}} \frac{\partial R_{in}}{\partial T} = \gamma_T^R + \gamma_T^{(1+A_V)} \tag{4.9}$$

If A_V is realized so that

$$\gamma_T^{(1+A_V)} = - \gamma_T^R \tag{4.10}$$

then R_{in} has a temperature coefficient equal to zero.

This procedure can be represented schematically as shown in Fig. 4.11 to realize a single pole of Z_{in} at -1/RC. If $\gamma_T^C = 0$ and the diffused resistor has a temperature coefficient $\gamma_T^{R_D}$, the Miller resistance R_M, which is R_{in} of Eq. 4.8, should be such that

$$\frac{d}{dT} (R_D + R_M) = 0 \tag{4.11}$$

or

$$\frac{R_D}{R_D + R_M} \gamma_T^{R_D} + \frac{R_M}{R_D + R_M} \gamma_T^{R_M} = 0 \tag{4.12}$$

This description is the basis of Miller effect compensation which is discussed in more detail in the next section.

4.6 Miller Sensitivity Formulation

In this section, the relations that must be satisfied to realize an insensitive positive feedback oscillator based on Miller

compensation of the basic oscillator are derived. Two configurations that do not change the gain insensitivity requirement of the basic oscillator are developed in detail. The derivations are based on a linear model of the oscillator system.

The parameter of concern is the total differential of frequency with respect to temperature. If there are n temperature sensitive parameters x_n, this total differential is given by

$$d\omega = \left(\frac{\partial \omega}{\partial x_1} \frac{\partial x_1}{\partial T} + \frac{\partial \omega}{\partial x_2} \frac{\partial x_2}{\partial T} + \ldots + \frac{\partial \omega}{\partial x_n} \frac{\partial x_n}{\partial T} \right) dt \tag{4.13}$$

The frequency sensitivity is given by

$$\gamma_T^{\omega} = \frac{1}{\omega} \frac{d\omega}{T} \tag{4.14}$$

As derived in Chapter 2, the basic positive feedback oscillator with no distortion has a frequency of oscillation given by

$$\omega_o^2 = \frac{1}{R_1 R_2 C_1 C_2} \tag{4.15}$$

The compensated oscillator can be realized by making this product invariant with temperature. This can be accomplished by compensation of the capacitances or resistances. Capacitor compensation produces realization problems in the actual final design due to bias considerations to avoid positive feedback at dc. Therefore, resistance compensation techniques are used. A linear sensitivity formulation

based on a harmonic oscillator model is valid for the very low distortion near-harmonic oscillators realized. The distortion is less than 2.5% over the temperature range considered for the actual oscillators.

Both series and shunt resistance compensation are possible. The series resistance compensation technique of Fig. 4.12 is considered first. If the model shown in Fig. 4.13 of the transistor is valid, the total input resistance is given by

$$R = R_a + \frac{R_b}{\beta} \tag{4.16}$$

For the case of equal total R's and C's, the frequency of oscillation is given by

$$\omega = \frac{1}{RC} = \frac{\beta}{(\beta R_a + R_b)C} \tag{4.17}$$

The sensitive parameters are β, R_a, and R_b. Therefore, the quantities of interest are $\partial\omega/\partial\beta$, $\partial\omega/\partial R_a$, and $\partial\omega/\partial R_b$. These are given by

$$\frac{\partial\omega}{\partial\beta} = \frac{R_b}{(\beta R_c + R_b)^2 C} \tag{4.18}$$

$$\frac{\partial\omega}{\partial R_a} = -\frac{\beta}{(\beta R_c + R_b)^2 C} \tag{4.19}$$

$$\frac{\partial \omega}{\partial R_b} = - \frac{\beta}{(\beta R_c + R_b)^2 C} \tag{4.20}$$

This gives

$$\gamma_T^{\omega} = \frac{1}{1 + \beta R_a / R_b} \gamma_T^{\beta} - \gamma_T^{R} \tag{4.21}$$

which is the primary design relation.

For a broad temperature range for insensitivity, it is desired to make d γ_T^{ω}/dT a minimum over the temperature range. d γ_T^{β}/dT is given by

$$\frac{\partial \gamma T}{dT} = - \frac{\partial \gamma_T^{R}}{\partial T} + \left[\frac{1}{1+\beta R_a / R_b} \frac{\partial \gamma_T^{\beta}}{\partial T} - \frac{\beta R_a R_b}{(\beta R_a + R_b)^2} (\gamma_T^{\beta})^2 \right] \tag{4.22}$$

Since $\partial \gamma_T^{R}/\partial T > 0$, $\partial \gamma_T^{\beta}/\partial T < 0$, and $\gamma_T^{\beta} > 0$, all the terms are negative, which means

$$\frac{d\gamma_T^{\omega}}{dT} < 0 \tag{4.23}$$

over any temperature range so the sensitivity can have no zero unless $\partial \delta_T^{R}/\partial T > 0$, this means $d\gamma_T^{\omega}/dT$ is monotonic over the temperature range so that γ_T^{ω} has at most a single zero in this temperature range.

The shunt resistance compensation technique is shown in Fig. 4.14.

In this case, the total input resistance is given by

$$R = \frac{R_a R_b}{\beta R_a + R_b} \tag{4.24}$$

The derivatives of frequency with respect to the sensitive parameters are then

$$\frac{\partial \omega}{\partial \beta} = \frac{1}{R_b C} \tag{4.25}$$

$$\frac{\partial \omega}{\partial R_a} = - \frac{1}{R_a^2 C} \tag{4.26}$$

$$\frac{\partial \omega}{\partial R_b} = - \frac{}{R_b^2 C} \tag{4.27}$$

This gives a frequency sensitivity of

$$\gamma_T^{\omega} = \frac{1}{1+R_b/\beta R_a} \gamma_T^{\beta} - \gamma_T^{R} \tag{4.28}$$

The derivative of sensitivty is given by

$$\frac{\partial \gamma_T^{\omega}}{\partial T} = \frac{1}{1+R_b/\beta R_a} \frac{\partial \gamma_T^{\beta}}{\partial T} + \frac{R_b/\beta R_a}{(1+R_b/\beta R_a)^2} (\gamma_T^{\beta})^2 - \frac{\partial \gamma_T^{R}}{\partial T} \tag{4.29}$$

which may have a zero. This means that γ_T^{ω} may have more than one zero in the temperature range for the shunt case. However, as it turns out for the actual design numbers as shown in Chapter 5, the series case given a smaller total derivation over the temperature range of 0^{o} C to 65^{o} C and is, by this measure, a more nearly optimum design.

The transistor model shown in Fig. 4.13 which is used in the immediately preceding derivation yields results that are straightforward to interpret in relation to an insensitive design, but it overlooks many potentially important parameters of a transistor and therefore does not indicate any criterion for optimum transistor realization in the monolithic circuit. If the transistor model of Chapter 2 is introduced to the circuit of Fig. 4.12, the Miller effect circuit that results is shown in Fig. 4.15. In this circuit, the series base resistance is included in G_f. The emitter-to-collector input impedance of the more complete transistor model of the Miller effect circuit is found to be

$$Y_{EC} = \frac{g_m(G_f g_c + y_\mu(G_f+g_c)) + y_\pi(G_f g_c + y_\mu(G_f+g_c) + g_o(G_f+g_c)) + y_\mu g_o(G_f+g_c) + G_f g_c g_o}{y_\pi(g_c+g_o+y_\mu) + y_\mu(G_f+g_c+g_o) + g_m y_\mu + G_f(g_c+g_o)} \qquad (4.30)$$

The model applied to the sensitivity derivation just done assumes that only the first term of numerator and denominator of Eq. 4.30 is significant which gives the input impedance $Y_{in} = \beta_o G_f$ as stated

in Eqs. 4.16 and 4.24. In typical designs, G_f is on the order of 10^{-4} mhos and $\beta_o \approx 70$. For a well designed transistor that has low basewidth modulation effects, and high collector series resistance $1/g_c$, Eq. 4.30 may be approximated by[51]

$$Y_{EC} \approx \frac{g_m g_c (G_f + y_\mu)}{y_\pi g_c + g_m y_\mu} \tag{4.31}$$

If the oscillation frequency ω_o is less than ω_β of the transistor, Eq. 4.31 may be written:

$$Y_{EC} \approx \frac{g_m g_c (G_f + g_\mu)}{g_\pi g_c + g_m} \tag{4.32}$$

Since $g_m g_\mu$ is equal to $g_\pi g_o$ and $g_\mu = g_o/\beta_o$, Eq. 4.32 becomes

$$Y_{EC} \approx \frac{g_m g_c (G_f + g_o/\beta)}{g_\pi (g_c + g_o)} \tag{4.33}$$

For the circuits realized in this laboratory, $g_o < 2\times10^{-5}$ mhos and $g_c > 2\times10^{-3}$ mhos. Therefore Eq. 4.33 is well approximated by

$$Y_{EC} \approx \beta G_f$$

for $G_f < 10^{-5}$ mhos which is just the assumption required to get Eq. 4.16.

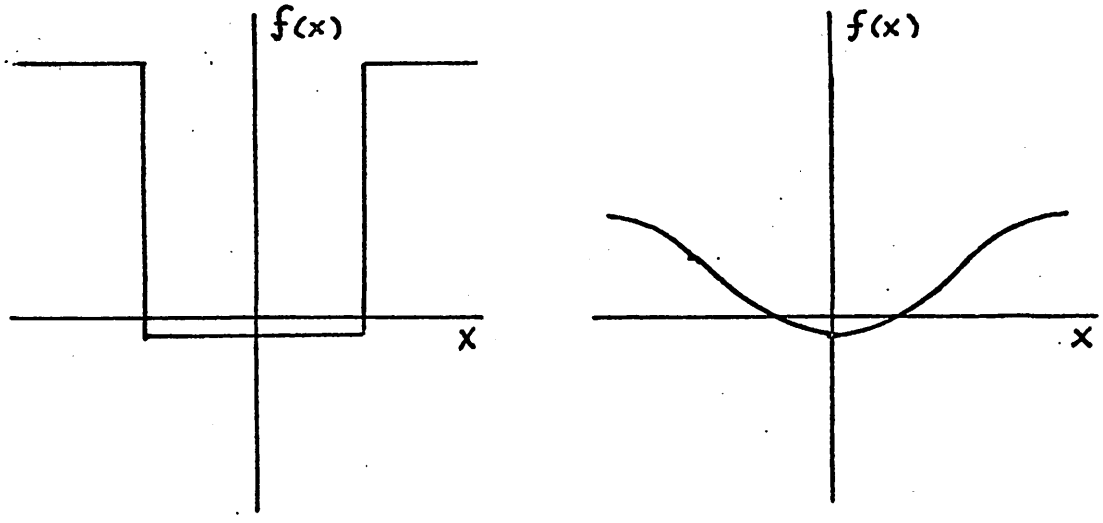

(a) Piecewise Linear Gain (b) Modified Gain

Fig. 4.1 Second-Order Lienard's Equation Nonlinearity f(x)

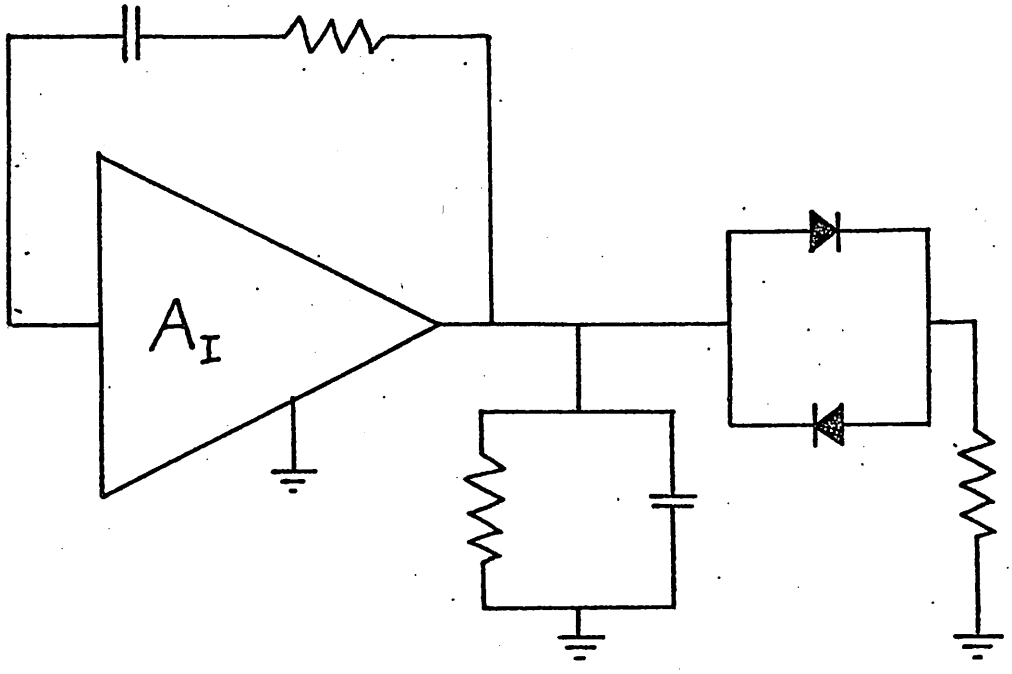

Fig. 4.2 Compensated Oscillator

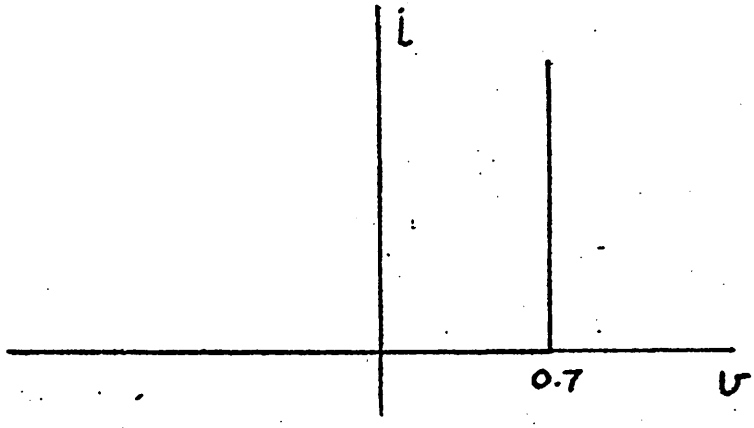

Fig. 4.3 Idealized Diode Characteristic

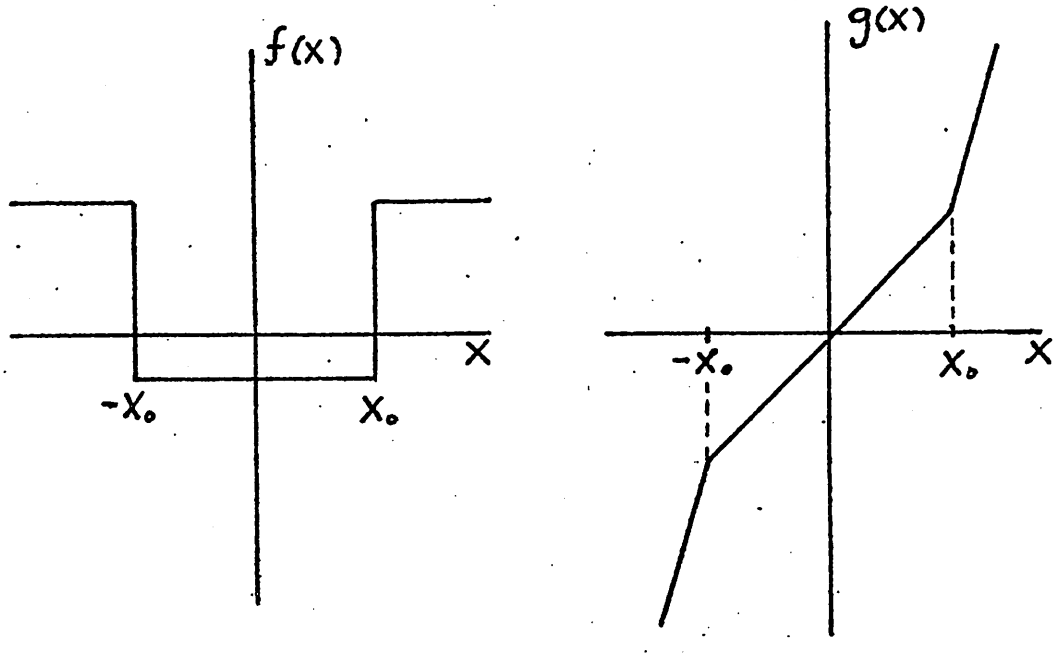

Fig. 4.4 Nonlinear Terms f(x) and g(x) for Compensated Oscillator

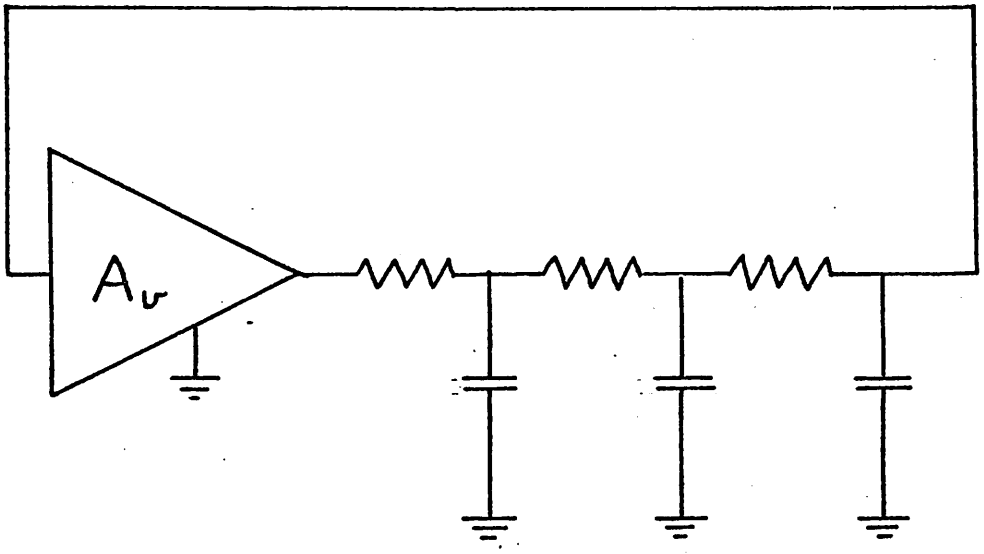

Fig. 4.5 Ladder-type Negative Feedback Oscillator

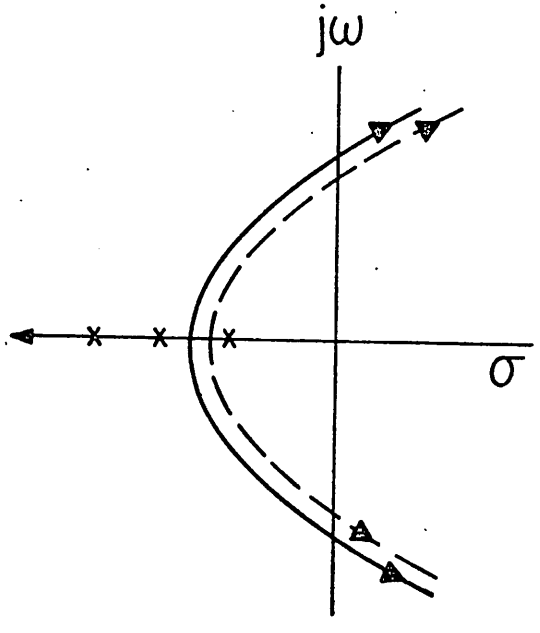

Fig. 4.6 Root Locus of Basic Negative Feedback Oscillator, Temperature Variations

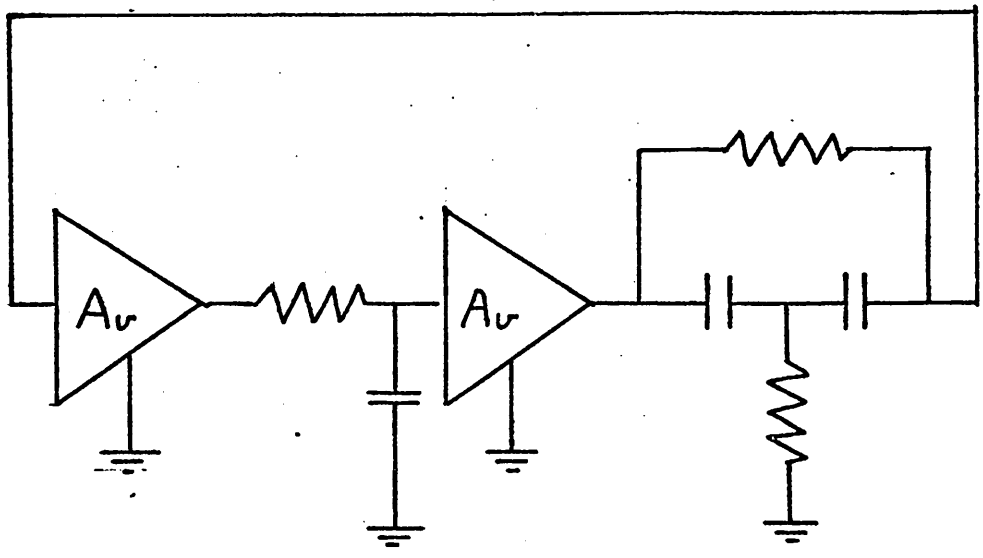

Fig. 4.7 Multipath Negative Feedback Oscillator

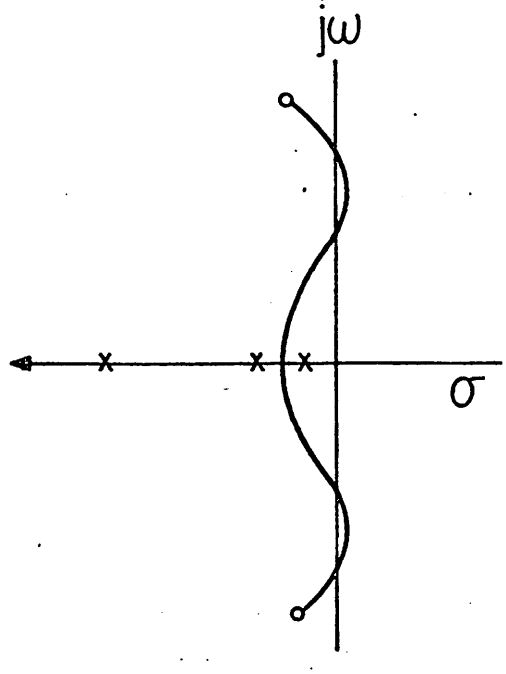

Fig. 4.8 Root Locus for Non-basic Negative Feedback Oscillator

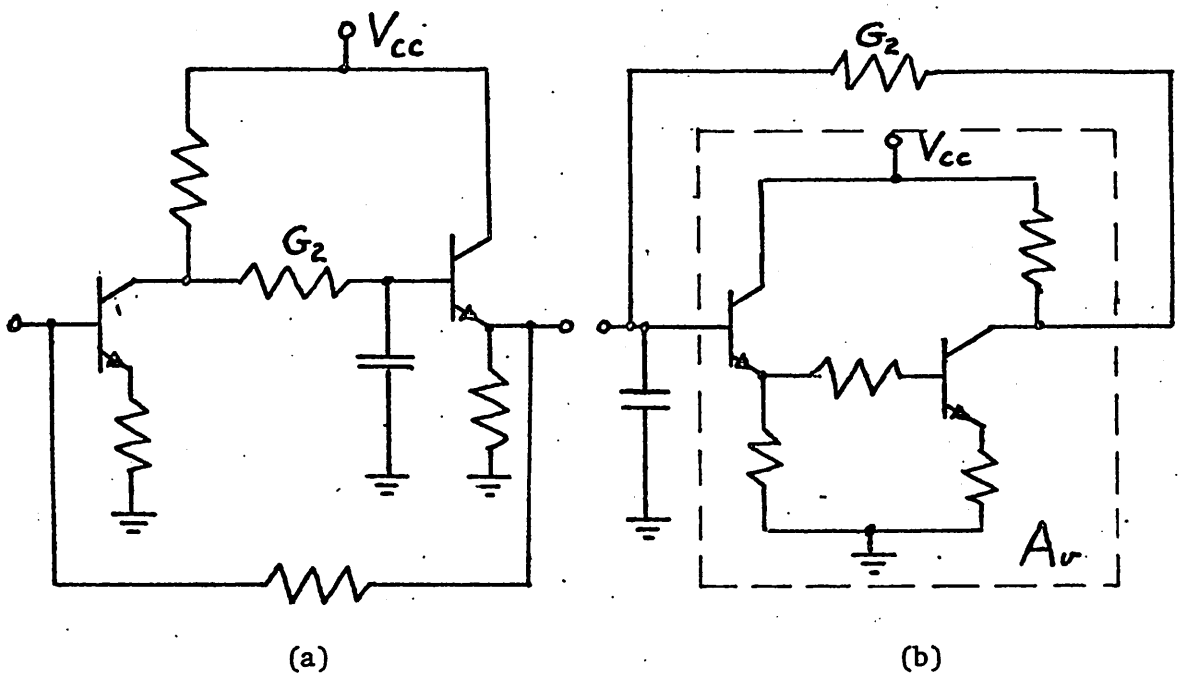

Fig. 4.9 Compensated Pole Realization Circuit

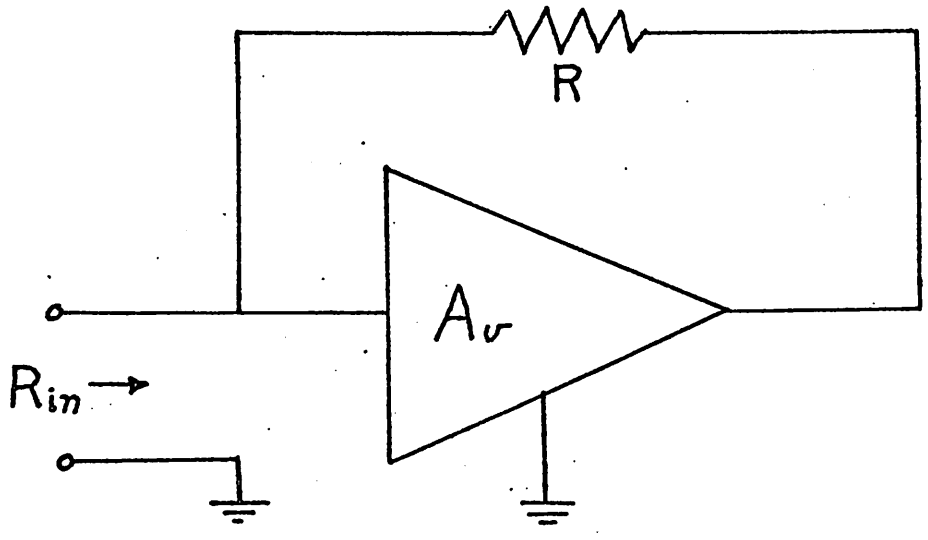

Fig. 4.10 Idealized Miller Realization

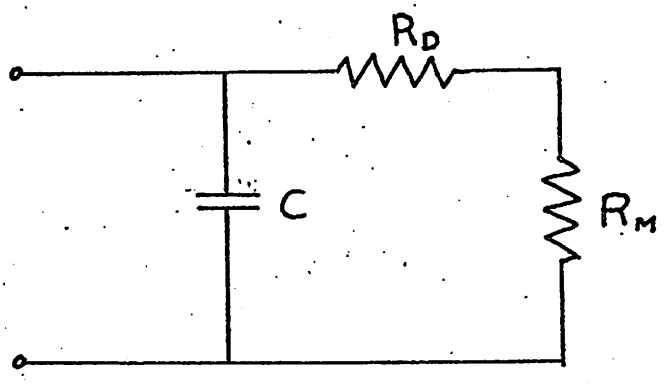

Fig. 4.11 Compensated Pole

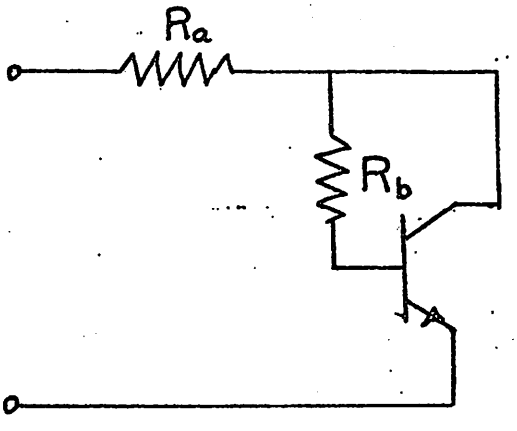

Fig. 4.12 Series Miller-type Compensation

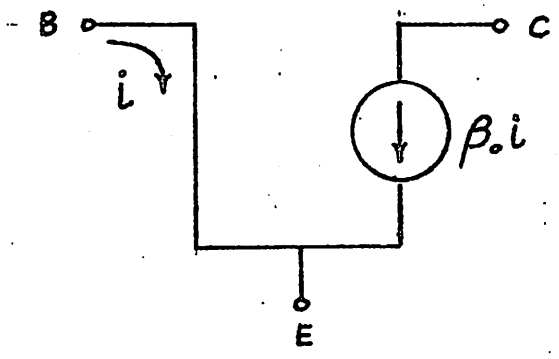

Fig. 4.13 Simple Current Transistor Model

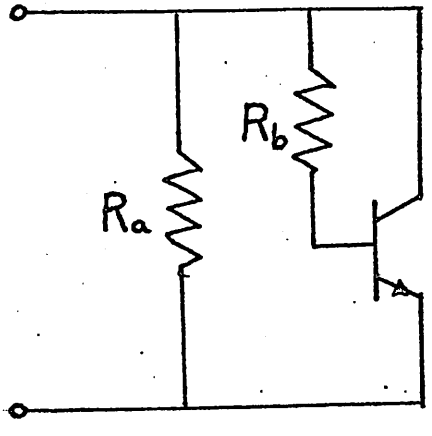

Fig. 4.14 Shunt Miller-type Compensation

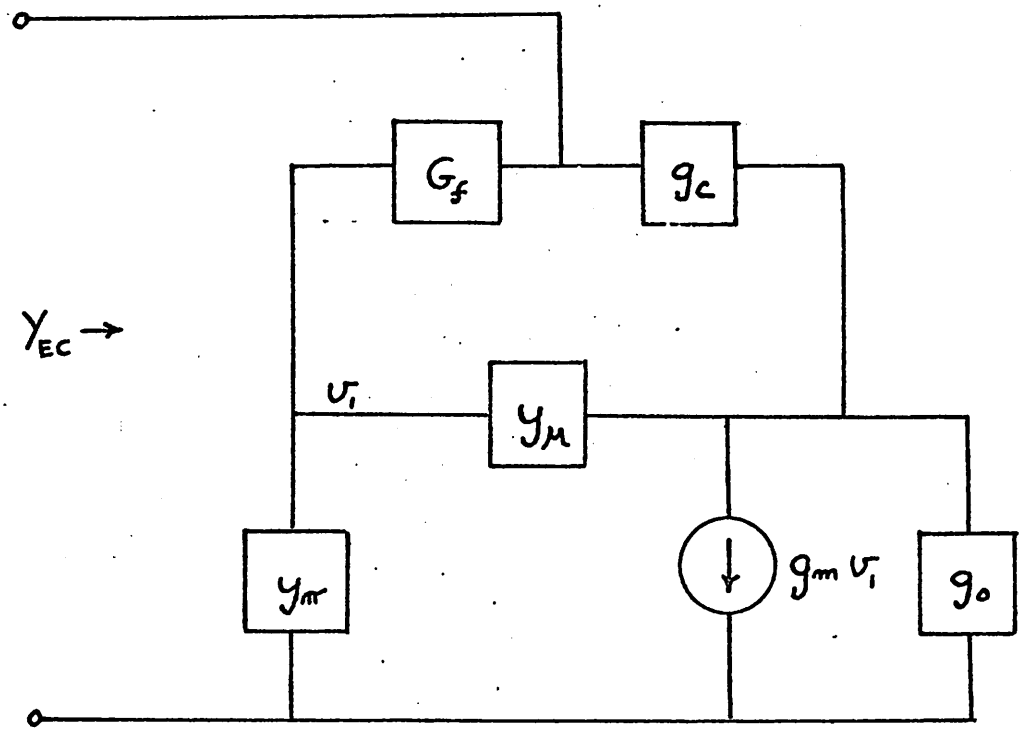

Fig. 4.15 Total Miller-type Compensation Model

V. INTEGRATED OSCILLATOR REALIZATIONS

5.1 Introduction

This chapter describes the actual integrated monolithic realization of both compensated and uncompensated oscillators. The results of experimental measurements on these oscillators are used to justify the assumptions and verify the conclusions of the theoretical results of the preceding chapters. Three different oscillators are realized, two of which are uncompensated and one of which is compensated. All three are positive feedback configurations. The first oscillator is the basic Wien-type uncompensated oscillator described and analyzed in Chapter 3. The second oscillator is a non-basic, uncompensated oscillator based on a modification of the first oscillator. The third oscillator is a compensated version of the first oscillator. Before a detailed description of the experimental investigation of these oscillators is given, a description of some of the laboratory considerations and techniques is provided.

5.2 Laboratory Considerations

There are two distinct considerations in the laboratory realizations of these integrated circuits. The first is physically designing the circuit elements of the realization so that they have acceptable circuit performance. This acceptable circuit performance implies the realized device is well approximated by an acceptable model. The other consideration is in obtaining adequate yields. In general, as the circuit area goes up, the yield goes down. The oscillators realized here have an area of 80×80 sq. mils which is large and gives low yields. Therefore, processing steps involving multiple masks and other special techniques described below are required to obtain non-zero yields for these circuits. Laboratory considerations concerning both yields and adequate circuit element performance are described in the following two sections.

5.3 Layout and Processing for Circuit Element Design

The circuit elements used in the monolithic realizations are bipolar transistors, diffused resistors and MOS capacitors. Some of the considerations of these circuit elements as monolithic components are discussed in Section 2.6 of Chapter 2, where it is pointed out there that the diffused resistors appear as lumped elements at the frequencies of interest. The elements that are most likely to have unsatisfactory performance are the bipolar transistors and the MOS capacitors as discussed below.

The model proposed for the monolithic bipolar transistors in Chapter 2 is repeated in Fig. 5.1. The processing affected parameters that are of interest are the collector series resistance $1/g_c$ and the basewidth modulation factor which determines y_μ and g_o of Fig. 5.1. The most desirable transistor is one with very little basewidth modulation and a low series collector resistance[53].

The collector series resistance is high in the transistors realized in this laboratory (300-1000Ω) because of the lack of a buried layer capability[54]. A possible method to reduce the collector series resistance might be to decrease the collector material resistivity. As the n-type collector material decreases in resistivity, the collector series resistance decreases, but so does the basewidth modulation factor and the collector breakdown voltage. Therefore, this is not a desirable way to minimize the collector series resistance. The collector region bulk resistivity is usually chosen as a compromise between a minimum collector series resistance and a reasonable base resistivity profile that exhibits negligible basewidth modulation (r_o > 20kΩ). Another method to reduce collector series resistance that might be tried is using a thicker expitaxial layer. This has the disadvantage that it increases the collector to substrate parasitic capacitance C_o by increasing the isolation wall area.

There are steps that can be taken to decrease the collector series resistance without having some of the drawbacks mentioned above. One is to surround the base diffusion region with an n^+

diffusion as shown in Fig. 5.2. Another is to decrease the physical dimensions of the transistor. A decrease in the surface area of the transistor base region with a close spacing of the n^+ ring decreases the bulk series resistance. The amount of this reduction is limited by the fabrication facilities, such as camera resolution in the mask producing setup and mask alingment control. The actual dimensions used are indicated in Fig. 5.2.

The vertical dimension of the transistor can be reduced by modifying the predeposit and diffusion processing. The more shallow structure has a lower collector series resistance since the thickness of the region under the base region is greater. This modification is equivalent to a thicker expitaxial layer, except that it does not change the collector to substrate parasitic capacitance C_o.

Transistors realized in this laboratory in a 12μ epitaxial layer with a 3.5μ collector junction depth and a single collector stripe have had a collector series resistance on the order of 1kΩ. Transistors made with the geometry of Fig. 5.2 according to the schedule in Table 5.1 have a collector junction of 2.5-3.0μ and a collector series resistance of 300Ω.

The other circuit element of importance is the MOS capacitor. This capacitor is formed by an aluminum coating over an oxide layer covering the silicon expitaxial layer as shown in Fig. 5.3. The circuit area that is to be capacitive is exposed in the emitter predeposit step so that the expitaxial layer in this area is an n^+ on n region. This minimizes the parasitic series resistance asso-

ciated with the capacitor due to the bulk resistance of the epitaxial layer that forms the bottom plate.

In order to obtain the capacitance values desired, a six mask process is adopted. In this way, a very thin oxide is creased in the capacitive areas which increases the capacitance realized from .06 pF/mil^2 to .24 pF/mil^2. The value of capacitance for 1500 Å of oxide is .24 pF/mil^2 and this is about the minimum oxide thickness possible for good yields.

5.4 Processing for Yield Improvement

Circuit failures are found to be due mainly to pinholes appearing in the oxide at some point in the processing. These pinholes can cause circuit failure by shorting p-type regions in the circuit to the substrate by p-type pipes. These pipes are formed through the pinholes during the isolation processing steps. Shorting of the aluminum interconnection pattern through a pinholes to the circuit can also occur. The former is the major cause of transistor and resistor failure and the latter is the major cause of MOS capacitor failure.

The pinholes causing these problems are not so much due to faults occuring during oxide growth as to photo-resist processing failures. These photo-resist failures occur in two ways: one is unintended dark spots in the final mask due to a faulty emulsion or dirt. The other problem is the appearance of flaws in the photo-resist coating due to dirt or mechanical damage.

To avoid the p-type pipes formed accidently in the isolation process, a dual mask system is used for the isolation predeposit photo-resist exposure. After the initial oxide is grown on the wafer, an isolation pattern is exposed and partially etched. The wafer is then returned to the furnace for further oxide growth. After the wafer is re-coated with photo-resist, the second isolation pattern is exposed twice through different masks with the identical pattern. Alignment is achieved by using the isolation pattern already partially etched into the oxide. In this way, as long as the flaws in the two masks do not coincide, mask failures do not occur.

Faults in the photo-resist are controlled by careful filtering of the photo-resist solution. Precautions are taken to avoid possible sources of dirt to keep the mask and wafer dirt free. In addition, a significant yield improvement for MOS capacitors can be obtained by coating the capacitor areas with additional photo-resist after the initial photo-resist layer has been exposed and developed but before etching the oxide.

A typical composite processing schedule is contained in Table 5.1.

5.5 Uncompensated Oscillator Realizations

The uncompensated oscillators are based on two of the positive feedback oscillator configurations introduced in Chapter 2. One

of these configurations is a basic form and is a current amplifier, Wien-type oscillator. The other is a non-basic modification of this configuration. The Wien-type oscillator is discussed first.

The basic Wien-type oscillator shown in Fig. 5.4 is considered first. The open-loop transfer function is Eq. 2.15 of Chapter 2. This equation is

$$T_I = \frac{A\, s/R_1C_2}{s^2 + (1/R_1C_1 + 1/R_2C_2 + 1/R_1C_2)s + 1/R_1R_2C_1C_2} \tag{5.1}$$

The starting condition is

$$A \geq 1 + \frac{R_1}{R_2} + \frac{C_2}{C_1} \tag{5.2}$$

If the equality sign holds, harmonic oscillation occurs at a frequency

$$\omega_o^2 = \frac{1}{R_1R_2C_1C_2} \tag{5.3}$$

For a very low distortion, near-harmonic mode of oscillation, Eq. 5.3 gives a very close approximation to oscillation frequency. In Chapter 3, it is shown from the expression for the current gain of the linearized amplifier (Eq. 3.42) that the nonlinear contribution to temperature sensitivity is on the order of 50 ppm/^{o}C. This is more than an order of magnitude less than the linear contribution

and therefore the temperature sensitivity can be approximated by linear contribution derived from Eq. 5.2. The MOS capacitors have a temperature sensitivity less than 50 ppm/^{o}C over the entire temperature range as shown in Fig. 3.3 of Chapter 3. Since this is a negligible contribution, the temperature sensitivity is found directly from Eq. 3.10 which is derived from Eq. 5.3. It is

$$\gamma_T^{f_o} = - \gamma_T^{R} \tag{5.4}$$

The actual monolithic realization had the circuit values shown in Fig. 5.4 which were determined by computer-aided analysis of a complete circuit model for near-harmonic oscillation. The actual oscillator was realized by removing the compensation elements from a compensated oscillator. The monolithic realization, which is shown in Fig. 5.5, had an oscillation frequency of 140kHz at 27^{o}C. The design value of the diffused resistors was 5% greater than the actual values shown in Fig. 5.3. With V_{CC} = 12.0V, I_{dc} = 6 ma and the dc input power to the circuit was approximately 90 (mw). The amplitude of the output at the collector of T2 was 3 volts peak.

The oscillation frequency dependence on temperature that was experimentally measured and that predicted by Eq. 5.5 from measured resistor sensitivity data are both shown in Fig. 5.6. The total frequency deviation of the oscillator is 11.5% over the temperature range 0^{o}C to 65^{o}C. The experimental and predicted results shown in

Fig. 5.6 corresponds well and indicate that the assumptions used to obtain Eq. 5.4 are reasonable.

The second oscillator considered is the uncompensated non-basic configuration shown in Fig. 5.7. This non-basic oscillator is analyzed in Chapter 2 and has the closed-loop transfer function of Eq. 3.10 which is repeated here.

$$Z_{21} = \frac{V_2}{I_1} = \frac{\Delta_{12}}{\Delta} \tag{5.5}$$

where Δ is the determinant of the nodal equations and found to be

$$\Delta(s) = g_{m1}g_{m2} \left[\frac{G_1+C_1s}{G_1C_1s} \quad G_E - G_L \ (G_2+G_2s) \right] \tag{5.6}$$

The circuit elements indicated in Eq. 5.7 are shown in Fig. 5.7. As discussed in Chapter 2, Eq. 5.6 is the dominant term of the determinant Δ by an order of magnitude. The natural frequencies of the system are found by setting $\Delta = 0$. The real part is set equal to zero to obtain harmonic oscillation and this requires for $G_1 = G_2 = G$, and $C_1 = C_2 = C$ that $G_E = 2G_c$. The frequency of oscillation is then

$$\omega_o = \frac{G}{C} \tag{5.7}$$

Again, if the resistors track closely with temperature and the oscillation is near-harmonic, Eq. 5.7 is a good approximation and the linear

contribution to temperature sensitivity is an adequate description of the oscillator performance. This is given by Eq. 5.4 which is

$$\gamma_T^{f_o} = -\gamma_T^R \tag{5.8}$$

The final circuit values are chosen by computer-aided analysis of a complete circuit model to achieve near-harmonic oscillation. The circuit model of the transistors used in the analysis was the intrincis hybrid π model with an added collector to substrate (ground) capacitance of 10 pF and series base resistance r_x of 50Ω. The circuit was designed to operate at 6 ma of input current at V_{CC} = 10V. The design oscillation frequency was 320 kHz with the elements of the RC frequency selective network having the values C = 100 pF and R = 5kΩ. The MOS capacitor area was chosen on the basis of an assumed .06 pF/mil^2. For the oxide thickness of 1500 Å used, the capacitance per unit area was .24 pF/mil^2. This is equivalent to an 80 kHz frequency of oscillation if R = 5 kΩ. The actual values of feedback R achieved were 5.8 kΩ, 15% higher than the design value. This corresponds closely to the actual oscillation frequency of 65.5 kHz.

The actual circuit values are shown in Fig. 5.7 and the monolithic circuit is shown in Fig. 5.8. The circuit has an oscillation frequency of 65.5 kHz at 27°C. The total frequency deviation over the temperature range of 0°C to 65°C is 13.5%. A comparison of actual

measured oscillation frequency dependence on temperature and that predicted from measured resistor sensitivity is shown in Fig. 5.9. Again, it is seen that the two compare well and the approximation to obtain Eq. 5.8 is reasonable.

The oscillation frequency dependence on temperature for f_o = 200 kHz was also measured by replacing the MOS capacitors with external, zero temperature coefficient capacitors. Again the relation of Eq. 5.8 held to within 10%.

The transfer characteristic of the amplifier was measured to determine the 3 db point with the positive feedback loop and MOS capacitors removed. The amplifier was driven by 4 kΩ current source and the voltage output on the collector of T2 was measured. (The input impedance of the amplifier measured as 50Ω at 200 kHz.) The 3 db point was found to be 2.2 MHz.

5.6 Selection of Compensation Technique

As is discussed in Chapter 4, linear compensation is more desirable than nonlinear compensation for the oscillator considered here. Moreover, the linear compensation technique selected should not increase the nonlinear contribution to temperature sensitivity. For root locus shaping, the closed-loop poles would have moved on the root locus to compensate for the 12% radial shift of the locus over the temperature range. It is difficult to find a straightforward circuit that can provide this radial closed-loop pole movement on

the locus and therefore this compensation method is not used. The Miller compensated realization is selected as best satisfying the requirement for no increase in the nonlinear contribution with a minimum complexity realization. If for the positive feedback oscillator the frequency determining resistors are both realized by identical Miller-type desensitizing schemes, their ratio remains invariant. For a realization of the oscillator as a voltage or current transfer type, the gain requirement is thus independent of temperature. As is pointed out in Chapter 3, amplifiers which have an insensitive gain are straightforward to realize.

Miller compensation of the capacitors is not used because of the requirement of zero open-loop transmission at dc to avoid possible bias instability. Therefore, Miller compensation of the resistors, which has been analyzed in the last chapter, is the basis of the design selected.

5.7 Design and Performance of the Compensated Monolithic Oscillator

The series of the Miller compensated resistance is selected over the shunt form because, for the element sensitivities encountered, it is possible to have a smaller total deviation of frequency over the temperature range considered for the series form. The linear contribution to temperature sensitivity for the series form shown in Fig. 5.10 is, by Eq. 4.21 of Chapter 4,

$$\gamma_T^{f_o} = \frac{R_b}{\beta R_a + R_b} \gamma_T^{\beta o} - \gamma_T^{R} \tag{5.9}$$

The design values of temperature sensitivities at 30°C are $\gamma_T^{\beta} = 6000$ ppm/°C and $\gamma_T^{R} = 1800$ ppm/°C which are based on experience. Setting $\gamma_T^{f_o} = 0$ gives

$$1 + \beta R_a/R_b = \gamma_T^{\beta o}/\gamma_T^{R} = 3.34 \tag{5.10}$$

Eq. 5.10 gives the value $R_b = 30R_a$ for $\beta_o \approx 70$. The resistance ratio is determined well by geometry control.

The circuit was designed to have an operating point of 2.0 ma in T1, 0.5 ma in T2 and T4, and 1.0 ma in T3. The design values for R_a and R_b were $R_a = 2$ kΩ and $R_b = 60$ kΩ. Taps were provided on R_a and R_b to provide adjustment so that the R_a would be set equal to 2.5 kΩ and $R_b = 50$ kΩ.

The realization had $\beta_o = 55$ and $R_b = 78$ kΩ. To make a zero of sensitivity near room temperature, the tap on R_a was chosen so that $R_a = 3.3$ kΩ (2.5 kΩ design). The final circuit values of the actual integrated realization are shown in Fig. 5.9. The monolithic circuit is shown in Fig. 5.11. With $V_{CC} = 15.0$V, I_{dc} of the power supply was approximately 3 ma. This corresponds to a power input of 45 mw. The oscillation frequency is 130 kHz with an output amplitude of 2.0v p-p. The temperature sensitivity and measured distortion over the temperature range o°C to 65°C is shown in Fig. 5.12. The

distortion was measured with an H.P. distortion meter that filtered out the fundamental and measured remaining RM7 voltage. The total frequency deviation is 2.4%. This is seen that the Miller compensation produces a zero of temperature sensitivity when the linear and nonlinear contribution cancel over the mid-temperature range. There is a reduction by a factor of 5 of the total frequency deviation over the temperature range $0^{o}C$ to $65^{o}C$.

No.	Step	Atm.	Temp. °C	Time - min.	Comment
1	Initial oxide	Steam	1175	20	-
2	Initial Iso. Pattern Exp. + Etch	-	-	-	Isolation Pattern
3	Isolation oxide	Steam	1175	20	
4	Double Exp. Iso. Patrn. + Etch	-	-	-	-
5	Iso Predep.	N_2+B_2H_2	985	60	
6	Iso. Drive-in	O_2	1175	5	
		N_2	1175	15 hrs.	
		Steam	1175	10	
		N_2	1175	3	
7	Single Exp. + Etch.Base Resistors	-	-	-	-
8	P Predep.	N_2+B_2H_6	950	20	60-70Ω/□
9	HF rinse (12%)				
10	Drive-in p-regions	Steam	1150	10	
		N_2	1150	90	~160Ω/□

Table continued on next page

No.	Step	Atm.	Temp. ^{o}C	Time - min.	Comment
11	Single Exp. Etch emitter, n^+ regions	-	-	-	
12	n^+ predep.	N_2 $+P_3N_5$	950	40	~7Ω/□
13	HF Rinse (12 1/2%)				
14	MOS oxide	Wet O_2	1050	15	3700 Å
15	Single Exp. MOS pattern + etch	-	-	-	Etch in oxide etch using color to determine oxide thickness
16	Drying	N_2	1050	5	
17	Double Expo. Etch windows	-	-	-	Extra PR coat
18	Emitter trim	N_2	1100	5	As needed
19	Metalization	-	-	-	-
20	Sinter	N_2	525	30	-

Table 5.1 Typical Processing Schedule

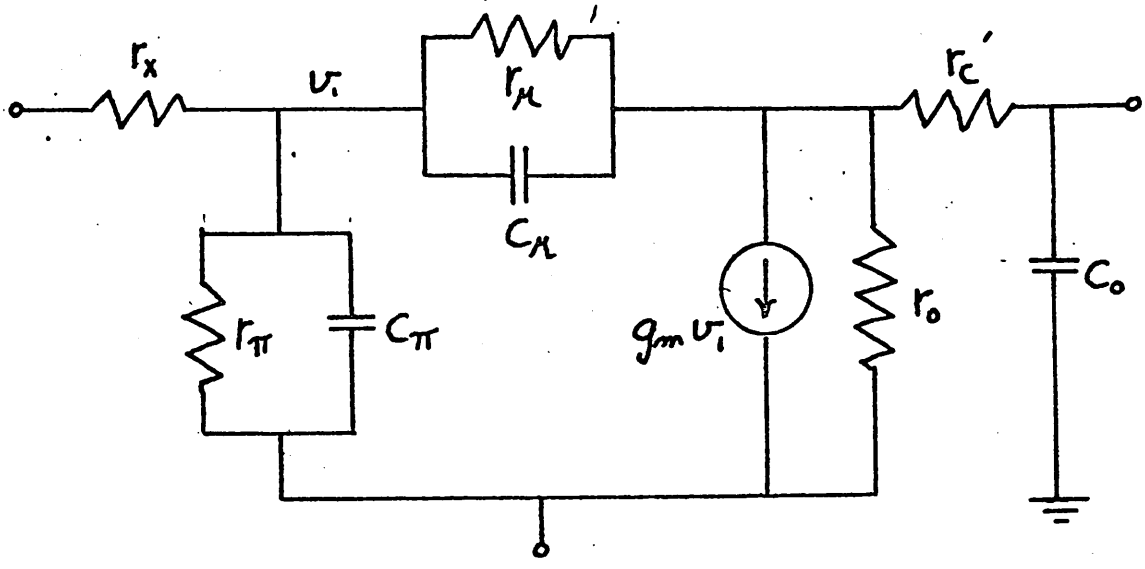

Fig. 5.1 Monolithic Bipolar Transistor Model

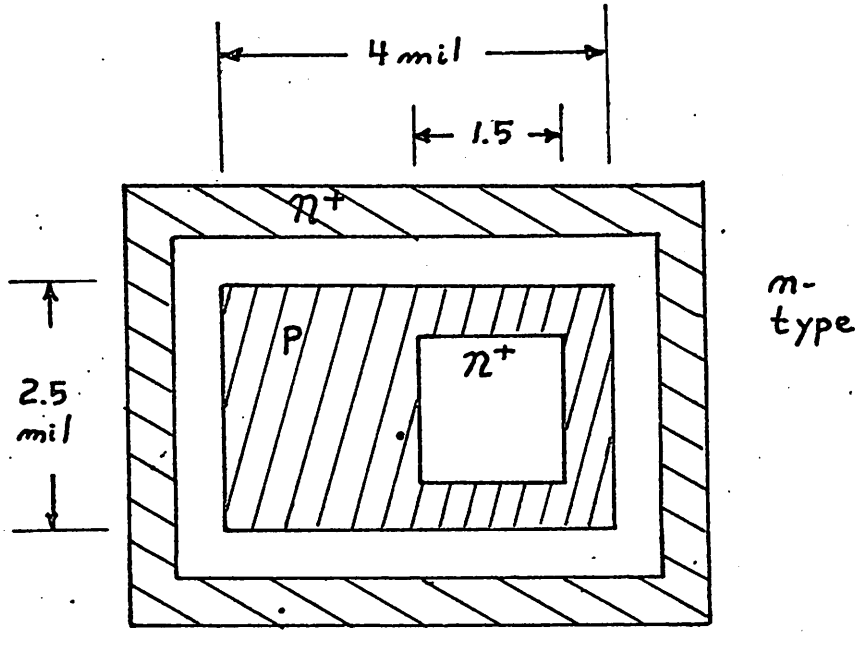

Fig. 5.2 Monolithic Bipolar Transistor, Physical Layout

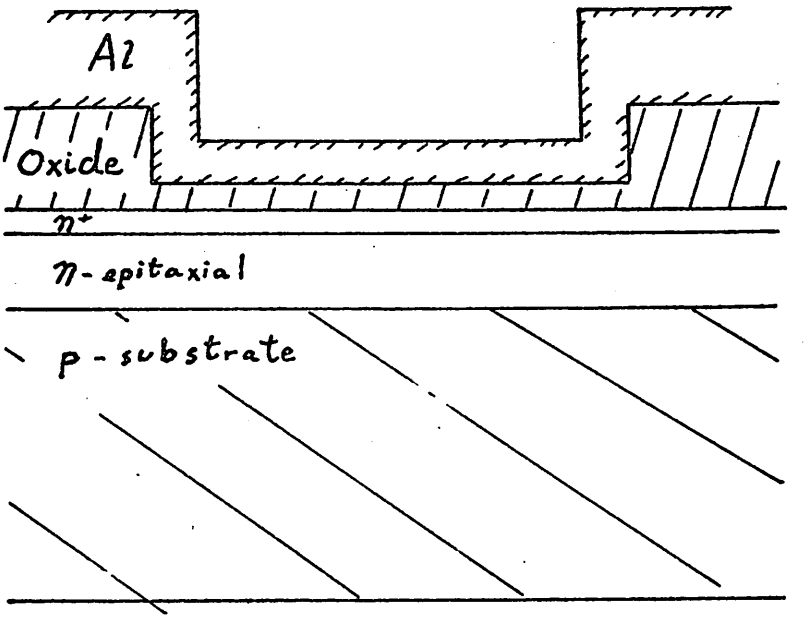

Fig. 5.3 MOS Capacitor Structure

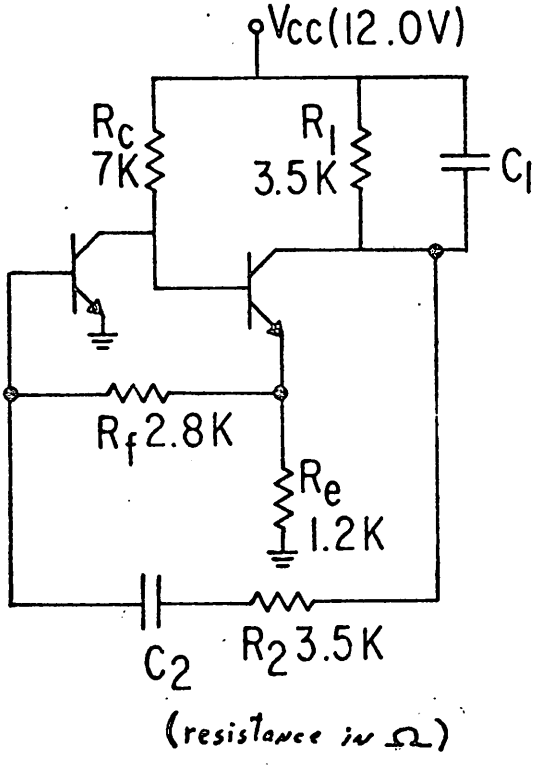

Fig. 5.4 Current Amplifier, Wien-type Oscillator

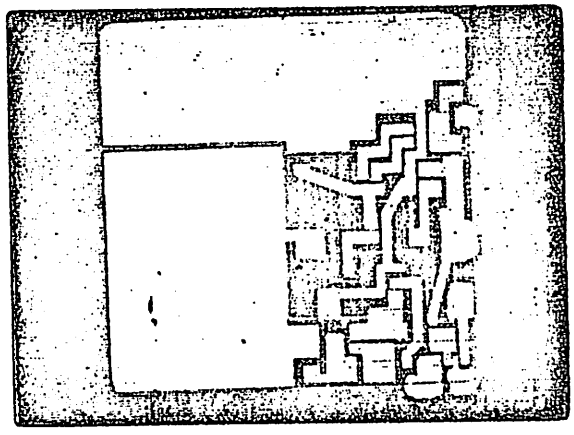

Fig. 5.5 Monolithic Realization of Wien-type Oscillator

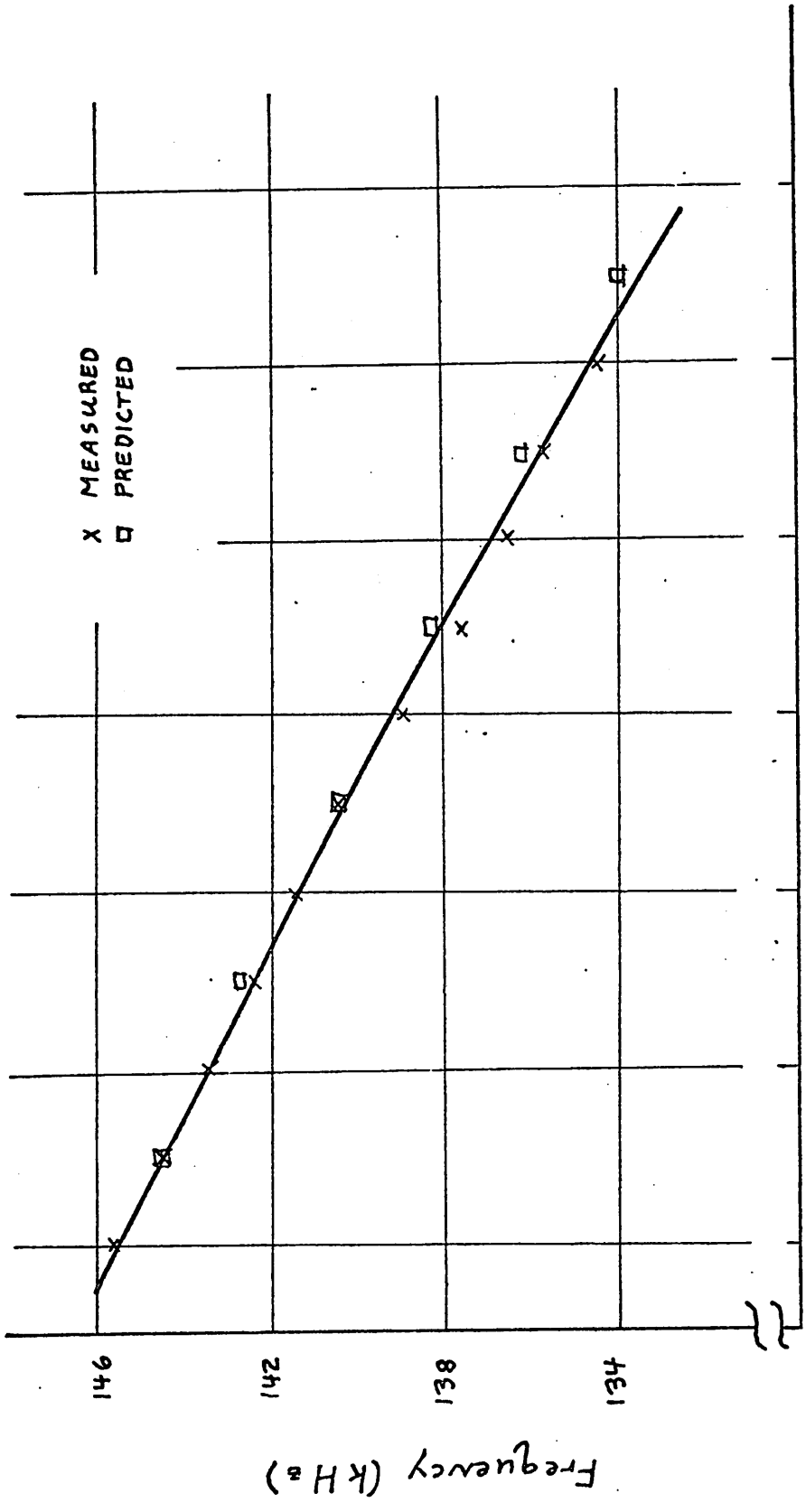

Fig. 5.6 Measured and Predicted Wien-type Oscillator Temperature Sensitivity

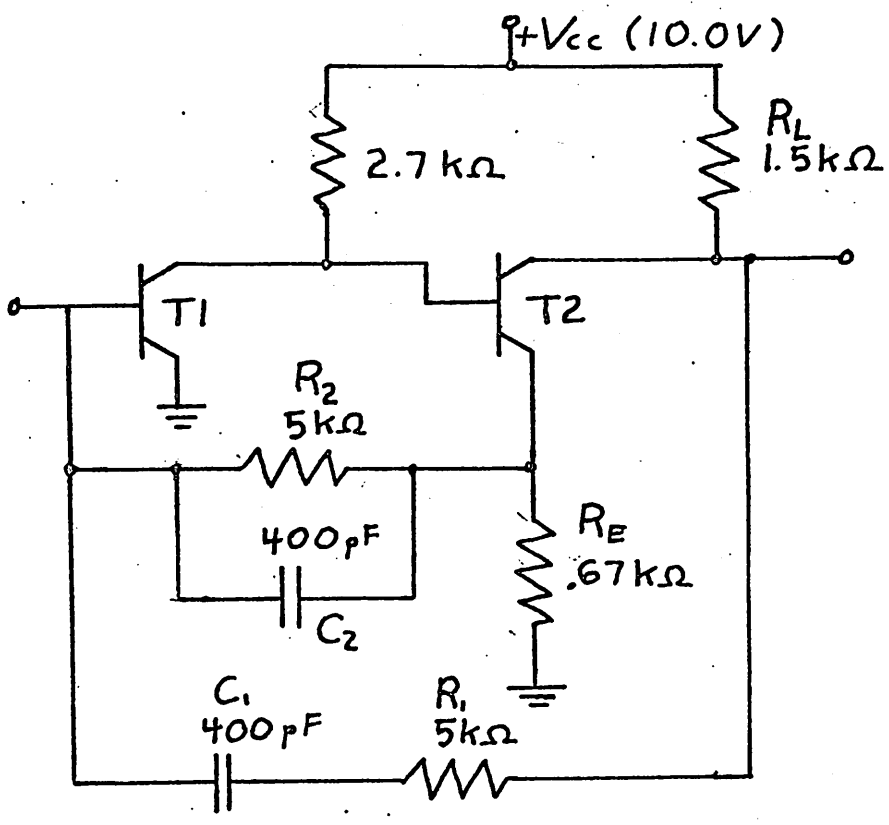

Fig. 5.7 Non-basic Uncompensated Oscillator

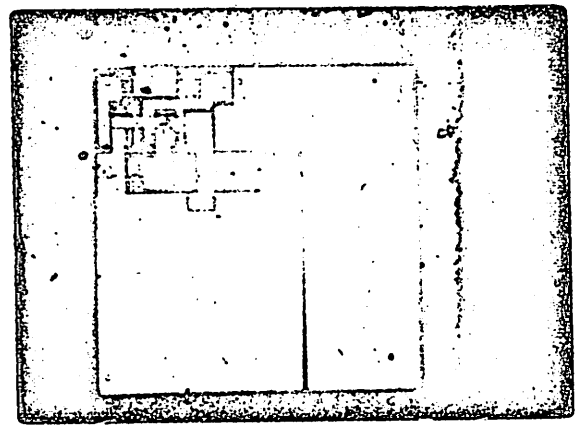

Fig. 5.8 Monolithic Realization of Non-basic Oscillator

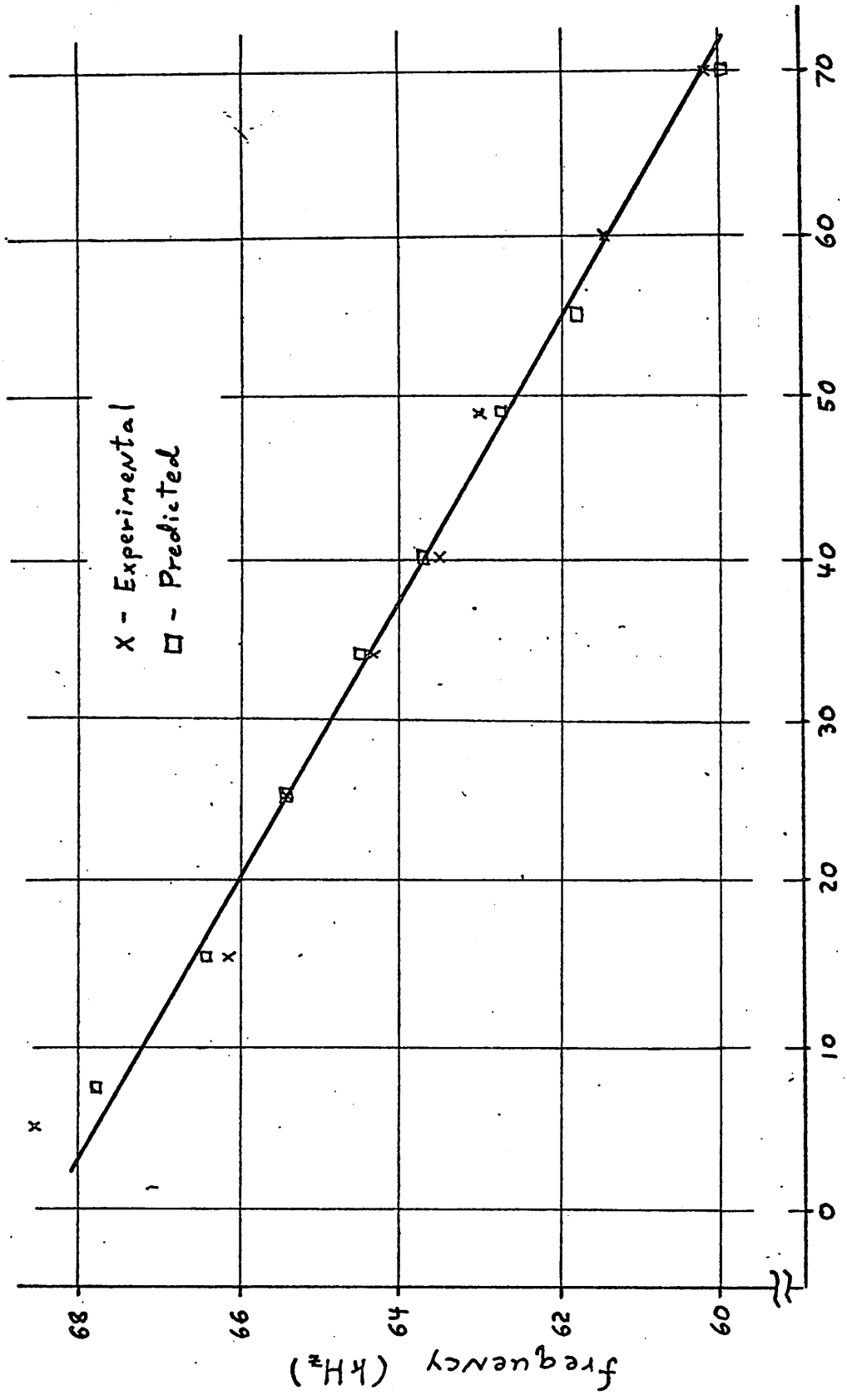

Fig. 5.9 Measured and Predicted Non-basic Oscillator Temperature Sensitivity

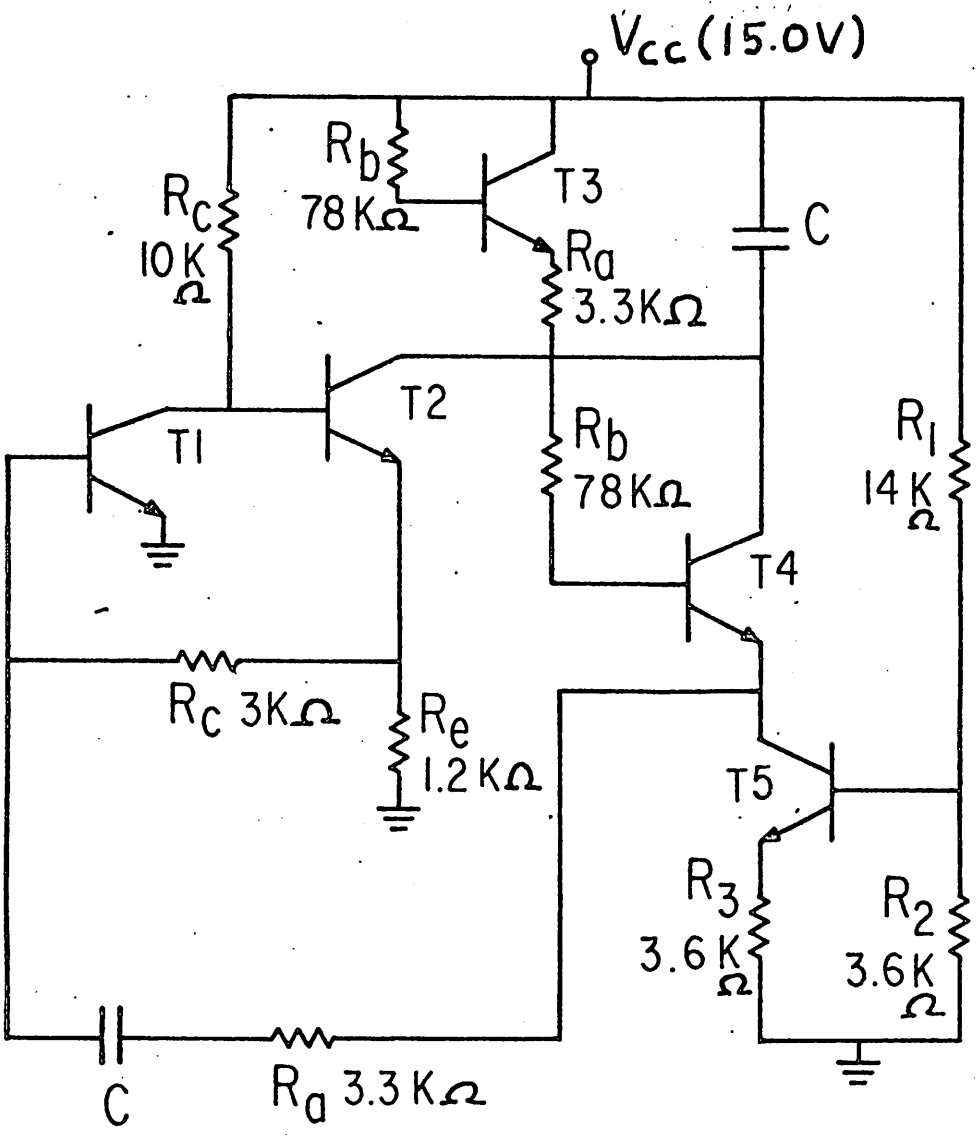

Fig. 5.10 Current Amplifier Wien-type Oscillator with Series Miller-type Compensation

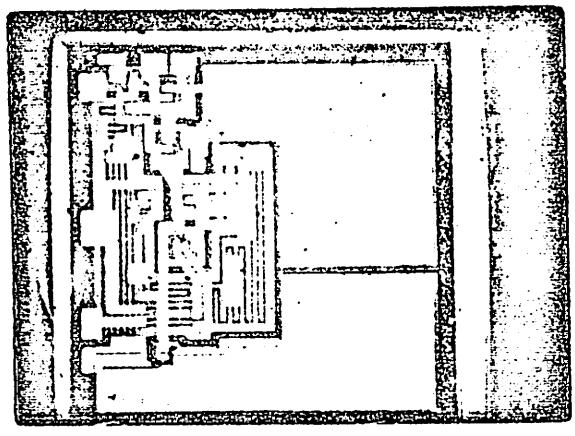

Fig. 5.11 Monolithic Realization of the Compensated Oscillator

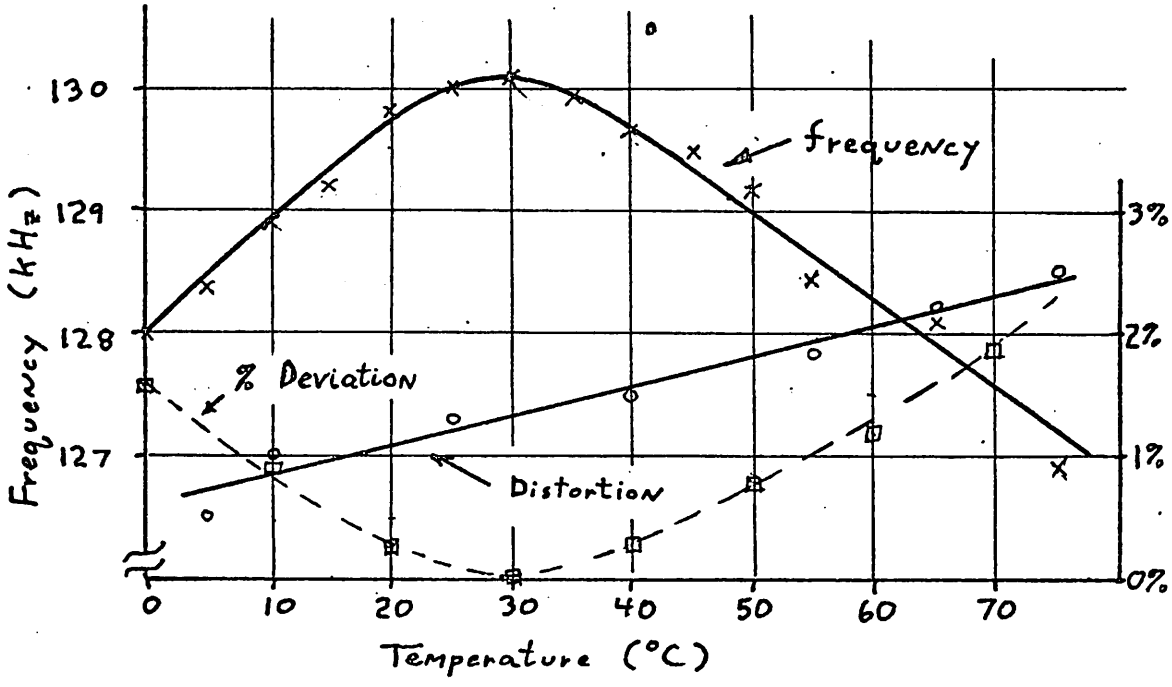

Fig. 5.12 Compensated Oscillator Temperature Sensitivity

VI. CONCLUSIONS AND RECOMMENDATIONS

The total sensitivity of an oscillator has been shown to be the sum of a term due to linear effects in the circuit and a term due to nonlinear effects. Circuit configurations were found such that the nonlinear term was negligible compared to the linear term in a monolithic realization. For these circuits, a compensation technique was found that produced a specified zero of sensitivity at a particular temperature and a reduced sensitivity over a given temperature range. At the sensitivity zero, the linear and nonlinear contribution to temperature sensitivity just cancel.

The oscillators realized experimentally had an oscillation frequency that is processing dependent. Better processing control than is available would give closer tolerances than the $\pm$15% seen in the results of Chapter 5. Final tuning could be accomplished by etching the aluminum of the MOS capacitors to remove excess capacitance and achieve the desired frequency.

For the compensated circuits, the temperature at which the zero of sensitivity occur depends on the circuit element sensitivities and the β_o realized for the transistors. A 10% error in β_o would cause about a 10^oC shift in the sensitivity zero. Again, better process control can yield a more predictable value of the zero.

Even though a reduction in overall sensitivity of the oscillator is obtained, the frequency does show considerable variation. with temperature. This is due to the large deviation of the temperature sensitivity of the compensated oscillator from zero at the temperature extremes. The major cause for this is the large difference in temperature sensitivity between the diffused resistors and the compensating transistors. A different processing schedule might make these sensitivity values more closely matched. As in pointed out in Chapter 3, the shallower transistor structures have a β_o with a lower temperature coefficient. In addition, the higher the emitter doping of the transistors, the lower the β_o temperature sensitivity is. Resistors also have temperature coefficients that are dependent on processing.

As the final point, the major concern in the monolithic realization of the oscillators considered is the linear contribution to temperature sensitivity. For oscillators that employ thin film devices in the frequency selection feedback network, the nonlinear term may become significant and nonlinear compensation resulting from extension of the results of Chapter 3 may become of interest.

APPENDIX A

The purpose of this appendix is to determine the effect of a frequency scale K on the closed-loop system poles. A frequency scale by K implies the closed-loop poles s_o becomes

$$s_o' = \frac{s_o}{K} \tag{A-1}$$

As is pointed out by Eq. 3.19, the frequency scale K is

$$K = 1 + \gamma_T^R \, \Delta T \tag{A-2}$$

Applying this to Eq. A-1 gives

$$\frac{s_o'-s_o}{\Delta T} = - s_o' \, \gamma_T^R \tag{A-3}$$

In the limit as $\Delta T \to dT$, Eq. A-3 becomes

$$\frac{ds_o}{dT} = - s_o \, \gamma_T^R \tag{A-4}$$

This is the result needed to show

$$\gamma_T^{s_o} = \frac{1}{|s_o|} \frac{\partial s_o}{\partial T} = - \frac{s_o}{|s_o|} \gamma_T^R$$

APPENDIX B

Consider a second-order system described by the generalized form of Lienard's equation

$$\ddot{x} + f(x)\dot{x} + g(x) = 0 \tag{B-1}$$

The functions $f(x)$ and $g(x)$ are assumed to have the properties:

i. $f(x), g(x) \in C(-\infty, \infty)$

ii. $df(x)/dx$ exists

iii. $f(x)$ and $df(x)/dx$ bounded

iv. $f(o) < 0$ and a period solution exists

The periodic solution of (B-1) can be expressed

$$x(t) = \frac{A_o}{2} + \sum_{n=1}^{\infty} A_n \cos(n\omega t + \psi_n) \tag{B-2}$$

Since Eq. B-1 equals zero,

$$\int_o^T (\ddot{x} + f(x)\dot{x} + g(x))dx = 0 \tag{B-3}$$

Considering Eq. B-3 term by term, one obtains

$$\int_0^T \ddot{x}\, dt = \dot{x}\Big|_0^T = 0 \tag{B-4}$$

and

$$\int_0^T f(x)\dot{x}\, dt = \oint f(x)dx = 0 \tag{B-5}$$

where the integral of the last line is taken over x from x(o) to x(T). Thus

$$\int_0^T g(x)\, dt = 0 \tag{B-6}$$

Multiplying Eq. B-1 by x and integrating the result over the period gives

$$\int_0^T (x\ddot{x} + xf(x)\dot{x} + g(x)x)dt = 0 \tag{B-7}$$

On a term by term basis, integration by parts gives

$$\int_0^T x\ddot{x}\, dt = \int_0^T \dot{x}^2\, dt \tag{B-8}$$

and

$$\int_0^T xf(x)\dot{x}\,dt = \oint xf(x)\,dx = 0 \qquad \text{(B-9)}$$

Substituting Eqs. B-8 and B-9 in Eq. B-7 gives

$$\int_0^T xg(x)\,dt = \int_0^T \dot{x}^2\,dt \qquad \text{(B-10)}$$

Eq. B-10 is the generalized relation between frequency and harmonic content.

APPENDIX C

The nonlinear equation considered is

$$\ddot{x} + f(x)\dot{x} + x = 0 \qquad \text{(C-1)}$$

A computer program for the periodic solution is written in Fortran IV for the IBM 7094. For this solution, Eq. C-1 is linearized about a point x_o on the limit cycle by putting Eq. C-1 into the form

$$\ddot{x} + 2\alpha\,\dot{x} + x = 0 \qquad \text{(C-2)}$$

where $2\alpha = f(x_o) = 3 - dF(x)/dx\Big|_{x=x_o}$. $F(x)$ is the amplifier gain characteristic. The linearized equation is solved for a small increment of time. A new α is calculated from the new value of x_o and time again incremented. This process continues until a well converged limit cycle is found. Summing the time increments to traverse the final limit cycle once gives the period.

The actual solution is carried out on a state-space basis. If $y = dx/dt$, the state of the system is given by (x,y). For given initial conditions, α is calculated from $f(x_1)$. The form of the solution is chosen on the basis of whether the roots of

$s^2 + 2\alpha s + 1 = 0$ are real or imaginary. The new set of initial conditions on the solution curve are found by incrementing time by Δt and solving

$$x_2 = Ae^{s_1\Delta t} + Be^{s_2\Delta t}$$

$$\dot{x}_2 = s_1Ae^{s_1\Delta t} + s_2Be^{s_2\Delta t} \qquad \text{(C-3)}$$

where A and B are determined from (x_1, y_1).

The time increment is chosen to limit the error in the linearized model to some predetermined maximum. This error limit is based on the predicted deviation of $f(x_2)$ from $f(x_1)$ for a given time increment. Define $h(x)$ as $h(x) = df(x)/dx$. In the linear portions of the curve, $h(x) = 0$. If x_1 is in the linear portion of the curve, t is chosen such that $h(x_2) \neq 0$. If $h(x_1) \neq 0$, Δt is chosen by an approximation, which for $\ddot{x} < 0$ is represented by

$$\Delta t = \frac{\delta}{(y_1 \cdot h(x_1))}$$

where δ is given by $\delta = |f(x_2) - f(x_1)|$. This represents the accuracy of the solution. Low accuracy and rapid convergence occur for δ large, which is used to determine the approximate limit cycle. δ is then varied to its smallest value which is chosen so that the

limit cycle is independent of δ to five places. The program is as follows:

```
C  OSCILLATOR WAVEFORM SOLUTION
   1   DIMENSION X(500),  Y(500),  T(401), W(400), DT(1), SL(9),
       F(400)
       1,D(27),G(400),JR(402)
1604   DATA SL/3.02,3.04,3.06,3.08,3.10,3.12,3,14,3.16,3.18/,(X(N),
       N=441, 1449)/0.7700,0.8500,0.9300,0.9900,1.0400,0.3125,0.8930,
       1.1750,31.2250/,(D(N),N=1,9)/9*0.01/
 614   Y(405)=3.0
2500   DEL=.025
 616   Y(406)=0.2
 617   DO 1771 K=6,7
2233   M=2
2234   N=1
   3   T(1)=0.0
 619   X(1)=X(K+440)
   5   Y(1)=0.0
3001   IF(K-6) 500,500,9500
 500   X(K+410)=9.0/(2.0*SL(K))
 501   Y(K+470)=4.0*SL(K)**3/81.0
 502   RB=Y(K+470)
 521   X(K+470)=X(K+410)
```

```
3002  GO TO 6
9500  X(K+410)=15./(4.0*SL(K-1))
9501  Y(K+470)=SL(K-1)/(5.0*X(K+410)**4)
9502  RB=Y(K+470)
9521  X(K+470)=X(K+410)
   6  DO 17 I=1,250
 970  JR(I)=0
 580  IF (ABS(X(I))-X(K+410)) 81,81,93
  81  IF(K-6) 3181,3181,3081
3081  F(I)=0.5*(3.0-SL(K-1)+5.0*RB*X(I)**4)
3044  GO TO 370
3181  F(I)=0.5*(3.0-SL(K)+3.0(RB(X(I)**2)
  84  GO TO 370
  93  F(I)=1.5
 370  P=F(I)
1370  IF (F(I)-1.0) 8,300,400
   8  W(I)=SQRT(1.0-F(I)**2)
1090  L=1
2091  GO TO 1200
 300  W(I)=1.0
1091  L=2
2090  GO TO 1200
 400  W(I)=-F(I)+SWRT(F(I)**2-1.0)
 401  F(I)=-F(I)-SQRT(F(I)**2-1.0)
1092  L=3
```

```
1200    IF(N-1) 1201,1201,1205
1201    DT(1)=D(K)
1202    JR(I)=1
1203    N=4
1204    GO TO 200
1205    IF(ABS(X(I))-X(K+410))2393,385,385
2393    N=2
2394    IF(ABS(Y(I))-0.001) 377,377,2395
2395    IF(X(I)*Y(I)) 1990,377,1380
1380    IF(K-6) 3380,3380,3480
3380    DT(1)=DEL/((6.0*RB*ABS(X(I))+.01*DEL)*ABS(Y(I)))
3381    GO TO 1381
3480    DT(1)=DEL/((20.0*RB*X(I)**4 +.01*DEL)*ABS(Y(I)))
1381    JR(I)=9
1382    IF(DT(1)-.10)200,200,1383
1383    DT(1)=.10
1384    JR(I)=10
1385    GO TO 200
1990    COR=1.0-0.5*X(I)/Y(I)
1991    IF(K-6) 3791,3791,3891
3691    DT(1)=DEL/((6.0*RB*ABS(X(I))+.01*DEL)*ABS(Y(I))*COR)
3692    GO TO 1992
3891    DT(1)+DEL/((20.0*RB*X(I)**4 +.01*DEL)*ABS(Y(I))*COR)
1992    JR(I)=11
1993    IF(DT(1)-.10)200,200,1383
```

```
 377   DT(1)=.001
 378   GO TO 200
 385   N=N+1
 386   IF(N-4) 390,200,4392
 390   IF(L-2) 1392,377,1390
1392   DT(1)=(ATAN((W(I)*Y(I))/((W(I)**2+F(I)**2)*X(I)+F(I)*Y(I))))
 955   JR(I)=5
1391   GO TO 200
1390   DT(1)=(ALOG(ABS(F(I)*(Y(I)-W(I)*X(I))/(W(I)*(Y(I)-F(I)*X(I))))))
      1/(W(I)-F(I))
 956   JR(I)=6
 391   GO TO 200
 870   DT(1)=0.0001
 871   JR(I)=13
 872   GO TO 200
4392   IF(ABS(X(I))-X(K+470)-0.0001) 870,392,392
 392   H=(P*Y(I)+0.5*X(I))
 900   IF(X(I)) 904,377,901
 901   IF(H-.0001) 908,902,902
 902   DT(1)= (Y(I)+SQRT(Y(I)**2-4.0*(X(K+470)-X(I))*H))/(2.0*H)
 962   JR(I)=12
 903   GO TO 376
 904   IF(H+.0001) 905,905,908
 905   U=-X(K+470)
 906   DT(1)= (Y(I)-SQRT(Y(I)**2-4.0*(U-X(I))*H))/(2.0*H)
 957   JR(I)=7
```

```
907   GO TO 376
908   DT(1)=-(X(K+470)-ABS(X(I)))/ABS(Y(I))
958   JR(I)=8
376   IF(DT(1)-0.001) 5377,5377,200
5377  DT(1)=0.0001
200   IF(L-2) 10,310,402
 10   T(I+1)=T(I)+DT(1)
 59   EX=EXP(-F(I)*DT(1))
 61   C2=COS(W(I)*DT(1))
 62   S2-SIN(W(I)*DT(1))
 64   A=X(I)
 65   B=(Y(I)+F(I)*X(I))/W(I)
 66   X(I+1)= (A*C2+B*S2)*EX
 67   Y(I+1)= (-A*(F(I)*C2+W(I)*S2)+B*(W(I)*C2-F(I)*S2))*EX
201   GO TO 17
310   T(I+1)=T(I)+DT(1)
313   X(I+1)+(X(I)*COS(W(I)*T(I))-(Y(I)*SIN(W(I)*T(I)))/W(I))*COS(W(I)*
     1T(I+1))+(X(I)*SIN(W(I)*T(I))+(Y(I)*COS(W(I)*T(I)))/W(I))*SIN(W(I)*
     2T(I+1))
314   Y(I+1)=-(X(I)*COS(W(I)*T(I))-(Y(I)*SIN(W(I)*T(I)))/W(I))*W(I)*
     1SIN(W(I)*T(I+1))+(X(I)*SIN(W(I)*T(I))+(Y(I)*COS(W(I)*T(I)))/W(I))*
     2W(I)*COS(W(I)*T(I+1))
315   GO TO 17
402   T(I+1)=T(I)+DI(1)
405   X(I+1)+((W(I)*X(I)-Y(I))*EXP(F(I)*(T(I+1))))/(W(I)-F(I))
     1+((F(I)*X(I)-Y(I))*EXP(W(I)*(T+1)-T(I))))/(F(I)-W(I))
406   Y(I+1)=F(I)*((W(I)*X(I)-Y(I))*EXP(F(I)*(T(I+1)-T(I))))/(W(I)-F(I))
     1+W(I)*((F(I)(X(I)-Y(I))*EXP(W(I)*(T(I+1)-T(I))))/(F(I)-W(I))
```

```
   17   CONTINUE
   50   PRINT 51,K
   51   FORMAT (1H1,I2)
   40   PRINT 41
   41   FORMAT (5H TIME, 10X, 7HX VALUE 7X, 7HY VALUE, 7X, 5HDECAY, 7X,
       14HFREQ, 7X, 4HTEST)
   18   PRINT 19, (T(J),X(J),Y(J),F(J),W(J),JR(J), J=1,250)
   19   FORMAT (E13.5,2X,E12.5,2X,E12.5,2X,E12.5,2X,E12,5,2X,I2)
 1671   CONTINUE
   20   PRINT 21, (X(M+410),X(M+470),Y(M+470), M=6,7)
   21   FORMAT (3(2X,E12.5))
  150   STOP
   44   END
```

APPENDIX D

Piecewise linear computer program to determine periodic solution of $\ddot{x} + f(x)\dot{x} + x = 0$ written for the IBM 1800.

LINK RFA

```
      COMMON XE(5),YE(5),XC(5),YC(5),T,I,W,S1,S2,ACT,DEC,X1,X2
      READ(1,1) X1,X2,DEC,ACT,YK
    1 FORMAT (5F10.5)
    3 WRITE (2,2) X1,X2,DFC,ACT,YK
    2 FORMAT (5F10.5)
      WRITE (2,61)
   61 FORMAT (1H1,2X,2HXE,10X,2HYE)
      YE(1)=YK
      XE(1)+X1
      W=SQRT(1.0-ACT**2)
      S1=-DEC-SQRT(DEC**2-1.0)
      S2=-DEC+SQRT(DEC**2-1.0)
      CALL LINK (KLA)
   44 END
```

LINK KLA

```
      COMMON XE(5),YE(5),XC(5),YC(5),T,I,W,S1,S2,ACT,DEC,X1,X2
      T=0.0
      A=(YE(1)-S2*XE(1))/(S1-S2)
      B=(YE(1)-S1*XE(1))/(S2-S1)
      T1=(ALOG(ABS(SL*(YE(1)-S2*XE(1))/(S2*(YE(1)-S1*XE(1))))))/(S2-S1)
      T2=1.8*T1
    4 C=A*EXP(S1*T2)
      D=B*EXP(S2*T2)
      XE(2)=C+D
      YE(2)=S1*C+s@*D
      IF(XE(2)-X1-.0005) 5,5,6
    6 H=DEC*YE(2)+0.5*XE(2)
      IF(H) 18,18,19
   19 T2=T2+(YE(2)+SQRT(YE(2)**2-4.0*(X1-XE(2))*H))/(2.0*H)
      GO TO 4
   18 T2=T2-(XE(2)-X1)/YE(2)
      GO TO 4
    5 T=T+T2
      A=XE(2)
      B=(YE(2)-ACT*XE(2))/W
      T1=(-ATAN(A/B))/W
      T2=1.1*T1
    7 XE(3)=(A*COS(W*T2)+B*SIN(W*T2))*EXP(ACT*T2)
```

```
      YE(3)=ACT*XE(3)+W*(B*COS(W*T2)-A*SIN(W*T2))*EXP(ACT*T2)
      IF(XE(3)-X2-.0001) 8,8,40
   40 T2=T2+(X2-XE(3))/YE(3)
      GO TO 7
    8 T=T+T2
      CALL LINK (KAA)
   44 END
```

LINK KAA

```
      COMMON XE(5),YE(5),XC(5),YC(5),T,I,W,S1,S2,ACT,DEC,X1,X2
      A=(YE(3)-S2*XE(3))/(S1-S2)
      B=(YE(3)-S1*XE(3))/(S2-S1)
      T1=(ALOG(ABS(S1*(YE(3)-S2*XE(3))/(S2*(YE(3)-S1*XE(3))))))/(S2-S1)
      T2=1.8*T1
   12 C=A*EXP(S1*T2)
      D=B*EXP(S2*T2)
      XE(4)=C+D
      YE(4)=S1*C+S2*D
      IF(XE(4)-X2+.0005) 10,11,11
   10 H=DEC*YE(4)+0.5*XE(4)
      IF(H) 21,22,22
   21 T2=T2+(YE(4)-SQRT(YE(4)**2-4.0*(X2-XE(4))*H))/(2.0*H)
      GO TO 12
```

```
22    T2=T2-(XE(4)-X2)/YE(4)
      GO TO 12
11    T=T+T2
      A=XE(4)
      B=(YE(4)-ACT*XE(4))/W
      T1=(-ATAN(A/B))/W
      T2-1.1*T1
16    XE(1)=(A*COS(W*T2)+B*SIN(W*T2))*EXP(ACT*T2)
      YE(1)=ACT*XE(1)+W*(B*COS(W*T2)-A*SIN(W*T2))*EXP(ACT*T2)
      IF(XE(1)-X1+.0001) 30,15,15
30    T2=T2+(X1-XE(1))/YE(1)
      GO TO 16
15    T=T+T2
      CALL LINK (RAA)
44    END
```

LINK RAA

```
      COMMON XE(5),YE(5),XC(5),YC(5),T,I,W,S1,S2,ACT,DEC,X1,X2
      WRITE (2,41) (XE(J),YE(J),J=1,4),T
41    FORMAT (2(2X,E12.5)/2(2X,E12.5)/2(2X,E12.5)/2(2X,E12.5)/6X,E12.5)
      CALL LINK (KLA)
44    END
```

APPENDIX E

This appendix lists a program written in modified Fortran II for the IBM 1800 computer with 8k of core storage. The program is useful only for determining the period of any periodic solution to an equation of the form

$$a_3\dddot{x} + a_2\ddot{x} + a_1\dot{x} + a_0 x = 0 \qquad \text{(E-1)}$$

where the coefficients depend on x in a piecewise linear sense. Each coefficient a_i may be given three values according to:

$$a_{i1} \text{ for } x > x_1 \qquad i = 0,1,2,3 \qquad \text{(E-2a)}$$

$$a_{i2} \text{ for } x_1 < x < x_2 \qquad i = 0,1,2,3 \qquad \text{(E-2b)}$$

$$a_{i3} \text{ for } x < x_2 \qquad i = 0,1,2,3 \qquad \text{(E-2c)}$$

The values of the coefficients are a part of the input data. The program is unending in that it runs until interrupted by the operator. The detail listing of the program is as follows. All the links are introduced by the same common state which is:

```
COMMON A(3,4),XR(3,4),X(10),Y(10),Z(10),X1,X2,K,L,TI,DT,R(3,3),
1S(3,3),T(3,3)U(3),V(3),IR,AQ(3),N,TA(10),JM
```

The main program consists of 8 links, the first of which is called by an XEQ RKA call card.

LINK RKA (1)

```
      READ (1,1) ((A(I,J),J=1,4),I=1,3),X1,X2,Y(1),Z(1),DT,IR
      WRITE(2,1) ((A(I,J),J=1,4),I=1,3),X1,X2,Y(1),Z(1),DT,IR
1     FORMAT (4F10.5/4F10.5/4F10.5/5F10.5,10X,I2)
      X(1)=X2
      TI=0.0
      K=0
      L=1
      CALL LINK (R3RD)
      END
```

LINK R3RD (2)

```
      DIMENSION XCOF(4),COF(4),ROOTR(3),ROOTI(3)
      COMMON A(3,4),XR(3,4)
      DO 11 K=1,3)
      XCOF(1)=A(K,4)
```

```
      XCOF(2)=A(K,3)
      XCOF(3)=A(K,2)
      XCOF(4)=A(K,1)
      CALL POLRT (XCOF,COF,M,ROOTR,ROOTI,IER)
      IF(ROOTI(1)) 1,2,1
 1    IF(ROOTI(2)) 20,21,20
20    IF(ROOTI(3)) 31,30,31
31    PAUSE 0003
      CALL EXIT
30    XR(K,1)=ROOTR(3)
      XR(K,2)=ROOTR(2)
      XR(K,3)=ROOTR(1)
      IF(ROOTI(2)) 33,33,34
33    XR(K,4)=-ROOTI(2)
      GO TO 99
34    XR(K,4)=ROOTI (2)
      GO TO 99
21    XR(K,1)=ROOTR(2)
      XR(K,2)=ROOTR(1)
      XR(K,3)=ROOTR(3)
      IF(ROOTI(1)) 22,22,23
22    XR(K,4)=-ROOTI(1)
      GO TO 99
23    XR(K,4)=ROOTI(1)
      GO TO 99
```

```
 2    IF(ROOTI(2)) 3,5,4
 3    XR(K,4)=-ROOTI(2)
      GO TO 6
 4    XR(K,4)=ROOTI(2)
 6    XR(K,1)=ROOTR(1)
      XR(K,2)+ROOTR(2)
      XR(K,3)+ROOTR(3)
99    A(K,1)=1.0
      A(K,2)-XR(K,1)-2.0*XR(K,2)
      A(K,3)XR(K,2)**2+XR(K,4)**2+2.0*XR(K,1)*XR(K,2)
      A(K,4)=-XR(K,1)*(XR(K,2)**2+XR(K,4)**2)
      GO TO 11
 5    XR(K,1)=ROOTR(1)
      XR(K,2)=ROOTR(2)
      XR(K,3)=ROOTR(3)
      XR(K,4)=0.0
      A(K,1)=1.0
      A(K,2)=-XR(K,1)-XR(K,2)-XR(K,3)
      A(K,3)=-XR(K,3)*(XR(K,1)+XR(K,2))-XR(K,1)*XR(K,2)
      A(K,4)=-XR(K,1)*XR(K,2)*XR(K,3)
11    CONTINUE
      CALL LINK (PRTA)
      END
```

LINK PRTA (3)

```
      CALL SSWTCH (0,NS)
      GO TO (21,20),NS
 20   WRITE(2,7) ((A(I,J),J=1,4),I=1,3),X1,X2,Y(1),Z(1),DT,IR
  7   FORMAT (4E12.5/4E12.5/4E12.5/5F10.5,10X,I2)
      WRITE (2,1)
  1   FORMAT (3HXR1,9X,3HXR2,9X,3HXR3,9X,3HIMG)
      WRITE (2,2) ((XR(I,J),J=1,4),I=1,3)
  2   FORMAT (4E12.5/4E12.5/4E12.5///)
      WRITE (2,3)
  3   FORMAT (1HT,11X,1HX,11X,1HY,11X,1HZ)
 21   N=3
      CALL LINK (CALC)
      END
```

LINK CALL (4)

```
      TA(1)=0.0
      DO 10 M=1,3
      R(M,1)=XR(M,3)-XR(M,2)
      S(M,1)=XR(M,2)**2-XR(M,3)**2
      T(M,1)=XR(M,2)*XR(M,3)**2-XR(M,3)*XR(M,2)**2
```

```
      R(M,2)=XR(M,1)-XR(M,3)
      S(M,2)=XR(M,3)**2-XR(M,1)**2
      T(M,2)=XR(M,3)*XR(M,1)**2-XR(M,1)*XR(M,3)**2
      R(M,3)=XR(M,2)-XR(M,1)
      S(M,3)=XR(M,1)**2-XR(M,2)**2
10    T(M,3)=XR(M,1)*XR(M,2)**2-XR(M,2)*XR(M,1)**2
      DO 11 M=1,3
      U(M(=XR(M,2)-XR(M,1)
11    V(M)=XR(M,2)**2-XR(M,1)**2-XR(M,4)**2
      N=3
      K=3
      JM=1
      IF(XR(3,4)) 7,7,8
 7    CALL LINK (SOLVR)
 8    CALL LINK (SOLVC)
      END
```

LINK SOLVC (5)

```
20    QC=XR(N,1)**2+XR(N,2)**2+XR(N,4)**2-2.*XR(N,1)*XR(N,2)
      TC=DT
      AC=(Z(L)-2.0*XR(N,2)*Y(L)+(XR(N,4)**2+XR(N,2)**2)*X(L))/QC
      BC=(-Z(L)+2.0*XR(N,2)*Y(L)+(XR(N,1)**2-2.0*XR(N,1)*XR(N,2))*X(L))
      1/QC
```

```
      C=(U(N)*Z(L)-V(N)*Y(L)+(XR(N,1)*XR(N,2)*U(N)-XR(N,4)**2*XR(N,1))
      1*X(L))/(XR(N,4)*QC)
45    EXC=EXP(XR(N,2)*TC)*COS(XR(N,4)*TC)
      EXS=EXP(XR(N,2)*TC)*SIN(XR(N,4)*TC)
      EX1=EXP(XR(N,1)*TC)*AC
      X(L+1)=EX1+BC*EXC+C*EXS
      Y(L+1)+XR(N,1)*EX1+(BC*XR(N,2)+C*XR(N,4))*EXC+(-BC*XR(N,4)+C*XR(
      1N,2))*EXS
      Z(L+1)=XR(N,1)**2*EX1+(BX*XR(N,2)**2-XR(N,4)**2)+C*(2.0*XR(N,4)*
      1XR(N,2)))*EXC+(BC*(-2.*XR(N,4)*XR(N,2))+C*(XR(N,2)**2-XR(N,4)**2
      2))*EXS
      GO TO (78,47,68),N
47    IF(K-2) 48,48,58
48    IF(Y(L+1)) 50, 50, 49
49    K=4
      N=2
      GO TO 57
50    IF(X(L+1)-X1) 53,53,51
51    IF(K=2) 55,52,52
52    TC=TC+DT
      GO TO 45
53    IF(K-2) 56,54,54
54    TC=TC-DT
      K=1
      GO TO 45
```

```
55    TC=TC-(X(L+1)-X1)/Y(L+1)+.01*DT
      GO TO 45
56    N=1
      K=1
57    TA(L+1)=TA(L)+TC
      GO TO 10
58    IF(Y(L+1)) 59,60,60
59    K=2
      N=2
      GO TO 67
60    IF(X(L+1)-X2) 61,61,63
61    IF(K-4) 65,62,62
62    TC=TC+DT
      GO TO 45
63    IF(K-4) 66,64,64
64    TC=TC-DT
      K=3
      GO TO 45
65    TC=TC+(X2-X(L+1))/Y(L+1)+.01*DT
      GO TO 45
66    N=3
      K=3
67    TA(L+1)=TA(L)+TC
      GO TO 10
68    IF (X(L+1)-X2) 72,70,70
70    IF(K-2) 74,74,71
```

```
71    TC=TC+DT
      GO TO 45
72    IF(K-2) 75,75,73
73    TC=TC-DT
      K=2
      GO TO 45
74    TC=TC-.9*((X(L+1)-X2)*Y(L+1))/(Y(L+1)**2-X(L+1)*X2+X(L+1)**2)+.01*
      1DT
      GO TO 45
75    TA(L+1)=TA(L)+TC
      K=2
      N=2
      GO TO 10
78    IF(X(L+1)-X1) 80,80,82
80    IF(K) 84,84,81
81    TC=TC+DT
      GO TO 45
82    IF(K) 85,85,83
83    TC=TC-DT
      K=0
      GO TO 45
84    TC=TC+.9*((X1-X(L+1))*Y(L+1))/(Y(L+1)**2-X(L+1)*X1+X(L+1)**2)+.01*
      1DT
      GO TO 45
85    TA(L+1)=TA(L)+TC
      K=4
```

```
      N=2
10    L=L+1
      TC=0.0
      IF(L-10) 12,13,13
13    CALL LINK (PANS)
12    IF(XR(N,4)) 15,15,14
14    CALL SSWTCH(2,MC)
98    GO TO (20,97),MC
97    CALL LINK (PCK)
15    CALL LINK (SOLVR)
      END
```

LINK SOLVR (6)

Link SOLVR is the same as link SOLVC except as noted here. Statement 20 of SOLVC is replaced by:

```
20    DO 11 M=1,3
11    G(M)=(R(N,M)*Z(L)+S(N,M)*Y(L)+T(N,M)*X(L))/(R(N,M)*XR(N,M)**2
      1+XR(N,M)*S(N,M)+T(N,M))
```

State 45 and the following 5 statements are replaced by:

```
45    EX1=EXP(XR(N,1)*TC)*G(1)
      EX2=EXP(XR(N,2)*TC)*G(2)
      EX3=EXP(XR(N,3)*TC)+G(3)
      X(L+1)+EX1+EX2+EX3
      Y(L+1)=EX1*XR(N,1)+EX2*XR(N,2)+EX3*XR(N,3)
      Z(L+1)=EX1*XR(N,1)**2+EX2*XR(N,2)**2+EX3*XR(N,3)**2
```

State 12 of SOLVC and all subsequent statements are replaced by:

```
12    IF(XR(N,4)) 14,14,15
14    GO TO 20
15    CALL LINK (SOLVC)
13    CALL LINK (PANS)
      END
```

LINK PCK (7)

```
      WRITE (2,1) x(L),Y(L),Z(L)
 1    FORMAT (3E12.5)
      CALL LINK (SOLVC)
      END
```

LINK PANS (8)

```
      CALL SSWTCH(1,MS)
      GO TO (3,4),MS
  3   WRITE (2,1)(TA(M),X(M),Y(M),X(M),M=1,9)
  1   FORMAT  (E13.6,E12.5)
  4   X(L-9)=X(L)
      Y(L-9)=Y(L)
      Z(L-9)=Z(L)
      TA(L-9)=TA(L)
      L=1
 10   IF(XR(N,4)) 14,14,15
 14   CALL LINK (SOLVR)
 15   CALL LINK (SOLVC)
      END
```

APPENDIX F

A perturbation analysis of the periodic solution of the nonlinear system is done by the method of Krylov, Bogoliubov, Mitropolsky[54]. The system is represented by the equation

$$\ddot{x} + \omega^2 x = \mu f(x)\, \dot{x} \tag{F-1}$$

It is assumed to have the solution

$$x = a \cos \psi + \mu\, u^{(i)}\, (a,\psi) + \ldots \tag{F-2}$$

where $u^{(i)}$ is a periodic function of ψ and a. ψ and a satisfy

$$\dot{a} = \mu A^{(1)}(a) + \mu^2\, A^{(2)}\, (a) \ldots \tag{F-3}$$

$$\dot{\psi} = \omega + \mu B^{(1)}(a) + \mu^2\, B^{(2)}\, (a) \ldots \tag{F-4}$$

This gives for the first approximation of the autonomous aystem:

$$x = a \cos \psi \tag{F-5}$$

$$\dot{a} = \frac{\mu}{2}\, F_1^*(a) \tag{F-6}$$

$$\dot{\psi} = \omega \tag{F-7}$$

and for the second approximation:

$$x = a \cos \psi + \frac{\mu}{\omega} \sum_{n=2}^{\infty} \frac{n F_n^*(a) \sin \psi}{n^2-1} \tag{F-8}$$

$$\dot{a} = \frac{\mu}{2} F_1^* (a) \tag{F-9}$$

$$\dot{\psi} = \omega + \mu^2 B^2(a) \tag{F-10}$$

The term of inerest is the second term in this approximation.

In the case of the van der Pol equation

$$f(x) = \varepsilon(1-\mu x^2) \tag{F-11}$$

This gives

$$F^*(x) = x - \frac{\mu x^3}{3} \tag{F-12}$$

or

$$F^*(a \cos \psi) = a(1 - \frac{\mu a^2}{2}) \cos \psi - \frac{\mu a^3}{12} \cos 3 \psi \tag{F-13}$$

The identity is made

$$F_1^*(a) = a\left(1 - \frac{\mu a^2}{2}\right) \tag{F-14}$$

$$F_3^*(a) = -\frac{\mu a^3}{2} \tag{F-15}$$

so that

$$\dot{a} = \frac{\varepsilon a}{2}\left(1 - \frac{\mu a^2}{4}\right) \tag{F-16}$$

Integrating by quadratures gives

$$\frac{a^2\left(1 - \frac{1}{4}\mu a_o^2\right)}{\left(1 - \frac{1}{4}\mu c^2\right)a_o^2} = e^{\varepsilon t} \tag{F-17}$$

As $t \to \infty$

$$a = 2/\sqrt{\mu} \tag{F-18}$$

If $\mu = 1$, $a = 2$ which is the known first order approximation amplitude for the van der Pol form.

In general, $B^{(2)}(a)$ is given by

$$B^{(2)}(a) = \frac{1}{\delta a \omega} F_1^*(a) \frac{dF_1^*(a)}{da} - \frac{1}{2\omega a^2} \sum_{n=2}^{\infty} \frac{n^2 F_n^{*2}(a)}{n^2 - 1} \tag{F-19}$$

For the second approximation, this gives

$$\dot{\psi} = \omega - \varepsilon^2\left(\frac{1}{8} - \frac{a^2}{8} + \frac{7a^4}{296}\right) \qquad \text{(F-20)}$$

For a = 2,

$$\boxed{\omega_o = 1 - \frac{\varepsilon^2}{16}} \qquad \text{(F-21)}$$

For the case where

$$f(x) = \varepsilon(1 - x^4) \qquad \text{(F-22)}$$

$F^*(x)$ is

$$F^*(x) = x - \mu\frac{x^5}{5} \qquad \text{(F-23)}$$

This leads to

$$F^*(a\cos\psi) = a\left(1 - \frac{5a^4}{40}\right)\cos\psi - \frac{5a^5}{80}\cos 3\psi - \frac{a^5}{80}\cos 5\psi \qquad \text{(F-24)}$$

Then

$$\dot{a} = \frac{a}{2}\varepsilon\omega\left(1 - \mu\frac{a^4}{8}\right) \qquad \text{(F-25)}$$

Integrating by quadratures

$$\int_{a_o}^{a} \frac{\frac{1}{2}\,da}{a^2(1 - \mu \frac{a^4}{8})} = \int_{o}^{t} \frac{\varepsilon\omega}{2}\,dt \tag{F-26}$$

gives

$$\log \frac{a^4(1 - \frac{1}{8}\mu a_o^4)}{(1 - \frac{1}{8}\mu a^4)a_o^4} = \mu\omega t \tag{F-27}$$

As $t \to \infty$

$$a^2 = \frac{2\sqrt{2}}{\sqrt{\mu}} \tag{F-28}$$

For $B_2(a)$

$$B_2(a) = -\frac{1}{8a}(a - \frac{a^5}{8})(1 - \frac{5}{8}a^4) - \frac{1}{2a^2}[\frac{9}{8}(\frac{a^5}{16})^2 + \frac{25}{24}(\frac{a^5}{16})^2] \tag{F-29}$$

For $\mu = 1$,

$$B_2(a) = \frac{28}{192} \tag{F-30}$$

so

$$\dot{\psi} = \omega + \varepsilon^2 \frac{28}{192} \tag{F-31}$$

Thus

$$\boxed{\omega_o = 1 - \varepsilon^2 \frac{28}{192}} \qquad \text{(F-32)}$$

Eqs. F-21 and F-32 show the dependence of the fundamental frequency of oscillation on the parameter ε. These results are considered in Chapter 3.

REFERENCES

1. R. S. Pepper and D. O. Pederson, "Integrated Near-Harmonic Oscillators," IEEE Region 6 Convention Record, 1966.

2. G. D. Hachtel and R. S. Pepper, "The Synthesis of Integrable Nearly Sinusoidal Potentially Bistable Oscillators," IEEE Journal of Solid State Circuits, Vol. SC-1, No. 2, pp. 111-117, December, 1963.

3. G. D. Hachtel, "Semiconductor Integrated Oscillators," Electronics Research Laboratory Report No. 65-32, University of California, Berkeley, August 1965.

4. G. D. Hachtel and G. W. Haines, Jr., "Unijunction Transistor Oscillators," Digest of Technical Papers, ISSCC, Lewis Winner, Publisher, New York, New York, February 1964.

5. G. D. Hachtel, "An Analysis of an Integrable Phase Shift Oscillator," University of California Electronics Research Laboratory Report No. 60-375, Berkeley, 1962.

6. W. G. Howard and D. O. Pederson, "Integrated Voltage Controlled Oscillations," Proc. of NEC, Vol. 23, pp. 279-284, 1967.

7. Berry, Miller, and Rickart, "A Tone-Generating Integrated Circuit," Bell Laboratories Record, Vol. 44, No. 9, Oct.-Nov 1966, p. 318.

8. Minorsky, Nonlinear Oscillations, Van Nostrand, Princeton, N.J., 1962.

9. D. K. Lynn, R. S. Pepper, D. O. Pederson, "The Minimum Period of Oscillation of Simple Tunnel Diode Oscillators," Institute of Engineering Research, University of California (Berkeley), Series No. 60, Issue 388.

10. G. D. Hachtel and G. W. Haines, op. cit.

11. R. S. Pepper and D. O. Pederson, op. cit.

12. N. Balabanian, Network Synthesis, Prentice-Hall, Englewood Cliffs, N. J., 1958.

13. W. G. Howard, op. cit.

14. W. G. Howard, op. cit.

15. L. O. Hill, D. O. Pederson, and R. S. Pepper, "Synthesis of Electronic Bistable Circuits," IEEE Trans. on Circuit Theory, Vol. CT-10, No. 1, March 1963, p. 25.

16. C. L. Searle, A. Boothroyd, E. Angelo, P. Gray, and D. O. Pederson, Elementary Circuit Properties of Transistors, SEEC, John Wiley & Sons, New York, 1964.

17. D. O. Pederson, Electronic Circuits, (Prelim. Ed.) McGraw-Hill, New York, 1966.

18. R. W. Warner, J. N. Fordemwalt, Ed., Integrated Circuits, Design Principles and Fabrication, McGraw-Hill, New York, 1965, p. 382.

19. D. A. Hodges, "Tapered RC Networks for use in Integrated Filter Circuits," University of California Electronic Research Laboratory Report No. 60-390, 1962.

20. W. G. Howard, Private Communication.

21. R. W. Warner, J. N. Fordemwalt, op. cit.

22. Ibid, p. 215

23. W. G. Howard, op. cit.

24. A. A. Gaash, R. S. Pepper, and D. O. Pederson, "Design of Integrated Desensitized Frequency Selective Amplifiers," IEEE Trans. on Solid-State Circuits, Vol. SC-1, No. 1, pp.29-35, Sept. 1966.

25. R. J. Widlar, "Some Circuit Design Techniques for Linear Integrated Circuits," IEEE Trans. on Circuit Theory, CT-12, No. 4, Dec. 1965, p. 586.

26. H. W. Bode, Network Analysis and Feedback Amplifier Design, Van Nostrand, New York, 1945.

27. A. A. Gaash, op. cit.

28. M. S. Hess, O. R. Viva, and W. J. Armstrong, "Properties of Diffused Resistors," Electrochemical Technology, Vol. 4, No. 11-12, pp. 544-546, Dec. 1966.

29. R. Bellman, Perturbation Techniques in Mathematics, Physics, and Engineering, Holt, Rinehart, and Winston, Inc., New York, 1964.

30. A. A. Gaash, op. cit.

31. G. Wilson, "Nonlinear Analysis of Sinusoidal Oscillators," Institute of Engineering Research, University of California (Berkeley), Series No. 60, Issue 420.

32. R. S. Pepper, op. cit.

33. K. K. Clarke, "Design of Self Limiting Transistor Sine Wave Oscillators," IEEE Trans. on Circuit Theory, Vol. CT-13, No. 1, March 1966, p. 58.

34. G. Wilson, op. cit.

35. L. L. Rauch, "Oscillation of a Third-Order Nonlinear Autonomous System", Contributions to the Theory of Nonlinear Oscillations, Vol. 1, Ed.: S. L. Lefschetz, Princeton University Press, 1956.

36. D. K. Lynn, op. cit.

37. S. P. Diliberto, "New Results of Periodic Surfaces and the Averaging Principle," University of California Department of Mathematics Tech. Report, University of California, Berkeley, August 1967.

38. A. A. Andronov, Theory of Oscillators, Pergamon Press, Oxford, 1966.

39. J. Stoker, Nonlinear Vibrations, Interscience, New York, 1950.

40. C. Hayaski, Nonlinear Oscillations in Physical Systems, McGraw-Hill, New York, 1964.

41. J. E. Littlewood, "Van der Pol Equation for Relaxation Oscillations," Contributions to the Theory of Nonlinear Oscillations, Ed.: S. L. Lefschetz, Princeton University Press, Vol. 2, 1966 (AS2).

42. J. Groszkowski, Frequency of Self-Oscillations, The Macmillan Co., New York, 1964.

43. J. Shohat, "On van der Pol's and Related Nonlinear Differential Equations," Journal of Applied Physics, Vol. 15, 1944, p. 568.

44. Stoker, op. cit.

45. Shohat, op. cit.

46. Minorsky, op. cit.

47. S. P. Diliberto, Private Communication.

48. F. H. Brownell, "Nonlinear Delay Differential Equations," Contributions to the Theory of Nonlinear Oscillations, Ed.: S. L. Lefschetz, Princeton University Press, Ud #1, 1950.

49. C. L. Johnson, Analog Computer Techniques, McGraw-Hill, New York, 1963.

50. A. A. Gaash, op. cit.

51. D. O. Pederson, Electronic Circuits, Preliminary Edition, McGraw-Hill, New York, 1965, p. 55.

52. R. W. Warner, J. N. Fordemwalt, op. cit.

53. Ibid.

54. Minorsky, op. cit., p. 342.